

**A SIZING AND VEHICLE MATCHING METHODOLOGY
FOR BOUNDARY LAYER INGESTING PROPULSION
SYSTEMS**

A Thesis
Presented to
The Academic Faculty

by

Jonathan C. Gladin

In Partial Fulfillment
of the Requirements for the Degree
Doctor of Philosophy in the
School of Aerospace Engineering

Georgia Institute of Technology
August 2015

A SIZING AND VEHICLE MATCHING METHODOLOGY FOR BOUNDARY LAYER INGESTING PROPULSION SYSTEMS

Approved by:

Professor Dimitri Mavris, Committee Chair
School of Aerospace Engineering
Georgia Institute of Technology

Professor Dimitri Mavris, Advisor
School of Aerospace Engineering
Georgia Institute of Technology

Dr. Brian Kestner
School of Aerospace Engineering
Georgia Institute of Technology

Dr. Brian German
School of Aerospace Engineering
Georgia Institute of Technology

Date Approved:

To myself,

Perry H. Disdaiful,

the only person worthy of my company.

A Sizing and Vehicle Matching Methodology for Boundary Layer Ingesting
Propulsion Systems

Jonathan C. Gladin

114 Pages

Directed by Professor Dimitri Mavris

This is the abstract that must be turned in as hard copy to the thesis office to meet the UMI requirements. It should *not* be included when submitting your ETD. Comment out the abstract environment before submitting. It is recommended that you simply copy and paste the text you put in the summary environment into this environment. The title, your name, the page count, and your advisor's name will all be generated automatically.

PREFACE

Theses have elements. Isn't that nice?

ACKNOWLEDGEMENTS

I want to “thank” my committee, without whose ridiculous demands, I would have graduated so, so, very much faster.

TABLE OF CONTENTS

DEDICATION	iii
PREFACE	iv
ACKNOWLEDGEMENTS	v
LIST OF TABLES	x
LIST OF FIGURES	xi
SUMMARY	xiv
I INTRODUCTION	1
1.1 Environmental Pressures and Aviation Technology	1
1.2 Boundary Layer Ingestion	2
1.2.1 BLI Benefits	4
1.2.2 BLI Risks	5
1.3 Design Methods	6
1.3.1 Conceptual Design Studies For BLI	7
1.4 Need for a Propulsion Systems Design Framework	8
II LITERATURE REVIEW	11
2.1 Cycle Analysis and Propulsion System Design Requirements	11
2.1.1 The Subsonic Airframe Integration Process	11
2.1.2 BLI as a Paradigm Shift	15
2.1.3 BLI Cycle Analysis Approaches	16
2.2 Boundary Layer Ingestion Models	17
2.3 Boundary Layer Ingestion Literature Review	17
2.3.1 Classic Studies	17
2.3.2 Recent System Studies	18
2.4 Modeling Requirements for BLI	23
2.5 Airframe Aerodynamics and Boundary Layer	24

2.5.1	Boundary Layer Characterization	25
2.5.2	Integral Properties	26
2.5.3	Observations	27
2.6	BLI Inlet Modeling	27
2.6.1	Pre-compression region	28
2.6.2	Inlet Sizing	28
2.6.3	Inlet Duct Recovery	30
2.7	Fan Modeling	30
2.7.1	Parallel Compressor Model	31
2.7.2	Higher Fidelity Models	32
2.7.3	Fan Distortion	32
2.7.4	Gap Analysis	35
2.8	Towards A Solution	35
2.8.1	Multi-Design Point Methodology Background	35
2.8.2	Short-Comings of the MDP Process for BLI	36
2.8.3	Research Objective	38
III	A GENERAL METHOD FOR BLI PROPULSION SYSTEM SIZ- ING (BLIPSS)	39
3.1	BLIPSS Methodology Overview	39
3.1.1	BLI Modeling Phase Overview	40
3.1.2	Architecture Integration Phase Overview	42
3.1.3	Vehicle Matching Phase Overview	42
3.2	Methodology Development: Research Questions and Hypotheses . .	43
3.2.1	BLI Modeling Phase	43
3.2.2	Architecture Integration Phase	81
3.2.3	Vehicle Matching Phase	93
IV	BLI MODELING PHASE	102
4.1	Baseline Design	103
4.1.1	Baseline Vehicle	103

4.2	Baseline Engine	104
4.3	BLI Modeling	104
4.3.1	Airframe Model	104
4.3.2	Power Balance and Drag Book-keeping	104
4.3.3	Inlet Model	104
4.3.4	Fan Model	104
4.4	Experiment 1 Results	104
4.4.1	Flight Condition Variation	104
4.4.2	BLI Design Space Variation	104
4.4.3	Off-Design Variation	104
4.5	Stall Margin Test Experimental Setup	104
4.5.1	Stall Margin Criteria and Allowables	104
4.6	Experiment 2 Results	104
4.7	Summary and Conclusions	104
V	ARCHITECTURE INTEGRATION PHASE	105
5.1	Implementation of Methodology on HWB Vehicle	105
5.2	Wake Correction Method	105
5.3	Experiment 3 Results	105
5.4	Experiment 4 Results	105
VI	VEHICLE MATCHING PHASE	106
6.1	Methodology Implementation	107
6.1.1	Algorithm Description	107
6.1.2	Solver Setup	107
6.1.3	Variable Area Nozzle Setup	107
6.2	Experimental Setup	107
6.2.1	Initial MDP Setup	107
6.2.2	Baseline Flight Envelope Requirements	107
6.2.3	Screening DoE Definition	107

6.2.4	Distortion Constraint Definition	107
6.3	Experiment 5 Results	107
6.3.1	Algorithm Validation	107
6.3.2	Screening Test Results	107
6.4	Impact of BLI Design Variables on Critical Flight Conditions	107
6.5	Impact of Cycle Design Variables on Critical Flight Conditions . . .	107
6.6	Impact of Requirements	107
6.7	Summary and Conclusions	107
VII	BLIPSS IMPLEMENTATION	108
7.1	Introduction	108
7.2	BLIPSS Process Description	108
7.3	BLI Modeling Phase	108
7.4	Architecture Integration Phase	108
7.5	Vehicle Matching Phase	108
7.6	Design Space Exploration	108
7.7	Results	108
VIII	SUMMARY AND CONCLUSIONS	109
	REFERENCES	110

LIST OF TABLES

1	NASA fuel burn targets for the next generation of aviation vehicles. [28]	2
2	Summary of the two prominent methods for boundary layer characterization and their pros and cons for system level conceptual design studies with BLI.	25
3	Fan efficiency assumption used for several system studies.	31
4	Table showing inlet shapes, $y(x)$, and r^*	65
5	Distortion Example Parameters	77
6	Design point mapping matrix for the 3 engine architecture highlighting the available design rules.	90
7	Table showing key design parameters for the baseline HWB vehicle. .	103

LIST OF FIGURES

1	Notional diagram of podded vs. BLI engine design	4
2	Notional inlet diagrams showing different conditions for which there are high inlet incidence angles [43]	14
3	Notional inlet incidence angle requirements vs. freestream Mach number [43]	14
4	Boundary layer ingestion system study estimates	22
5	Notional cycle analysis for a BLI propulsion system. Boxes outlined in red show the components which need modification for BLI.	24
6	Boundary layers profiles based on the Boeing HWB design and CFD analysis. Plot of height above the airframe vs. axial Mach number. [?]	26
7	Plot of Mach number, displacement, momentum, and kinetic energy defects vs. the axial length along the HWB centerline based on the Boeing CFD data.	27
8	Notional picture of the regions of the flow field before the fan face.	28
9	Mass averaged total pressure and temperature prior to the pre-compression region for the Boeing HWB design.	29
10	Illustration of the parallel compressor model on a notional fan map.	31
11	Typical circumferential distortion distribution for a single-per-rev type distortion profile at the i_{th} radial ring.	33
12	Simultaneous multi-design point cycle analysis equation setup [54]	36
13	MDP Methodology Data Flow Chart	37
14	BLIPSS Methodology Data Flow Chart	41
15	Diagram of the podded case illustrating the various components of the power balance equation.	47
16	Diagram of the BLI case illustrating the various components of the power balance equation.	49
17	Diagram of a class 1 geometry type with trailing edge boundary layer shown. The dissipation integral is performed along the z-direction.	56
18	Illustration of a class 1 geometry aerodynamic wake for the isolated airfoil and case with a BLI propulsor.	56

19	Illustration of the distribution of the kinetic energy defect over the length of a notional “class 1” aerodynamic body.	57
20	Illustration of the distribution of the kinetic energy defect over the length of a notional “class 1” aerodynamic body.	59
21	Illustration of the the wake defect for a class 2 body with BLI.	60
22	General cross-section diagram.	61
23	Influence of mass flow on the cross-section width solution.	63
24	Influence of inlet aspect ratio on inlet width sizing.	64
25	Influence of inlet aperture shape on inlet width sizing.	64
26	Plot showing trend of boundary layer thicknesses vs. airfoil angle of attack for a NACA 2012 airfoil at Mach = 0.7, Re = 10^6 as predicted by XFOIL	71
27	Standard ARP 1420 test rig showing static and total pressure probe locations	74
28	Illustration of a one-per-rev distortion type for a single probe ring. . .	75
29	Illustration of the definition of delta PRS with distortion	75
30	Illustration of the Notional Fan Face AIP	77
31	Example fan face ring total pressure distribution.	78
32	DC(θ) descriptor plotted vs. boundary layer thickness ratio.)	78
33	Examples of potential propulsion system architectures for an HWB aircraft.	81
34	Illustration of Sequential Single Point Design	83
35	Illustration of Multi-Design Point Process	84
36	Illustration of Multi-Engine Multi-Design Point Process	85
37	Illustration of 3-Engine Boeing N2A.	89
38	Plot showing size effects of a typical gas turbine axial compressor at very small exit corrected flow INSERT REFERENCE HERE.	92
39	Turbofan specific thrust vs. Mach number for different altitudes. . . .	95
40	Commercial turbofan variation in fan operating line with flight condition. Trends show that SLS hot day is critical and is worse at higher BPR.	98

41	Option 1 of 3 for determining the flight conditions where all off-design conditions are checked and iterated with the MDP sizing procedure. .	99
42	Option 2 of 3 for determining the flight conditions where all off-design conditions are included as constraint points within the MDP.	100
43	Option 3 of 3 for determining the flight conditions where a subset of critical conditions are identified using a screening design of experiments; all subsequent cases do not run off-design iteration checks. . .	101
44	HWB baseline key design dimensions.	104

SUMMARY

The current trend in industry standards for aviation technology is towards technologies with more fuel efficient and less noisy vehicles and power systems. One concept which has been used to much success in marine propulsion applications, and has been identified for future potential fuel burn savings for aviation is the "Boundary Layer Ingesting" (BLI) propulsion system. This technology has been investigated at the theoretical level for aviation applications over the years by a few authors and has been the subject of extensive research in recent years in academia, industry, and government, due to the increased synergy of the concept with new vehicle designs such as the hybrid wing body.

The benefit of the BLI propulsion configuration comes from the basic fact that ingesting a portion of the aircraft upper surface tends to re-energize the low velocity boundary layer flow and thereby increase the propulsive efficiency of the system. This, however, is counteracted by the fact that gas turbine component tend to operate with less efficiency and stability when subject to heavily distorted flow conditions. The design challenge for BLI, then, is to maximize the amount of boundary layer which can be ingested while minimizing the negative impact of BLI on the gas turbine operation. However, this task is made difficult due to the strong multi-disciplinary nature of the interactions between the engine and the airframe.

For the civil aviation engine designer, BLI poses a problem at the conceptual level because there are many new interaction effects where data must be filled into cycle analysis models, and such data may not be available in conceptual design. This leaves the cycle analyst with a difficult task to quantify these effects and understand

the impact of the uncertainty in the interactions on the choices made with regard to the engine cycle, the number of engines chosen, and other such conceptual level considerations. Methods used to date have employed simple approaches for cycle analyses whereby the boundary layer is characterized using data from a single CFD solution or from closed form boundary layer approximations. The losses are sometimes ignored, or are modeled parametrically with independent efficiency parameters in the cycle model. Furthermore, cycle analysis methods to date have typically only employed a single design point methodology, thus ignoring the impacts of BLI at important design points like take-off, top of climb, and sea-level-static conditions and also ignoring the fact that engines often operate at different inlet conditions during flight causing a disparity in engine thrust. Finally, conceptual level approaches typically ignore the impact of fan operability on the design trades made.

The present thesis presents a conceptual level method for cycle analysis which employs multiple design conditions and multiple inlet conditions in the propulsion system sizing process. The effects of BLI are modeled using a physics based approach, but are also modeled probabilistically so that uncertainty in the loss parameters can be mapped to the system level performance to determine the most important factors and design conditions for future development and experimentation. A method for sizing the propulsion system in the presence of uncertainty is proposed which can provide a means for designing for additional thrust given that loss parameters may be higher than initially estimated on the real vehicle. These methods will be tested on a hybrid wing body vehicle model with ultra hi-bypass geared turbofan engines ingesting a portion of the aircraft boundary layer. An investigation of the effects of operability constraints on the propulsion system design space will also be tested.

CHAPTER I

INTRODUCTION

1.1 Environmental Pressures and Aviation Technology

The current trend in industry standards for aviation technology is towards more fuel efficient and less noisy vehicles and power systems. Many entities including government agencies such as NASA and the FAA are interested in studying the effects of specific technologies to assess the potential return on investment to properly appropriate scarce government research dollars. In this context, many technologies require reasonable assessments of improvements at the conceptual level, when much design information is utterly lacking. In many cases, the technologies of interest are new materials, which may simply require refinement of the manufacturing processes required to achieve the necessary material strengths and thermal properties. Other types of technologies are related to the design of specific components which improve efficiencies or operability and durability throughout the component lifetime. Another class of technologies are those which alter the aerodynamics of the vehicle, such as winglets, ribs, or boundary layer laminar flow control. Such technologies are more dependent on the design of the vehicle and require proper design as well. The environmental and economic benefits of these technologies thus rely upon having reasonable design methods to assess their potential improvements. One such technology which falls into the latter class and is the subject of this thesis is boundary layer ingestion or "BLI". Rather than being a "technology", it is instead a novel arrangement of the propulsion system such that it interacts positively with the aircraft wake to produce

higher propulsive efficiencies. This is done by at least partially embedding the engine into the aircraft surface and ingesting the low-momentum boundary layer flow into the propulsor. Ingesting the boundary layer is beneficial because of the natural tendency for turbomachines, such as a fan, to do more work on sections of the flow with lower total inlet pressure [57]. BLI therefore has the effect of re-energizing the aircraft wake thereby reducing total drag relative to an aircraft with podded engines and improving the propulsive efficiency of the system. NASA has identified aggressive fuel burn targets for the next generation of aircraft and beyond as shown in figure 1. Boundary layer ingestion has been identified as a potential technology to help enable the achievement of these fuel burn targets.

Table 1: NASA fuel burn targets for the next generation of aviation vehicles. [28]

TECHNOLOGY BENEFITS*	TECHNOLOGY GENERATIONS (Technology Readiness Level = 4-6)		
	N+1 (2015)	N+2 (2020**)	N+3 (2025)
Noise (cum margin rel. to Stage 4)	-32 dB	-42 dB	-71 dB
LTO NOx Emissions (rel. to CAEP 6)	-60%	-75%	-80%
Cruise NOx Emissions (rel. to 2005 best in class)	-55%	-70%	-80%
Aircraft Fuel/Energy Consumption† (rel. to 2005 best in class)	-33%	-50%	-60%

* Projected benefits once technologies are matured and implemented by industry. Benefits vary by vehicle size and mission. N+1 and N+3 values are referenced to a 737-800 with CFM56-7B engines, N+2 values are referenced to a 777-200 with GE90 engines

** ERA's time-phased approach includes advancing "long-pole" technologies to TRL 6 by 2015

† CO₂ emission benefits dependent on life-cycle CO_{2e} per MJ for fuel and/or energy source used

1.2 Boundary Layer Ingestion

Boundary layer ingestion (BLI) has been known and practiced within maritime engineering for quite some time now. The main effect comes from the propulsive efficiency gains from ingesting the low-momentum flow into the propulsor and re-energizing the flow to a velocity much higher than it would be otherwise, thereby reducing the overall propulsive power required to overcome the dissipative forces acting on the

vehicle. In aviation, the gains from BLI are theoretically plausible and have been studied at some length but have yet to come to fruition in civil applications due to the additional difficulty of designing a proper aerodynamic intake which can deliver reasonable levels of distortion to the fan and compression system at transonic flight speeds and Reynold's numbers. However, the next generation of aircraft may have much better performance synergy with the integrated propulsive systems such that the costs of designing to negate the impacts on the engine operation of BLI are offset by the reduction in fuel consumption. One such futuristic aircraft which synergizes well with the BLI concept is the hybrid wing body. The synergy with BLI arises from the large space on the upper surface of the aircraft which is available for the placement of engines within the airframe. There are other aircraft configurations for which BLI could be a plausible option, including the "double bubble" aircraft [24], which is an aircraft resembling a conventional tube and wing aircraft but with a significantly flatter and wider body on the upper surface allowing for 2 or 3 embedded BLI engines. In fact, the configuration is such that almost the entire upper fuselage boundary layer can be ingested into the engine, which is a relatively large percentage of the total vehicle drag.

There are multiple engine architectures which are possible for a BLI system, especially for the HWB vehicle, including traditional turbofan direct-drive engines, geared turbofans, single-core/multi-fan type systems (e.g. tri-fan), and distributed propulsion. The single-core/multi-fan type systems have the benefit of being able to ingest much more boundary layer while avoiding the negative impacts on the gas turbine core. A distributed propulsion system is a system with many small propulsors "distributed" over the upper surface in an array type configuration. This type of system is synergistic with BLI because it allows a very large percentage of the aircraft boundary layer to be ingested. For each of these architectures, there are further options in terms of the inlet design used – high or low aspect ratio, embedded or flush mounted, long

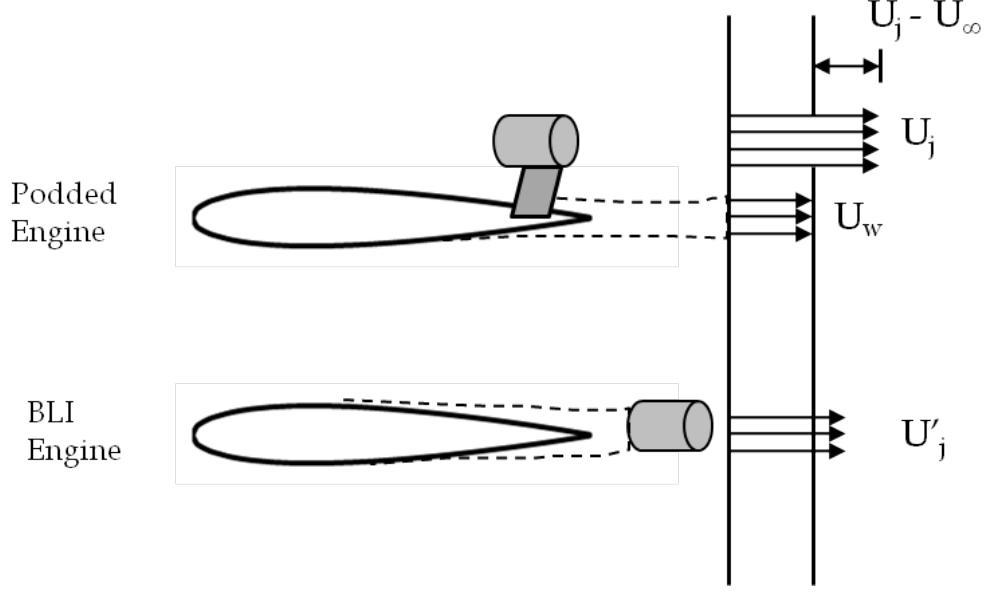


Figure 1: Notional diagram of podded vs. BLI engine design

or short, etc. Any design method for BLI systems must be able to include the physical performance differences between these engine configurations in order to properly trade between different system options in the early stages of design.

1.2.1 BLI Benefits

Figure 1 illustrates the basic difference between an ideal BLI engine and a podded engine [45]. Here U_∞ represents the free-stream velocity and U_w represents the averaged wake velocity in the podded case. From classical propulsion theory, the input power required is given by equation 1 for the podded case and by equation 3 for the BLI case, where U_j is the jet velocity exiting the nozzle and is assumed to be the free-stream velocity in the BLI case.

$$P_{Podded} = \frac{\dot{m}}{2} (U_j^2 - U_\infty^2) = \frac{F_{nPodded}}{2} (U_j + U_\infty) \quad (1)$$

$$F_{nPodded} = \dot{m} (U_j - U_\infty) \quad (2)$$

$$P_{BLI} = \frac{\dot{m}}{2} (U_j^2 - U_w^2) = \frac{F_{nBLI}}{2} (U_j + U_w) \quad (3)$$

$$F_{nBLI} = \dot{m} (U_j - U_w) \quad (4)$$

Since U_w is inherently less than the free-stream velocity, comparing equations 1 and 3 shows that the power required for the BLI case is less than for the podded case, assuming a constant jet velocity for both systems. The benefits of BLI can be described, then, as a reduction in the total power requirement of the vehicle due to an increase in propulsive efficiency. Additionally, the weight of the propulsion system is typically improved because of the elimination of the need for an engine pylon. There is also a nacelle wetted area reduction since the pylon and nacelle wetted area is less with the embedded or flush mounted engines having some of their surface area contained within the aircraft and not wetted by the air. Lowering the engine closer to the airframe also incidentally has the effect of improving the pitch control of the aircraft with the thrust vector momentum arm being smaller.

1.2.2 BLI Risks

Perhaps the most significant risk with regard to BLI is the performance of the inlet and fan system. The intake of an aircraft engine, while simple, is an absolutely essential component whose performance has a high impact on the specific fuel consumption of the engine. The intake must supply the necessary amount of air flow to the compression system to accommodate the required level of thrust without significant losses or flow distortion which can lead to performance degradation or compression stability concerns. Two risks arise from this problem: 1.) Engine performance degradation (related to inlet total pressure recovery and fan distortion); 2.) Compromised stability of the compression system due to the presence of both steady-state and dynamic inlet total pressure and swirl distortion. There is therefore a risk that the BLI induced gains in propulsive efficiency may be offset by the presence of a poorly performing inlet configuration and also a risk that the engine, while more efficient, may not be operable over the required flight envelope of a civil air transport. Nichols, in an evaluation of the Silent Aircraft Initiative, also identifies these risks as the primary

factors of uncertainty for the concept [41].

There are other ancillary risks such as the effect of the distortion on component degradation and lifetime. Such factors can significantly impact operability costs and potentially offset some of the fuel burn cost savings. There is also the additional difficulty of designing a system which has a highly integrated airframe and propulsion system. This concern is exacerbated by the fact that these components are produced by separate companies requiring the need for intercorporate cooperation to certify this new technology and provide for an economical design. There are also other detailed factors such as the control of a system which is specifically designed to have steady-state and transient turbulent distortion present during operation or vibration which might arise from the same phenomenon. Significant research funding has gone into investigating the possibility of designing a "distortion tolerant fan" which can operate under the types of distortion related to BLI with improved efficiency and stall margin [21]. However, this possibility remains uncertain as the research is still in progress.

1.3 Design Methods

Before talking about the methods of engine design with BLI, it is worth discussing some general design terminology and concepts. Broadly speaking, there are 3 primary phases of the design process: conceptual, preliminary, and detailed. The conceptual design phase is the very earliest phase in which system requirements, architecture, and basic performance characteristics are formulated. Preliminary design moves the system towards a more concrete physical definition by giving some of the components geometric definition, and initial conceptual performance estimates are modified in light of the new design information. Detail design is the next phase in which every single detail of the design is decided up to the point where manufacturing takes place. This last phase is the most involved, most expensive, and therefore the most costly should errors in the process necessitate design changes. Recent advances in design

over the course of the last few decades have transitioned towards including elements of the latter two design phases in the conceptual phase using higher-order physics based tools to estimate detailed design performance. This is happening because some of the newer technological concepts require detailed design understanding and quantification in order to determine the feasibility of the technology up front. BLI is certainly a great example of where this design paradigm is most appropriate, since the propulsion design essentially depends upon the characteristic of the engine intake and the thrust requirement coming from the vehicle aerodynamics and flight conditions, thus lending itself to higher fidelity multi-disciplinary methods.

Conceptual design is the most important phase in the design process, especially for complicated systems with many subsystems. Early design mistakes due to large uncertainty in performance or system feasibility can have large influence on costs later in the design phases, since all component designs depend on conceptual design choices. As such, changes in the conceptual design of the system can have critical consequences if made in the detail phase and are amplified as the product matures. This thesis is primarily focused on the conceptual design of boundary layer ingestion propulsion systems.

1.3.1 Conceptual Design Studies For BLI

There have been a number of conceptual design studies performed on BLI propulsion systems in recent years which will be discussed in more detail in Chapter 2. The most common employ the thermodynamic cycle analysis while also incorporating some method for quantifying the impact of BLI on the engine performance. Typically these are "0-D", axisymmetric analyses that aim to provide thermodynamic gas path properties, thrust, and fuel flow. These estimates are used for architectural trade studies to determine the number of engines, engine placement, engine cycle, and other BLI related parameters which have an impact on the efficiency of the system.

Typically higher order analyses are required for determining the detailed design of the inlet and external cowl shape, but such analyses require a cycle model to create powered boundary conditions for the analysis to begin with. Furthermore, the computational complexity of the higher order tools preclude their use in a parametric cycle design trade study, which requires potentially thousands of function calls to the aerodynamic tools. Building a fast, parametric, conceptual level cycle model also allows up-front sensitivity studies on the CFD analysis results. While this level of analysis is not going to yield the ultimate design or performance estimate due to the lack of fidelity of the aerodynamic tools, it is still desired that the overall system cycle and architecture design is chosen to maximize the performance of the system while maintaining compression system operability. Otherwise, preliminary and detail design choices made in later phases will be aimed at optimizing an already inferior system. Such considerations establish the basic need for properly understanding how to conduct a BLI propulsion system sizing and trade study in the conceptual design phase while maintaining a reasonable level of accuracy and remaining within the computational constraints that are typically present at this level.

1.4 Need for a Propulsion Systems Design Framework

A recent report by Boeing and NASA state that the BLI technology is currently "TRL 2" [7]. Technology readiness level, or TRL, is a qualitative measure of how ready or proven a given technology is for practical usage. The study states that the current state of the technology includes [7]:

- Concepts for reducing distortion have been studied.
- Some BLI configurations have been conceived.
- Some studies have shown benefits for BLI.

To mature the technology to TRL 3, the maturation plan for BLI is stated as:

- A conceptual BLI aircraft configuration will be developed as a focal point for more detailed development and as target for assessment of system-level benefits.
- A BLI engine installation will be designed and analyzed with goals of ingesting substantial boundary layer flow while keeping the boundary layer flow away from the engine core.
- Approaches for reducing distortion from ingested boundary layer flows will be analyzed.
- The BLI aircraft aerodynamic lines will be adjusted for the BLI engine installation.
- Aerodynamic analysis of the integrated BLI configuration will be performed for cruise and significant off-design conditions.
- BLI-compatible engines will be designed for best efficiency given the anticipated engine flows.
- A concept for BLI engine structural integration will be developed and analyzed.
- A system-level assessment of the benefits of BLI will be made from the results of the analysis studies.

The second bullet in the above list is the selection of a BLI installation for ingesting maximum boundary layer. The following bullets then discuss the potential tactics for battling the inlet distortion, improving aerodynamic efficiency, and finally designing an engine which maximizes efficiency given the aerodynamics of the configuration. The problem with this design process is that the initial analysis which determines the BLI engine installation will need to account for some of the information which is to

be defined in later steps. This provides the basic motivation for a conceptual, physics based, system level analysis tool which can account for changes in performance and distortion related operability problems related to design choices made at the system level. As such, the thesis that follows attempts to build upon prior knowledge to construct a methodology for conducting propulsion system sizing and performance analysis for BLI vehicles.

The thesis will be structured as follows:

- Chapter 2 will discuss the past literature and identify gaps in previously used methods to establish the need for the methodology developed.
- Chapter 3 will discuss the theoretical justification for the methodology and establish a set of research questions and hypotheses to be investigated.
- Chapters 4-6 will present the modeling and simulation approach, and discuss the results of the experiments to validate the hypotheses and the use of the methodology.
- Chapter 7 will demonstrate the full methodology as applied to an example problem by employing a design space exploration for the propulsion system.
- Chapter 8 will provide a summary, conclusion, and recommendations for future work.

CHAPTER II

LITERATURE REVIEW

2.1 Cycle Analysis and Propulsion System Design Requirements

As discussed previously, the typical tool set for the engine designer at the conceptual level is engine thermodynamic cycle analysis. The point of the cycle analysis at the conceptual level is to establish an engine aerothermodynamic cycle which can satisfy all of the requirements of the engine while minimizing operational costs such as fuel burn. In the early years of cycle analysis, cycle trade studies were the primary tools for conducting the parametric engine cycle design studies, while the advent of the modern computer and computer aided design has enabled the integration of other aspects of the design process such as engine flowpath, aircraft mission and cost analyses. Additionally, modern design techniques enable broad trade space exploration and optimization within the context of these computational models. Along the same lines, engine and airframe integration, especially in the military realm, has had a similar history with increasing tendency towards integrated design processes to facilitate increasing design knowledge early in the design phase to eliminate costly design changes in the later phases. This section will look at the latest cycle analysis techniques and the basics of sub-sonic inlet integration.

2.1.1 The Subsonic Airframe Integration Process

Since this thesis primarily will focus on BLI for reduction in civil aviation fuel burn, it is worth looking at the current inlet and engine integration processes and requirements which are typical and to also consider how the BLI concept might change this

paradigm. Firstly, civil transports of the kind to be considered for BLI will spend the vast majority of their time at the cruise condition. For that reason, cruise fuel burn is typically considered the metric of interest in most studies. However, of course it is worth mentioning that cruise does not take place at a fixed altitude, but rather a range of altitudes and Mach numbers during flight, with the vehicle lift, angle of attack, and pressure distribution changing as fuel is burned. Typically the engine is sized for some value of thrust at the top-of-climb condition where mass flow is a maximum. Additionally, there is typically some maximum specified turbine inlet temperature at take-off where the engine is running at its hottest, and the engine has to be able to supply the necessary thrust to achieve a particular take-off field length and climb rate. The point is that there are a large range of operating conditions from take-off through climb, cruise, and descent which the inlet must supply sufficiently clean air for the propulsion system to supply the necessary thrust power to fly the vehicle. At each of these flight conditions, there is a different interaction between the airframe boundary layer and the engine than at the cruise condition. This difference will have an impact on performance through the BLI effects discussed in previous sections, but also on the ability of the propulsion system to meet the requirements. Uncertainty in these interactions could lead to mistakes in design choices or fundamentally overestimated benefit of the technology, leading to a totally inferior aircraft relative to the state of the art podded engines. Such mistakes could have catastrophic consequences considering the modern economic climate.

Subsonic Flow Incidence Requirements

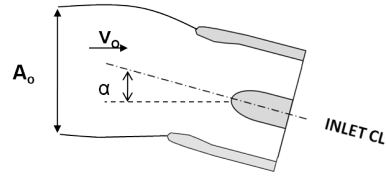
Although the inlet and airframe integration process is somewhat less tedious than for the military case, since civil transports clearly do not have as many critical maneuvers as military planes, the point still remains that there are multiple conditions in which the geometric orientation of the airframe causes potential problems for an engine

inlet. Perhaps most important among these are conditions such as take-off, climb, and landing where the vehicle and engine might be at an increased angle of incidence relative to the free-stream. The inlet mass flow ratio is the parameter that best describes the approaching flow and is given by equation 5.

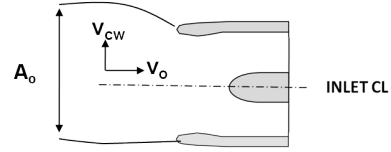
$$\frac{A_o}{A_i} = \frac{\left(\dot{m}_2\sqrt{\theta_2}/\delta_2\right)\left(\delta_2/\delta_o\right)}{\left(\dot{m}\sqrt{\theta}/\delta A\right)_o\left(A_i\right)} = \frac{\left(\dot{m}\sqrt{\theta}/\delta\right)_2\left(\pi_d\right)}{\left(\dot{m}\sqrt{\theta}/\delta A\right)_o\left(A_i\right)} \quad (5)$$

Oates states that: "For subsonic inlets, the numerical value of A_o/A_i is a direct indication of the general incidence of the flow approaching the inlet. A value of unity means that the inlet is capturing its projection in the freestream and the stagnation point will occur at the inlet highlight for level flight. A value less than unity indicates flow is prediffusing in the freestream, such that an outward flow incidence occurs; this is generally the case for cruise flight speeds. Conversely, A_o/A_i will exceed unity at low flight speeds and moderate to high power settings, such that an inward flow incidence develops with the stagnation point on the outer portion of the lip." Furthermore, other flight conditions in which flow incidence is induced produce a velocity component normal to the freestream on top of the basic mass flow effect. Figure ?? illustrates these issues [43] for different flight conditions. For each of these flight conditions, there is a danger that the flow could separate as it passes over the lower inlet lip, thus producing potentially unacceptable distortion levels. The engine must still be able to supply relatively low distortion flow to the inlet such that the engine maintains thrust and does not surge. Furthermore, this condition must be satisfied over a range of free-stream Mach numbers, since the aircraft is accelerating during climb and decelerating during landing. Typical engine incidence requirements are shown plotted vs. freestream Mach number in figure 3.

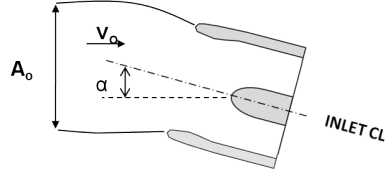
Finally, it is worth discussing the take-off with engine out condition. This is critical since the engine is operating at peak temperature during take-off meaning that a failure is likely to happen at that condition since the majority of the damage



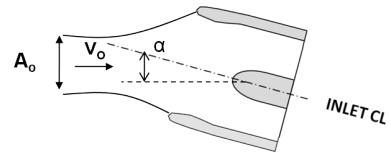
- Takeoff Rotation and Climb
- $A_o/A_i > 1, \alpha > 0$



- Crosswind Takeoff
- $A_o/A_i > 1, \alpha_{eff} > 0$



- Landing Approach
- $1 < A_o/A_i < (A_o/A_i)_{TO}, 0 < \alpha < \alpha_{TO}$



- Takeoff Climb with Failed Engine
- $A_o/A_i < 1, \alpha > 0$

35

Figure 2: Notional inlet diagrams showing different conditions for which there are high inlet incidence angles [43]

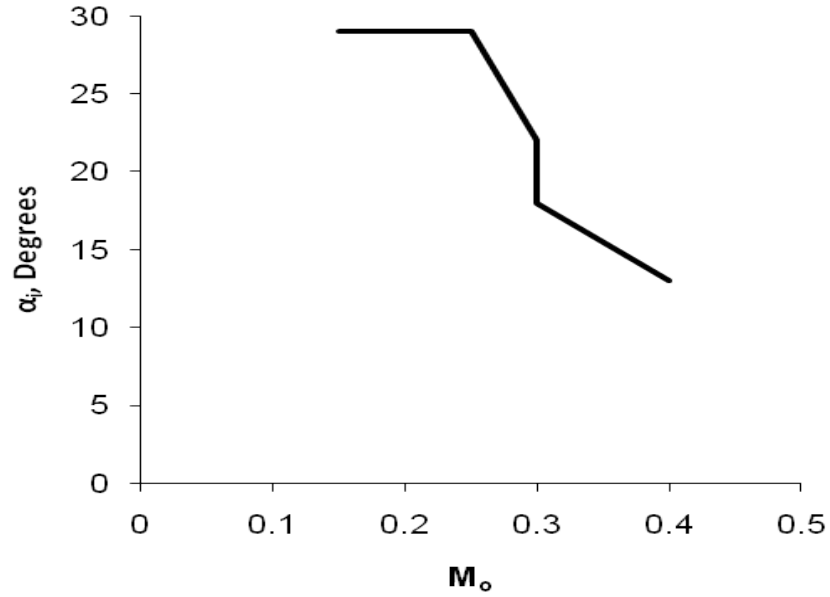


Figure 3: Notional inlet incidence angle requirements vs. freestream Mach number [43]

to the components occurs there. If an engine goes out, the ingested mass flow ratio is significantly less than unity since the engine is windmilling. At this condition, the external cowl can produce significant drag due to the flow accelerating rapidly over the cowl lip. The remaining operating engines must be able to overcome this drag on it's own with sufficient climb rate.

2.1.2 BLI as a Paradigm Shift

With the preceeding understanding of the limiting flight conditions for typical subsonic inlet integration, it is now necessary to consider how the above might change if there is some base level of distortion being ingested into the engine. Firstly, the fundamental difference between the embedded engine and the podded engine is that the danger due to separation is coming from the airframe itself rather than the inlet lip. This means that the level of distortion is inherently greater and the consequence of flow separation potentially greater as well. It is logical to speculate then, that the BLI engines will struggle to meet the vehicle incidence requirements. Indeed, the angle of attack envelope of the vehicle may need to be limited by the distortion limits of the engine as a function of Mach number. All of this has hitherto been unaddressed in the analysis literature, even with computational fluids tools, much less in the system study literature. Since these concerns may ultimately limit the possible engine configurations and also impact the cycle designs, there is a need to integrate these design conditions into conceptual design cycle analysis framework to at minimum understand their impact.

Another level of complexity generated by the boundary layer ingesting engine has to do with the placement of the engines on the airframe. First, the placement of each engine (or array of engines in the case of distributed propulsion) is now a design variable, although it is certainly subject to key constraints such as stability and control

and similar practical concerns. Furthermore, since preceding sections have substantiated that having smaller engines distributed across the airframe suction surface potentially offers higher BLI propulsive efficiency gains, there is a problem of having different airframe-engine interference for different sets of engines. For instance, if there are three engines such as in the work of Rodriguez [48], then the center-line engine may have quite different inlet flow properties – primarily boundary layer thickness – and subsequent performance impacts. As a corollary to this, Rodriguez showed that a proper inlet aerodynamic optimization might yield different inlet designs and slightly different inlet orientation for the inboard and outboard. This would then mean that the recoveries and distortion levels between the engines are different even though each engine is subject to the same operability constraints. To date, one system study has looked at the possibility of quantifying the impact of this [52] effect in terms of the BLI propulsive efficiency benefit. This study determined that if one does not consider the effect in the fuel burn calculations, then BLI benefit is rather significantly over predicted (which for BLI could mean 1 or 2%). Another computational fluids study [29] which showed this effect was done for the Boeing N2B design, in which the boundary layer thickness was found to differ by as much as a factor or two between inboard and outboard propulsors.

2.1.3 BLI Cycle Analysis Approaches

To date, the cycle analysis requirements specified in the BLI engine design literature have been of the traditional style. Typically a sizing point is set, such as top-of-climb, and the engine size is based on the required mass flow to achieve the engine thrust at that point. A few authors have additionally included analyses of the off-design points to check for sufficient sea-level static and take-off thrusts [31] [52]. Most of the higher fidelity studies do not touch the engine models, with perhaps the exception of Rodriguez who did vary the engine bypass ratio independently and used the cruise

point as the engine sizing point [48] [49].

2.2 Boundary Layer Ingestion Models

There are various approaches for modeling the effect of boundary layer ingestion on an aircraft. The primary differences between these methods is the fidelity of the models and the design capabilities that they allow. Some of the simpler models have basic, conceptual level parameters which define inputs to the model and with which the designer can understand the relevant trends. Higher order methods tend to be less parametric and require much more computational time, and for that reason are typically reserved for the later stages of design where detailed design features need to be set, and the uncertainty in the result must be inherently lower. Since this thesis work focuses on engine design at the very earliest conceptual stages in the context of BLI, the focus of this chapter is to outline some of the major approaches that have been taken to model BLI at the conceptual level. The purpose of this chapter is to outline the basic theory of each of these models, summarize the results from previous studies which employed them, and to assess the relative short-comings and benefits of each of them to provide a basis for later model selection and adaptation. Additionally, this chapter will substantiate the need for the current work by outlining the overall shortcomings of previous approaches to identify areas of improvement in both modeling and design methodology.

2.3 Boundary Layer Ingestion Literature Review

2.3.1 Classic Studies

Boundary layer ingestion really stems from considerable usage in marine propulsion where it is much easier to take advantage of the large ship wake that can be ingested by an aft mounted propeller. It has been researched somewhat in previous investigations for aircraft applications however. The first investigation of BLI was conducted by

A.M.O. Smith [56]. In 1946, Smith conducted an analysis of a turbojet engine and aircraft design with standard inlets and with BLI inlets. The BLI inlets were idealized as slots installed over the wing. Smith showed a 30% improvement in fuel efficiency and a 7% higher optimum cruise speed, though this is in comparison to designs of the time.

Lynch [39] performed a momentum analysis on an early turbofan engine design that ingested fuselage boundary layer and obtained a 3% improvement in propulsive efficiency accompanied by a 6-10% decrease in maximum engine thrust. Lynch's analysis also depended on the assumption of minimal inlet losses.

Douglass [13] performed an energy wake analysis on an aircraft with aft fuselage-mounted engines. The engines were assumed close enough to the fuselage to ingest the boundary layer. Douglass analysis suggests up to a 10% improvement in propulsive efficiency compared to an equivalent pylon mounted engine installation.

2.3.2 Recent System Studies

There has been a significant amount of research conducted on the BLI concept in essentially the last decade. This work has focused on many different vehicle concepts as well as many different aspects of the problem ranging from system level trade studies and technology risk assessment to high-order computational analyses and optimization of inlets and nacelles. There have also been some funded experimental studies, leaving at least a small amount of experimental data for certain designs – most commonly the inlet and fan. This thesis pertains to system studies at the conceptual level and so the following section will summarize in some detail the goals, general modeling approach, and conclusions of recent system level studies as well as show a comparison of the high level benefit for each of the identified studies.

Boeing Studies

Dagget et. al. conducted a study for the Boeing company under the Ultra Efficient Engine Technology/Propulsion Airframe Integration Project. The study was designed to analyze the effect of BLI on the BWB aircraft with active flow control (AFC). The engine analysis was done using the "ram drag" approach, meaning that the ram drag term contained within the net thrust is reduced by a percentage which is calculated based upon the boundary layer characteristic averaged over its height. The analysis included 3 tasks: first the establishment of a baseline; second, the evaluation of embedded engines with BLI; third, evaluation of active flow control (AFC) to inlets. A podded engine based off of typical engine technology was established as the baseline engine. For the BLI configuration, a long S-Duct, highly off-set embedded inlet was used to establish the fuel burn benefits from the ram drag reduction. It was determined that the baseline BLI configuration would offer 3.1% fuel burn improvement, which is relatively substantial. With the addition of the AFC technology, the inlet duct can be shortened which has weight, wetted area, and total engine length benefits. This also allows the use of high aspect ratio inlets which allows for larger ingested boundary layer. The fuel burn benefit with the AFC technology and the shorter low-offset inlets was estimated as 5.5%.

Another study conducted by the Boeing company focused on the inlet configuration and the potential benefits offered by increasing the aspect ratio of the inlet. The approach and general vehicle configuration was very similar to that studied in ref. XX. The study also refined the calculation for the nacelle viscous drag by "proper analyses of viscous changes where reductions in nacelle drag account for local Reynolds Number effects". This accounting difference led to a much greater estimate of the potential of BLI with AFC and flush mounted inlets which was estimated at 10% maximum. It was determined that the lower aspect ratio inlet (higher height than width) resulted in a better net fuel burn than the larger width inlets due to the fact

that the inlet pressure recovery was assumed to be 1% different. The result of this is therefore dependent on the validity of this assumption. If the lower and wider inlet (higher AR) can be kept at sufficiently similar levels of inlet recovery, it should offer larger benefit due to the increased amount of drag ingestion and improved ram drag effect.

Nickols

Nickols and McCullers conducted a configuration system study for the Hybrid Wing Body concept. This study was a relatively low fidelity study which did not truly employ engine design techniques or cycle analysis. Instead the study assumed a certain percentage drag reduction to be applied to the aircraft drag polar within the mission analysis, as well as a nacelle wetted area reduction factor, pylon weight structural factor, and SFC penalty due to the lower inlet pressure recovery. The final analysis showed an impact of 5.2% fuel burn benefit for the BLI technology.

Rodriguez

Rodriguez, as a part of his doctoral work, developed a method for multi-disciplinary inlet optimization which combined high fidelity CFD methods with a propulsion model. The method was applied to the BWB vehicle with 3 boundary layer ingesting high-bypass ratio engines. The method consisted of optimizing the inlet and external cowl shape such that the fuel burn rate is minimized while maintaining an acceptable level of inlet distortion. The method itself did show significant improvement from the baseline design, which highlights the importance of higher-order methods in the detail aerodynamic design phase. However, the work showed that the same optimization applied to the podded case yielded the result that BLI did not provide any benefit (BLI was actually worse, in fact). This could have resulted from the fact that there were a limited number of design variables for the outboard engines, yielding excess

and potentially removable wave drag from the outboard engines. Furthermore, the inlet pressure recovery was very low in comparison to recent studies which have shown potentially much higher values of inlet recovery using other optimization methods.

Plas

As part of NASA's silent aircraft initiative, Plas conducted a study of boundary layer ingesting engines in which the following 3 contributions were intended: Creation of a conceptual and theoretical framework for BLI in aircraft design; development of high fidelity models for representing an aircraft with BLI embedded engines; Quantification of the benefits of BLI. This work is the first of its kind that actually analyzes the impacts of BLI while including an actual model of the turbomachinery operating in non-uniform flow. The study assumed that the configuration of interest was a ducted fan type. The work included an assessment of three different degrees of fidelity within the fan modeling: a one-dimensional parallel compressor approach, an integral boundary layer approach, and a 3-D body force model. The highest fidelity of these approaches showed that BLI for the aircraft under consideration in the silent aircraft initiative gave power savings between 3-4%. The study also concluded that a principal feature required to estimate power saving for the propulsor is the distortion transfer across the fan (i.e. level of distortion downstream of the fan). It was also found that the power savings differed by 10-40% between the different fidelity fan models, although the trends remained roughly the same regardless of the modeling fidelity.

NASA and UTRC

Hardin et. al conducted an aircraft system study of a BLI propulsion configuration. The analysis included a detailed cycle model for an ultra-high-bypass propulsion system with BLI. The system study employed lower order models for the different components of the BLI problem, including the BLI theoretical benefits; nacelle weight

and drag; fan performance; and inlet pressure losses. Aircraft trade factors were used to estimate fuel burn based on the engine cycle calculations and weight estimates, and the results of the study showed that a 3-5% BLI fuel burn benefit could be achieved for the "N+2" generation aircraft relative to a pylon mounted baseline. Another key conclusion was that the inlet pressure recovery and fan efficiency have a strong impact on the level of fuel burn achieved with 1% pressure recovery loss translating to 3% fuel burn increase. This provides the motivation for low loss inlets and distortion tolerant fan configurations to maximize the potential benefit of the technology.

Summary

A few trends arise from an analysis of the system study literature:

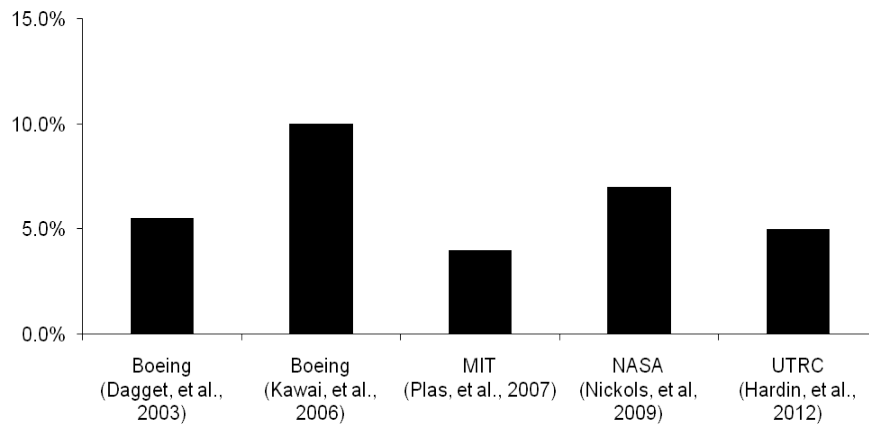


Figure 4: Boundary layer ingestion system study estimates

- The fuel burn analysis for BLI is a function of the trade-offs between propulsive efficiency gains obtained via drag ingestion, thermal efficiency penalty due to distorted inlet flow, propulsive efficiency changes due to changes in nacelle and interference drag, and the effect on the engine and support structure weight – all of which affect the aircraft fuel burn.
- There is a wide uncertainty on the potential benefit that BLI offers for the HWB aircraft, typically ranging from 0-10%. (See fig. 4)

- The quality of the inlet, level of inlet distortion, and impact on the fan efficiency have a strong impact on the potential benefits. This is shown by simple cycle analysis results, as well as by the study of Rodriguez, which predicted no benefit for BLI with very high loss inlets relative to studies with much improved assumptions.
- Configurations which can reasonably ingest more boundary layer across the upper surface of the aircraft stand to offer larger potential benefits.

2.4 Modeling Requirements for BLI

The boundary layer ingestion problem can be broken down into two areas with regard to performance: propulsive efficiency improvement (BLI effect) and thermal efficiency degradation. This is the basic trade-off upon which the economic viability of the system depends. This is an almost trivial statement, since of course the overall efficiency of the engine is ultimately a product of the thermal and propulsive efficiencies. However, the thing that makes the BLI problem interesting at the conceptual level is that the negative (thermal) efficiency impacts and the positive (propulsive) efficiency impacts are both functions of how much boundary layer (distorted flow) enters the engines. As more drag is ingested into the engine, the propulsive efficiency benefits increase, however the level of distortion and general total pressure recovery decreases which impacts the performance of the propulsor and potentially the gas turbine core. The design challenge then, stated clearly, is to maximize the amount of drag ingested while maintaining sufficiently low levels of distortion and total pressure loss such that the benefits of the propulsive efficiency gain are not prohibitive. To do this, the designer must have proper modeling fidelity for each of the components which are impacted by the ingestion. Design trades would then emerge from the combination of the various impacts on each component via typical cycle analysis techniques. Fig. 5 shows the components which require modification or addition for BLI. These are

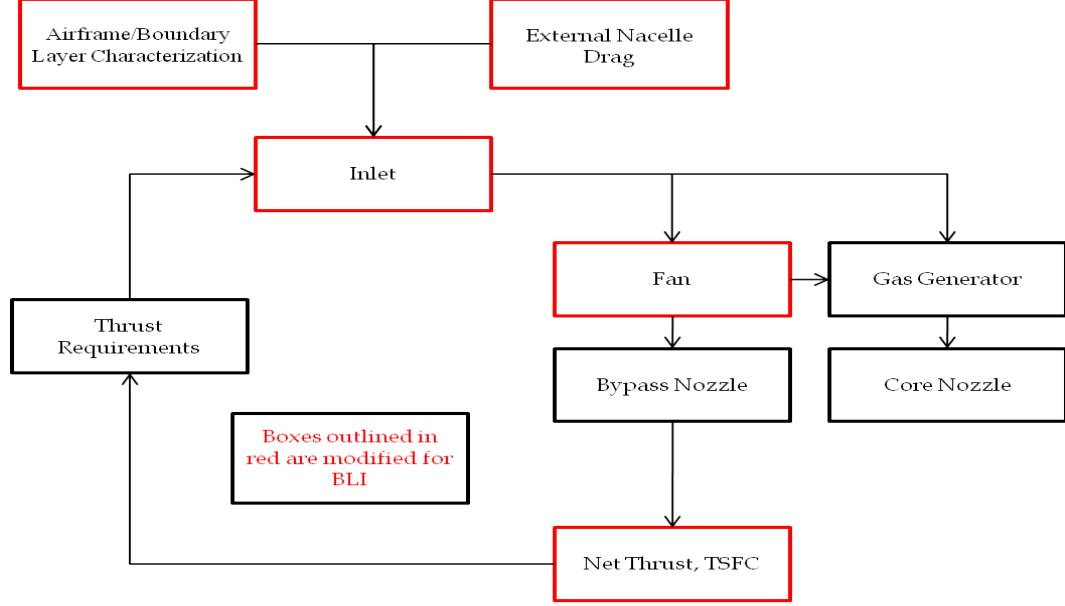


Figure 5: Notional cycle analysis for a BLI propulsion system. Boxes outlined in red show the components which need modification for BLI.

the most basic components that require modeling, however there can be other effects which impact system performance. These include but are not limited to: impact on bypass nozzle gross thrust coefficient; impact on propulsion system weight relative to equivalent podded case; compression system stability (fan or core stall). The rest of the chapter will focus on describing the state of the art system level approaches taken for each of the above components which require BLI impact modeling. Some space will also be taken to describe cycle analysis methodology.

2.5 Airframe Aerodynamics and Boundary Layer

The previous section discussed the power balance method and the metrics by which BLI performance can be estimated. These turned out to be a function of the characteristics of the aerodynamics of the vehicle and specifically the boundary layer properties such as the momentum and kinetic energy thicknesses as well as the shape factors. This section will discuss the methods by which system studies have estimated the inviscid airframe properties as well as the boundary layer properties needed for

the performance analysis.

2.5.1 Boundary Layer Characterization

There are a few general methods used to generate the airframe boundary layers. The two primary methods for conceptual level system studies are summarized in Table 2. Studies which use the first method include [52] [46], and studies which use the

Approach	Pros	Cons
1-D Boundary Layer Profiles	<ul style="list-style-type: none"> • Simple • Fast • Closed form solution • Scalable with Reynolds 	<ul style="list-style-type: none"> • Can't capture 2-D/airframe effects • No angle of attack variation
CFD Based Boundary Layer Profiles	<ul style="list-style-type: none"> • Captures Airframe Effects 	<ul style="list-style-type: none"> • Not scalable • Data only at points where CFD is run • Expensive/time consuming

Table 2: Summary of the two prominent methods for boundary layer characterization and their pros and cons for system level conceptual design studies with BLI.

second type of method include [31] [26] [27]. The majority of system level studies avoid using CFD in the multi-disciplinary analysis loop, but rather assume that the boundary layers do not change much from the cruise point and simply use those profiles as a starting point. From the first method, typical approaches are to assume a Coles wake profile or a $1/7^{th}$ power law profile which is typical of flat plate turbulent boundary layers. Figure 6 shows CFD data at the centerline of a Boeing HWB design [31]

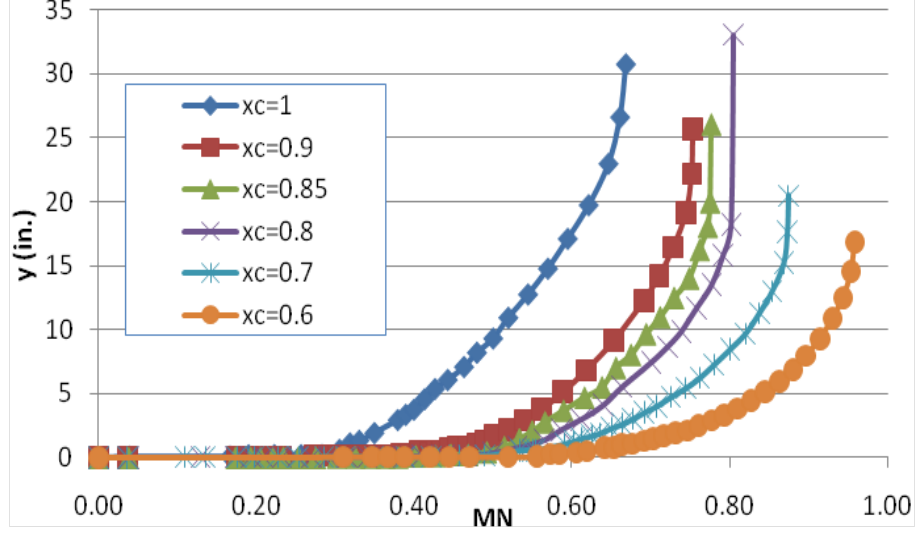


Figure 6: Boundary layers profiles based on the Boeing HWB design and CFD analysis. Plot of height above the airframe vs. axial Mach number. [?]

2.5.2 Integral Properties

Based on this data, the boundary layer integral properties can be calculated along the airframe and the inviscid Mach number at the edge of the boundary layer can also be computed. This data is shown in figure 7 vs. the axial position along the aircraft centerline and shows that the properties grow as essentially the Reynolds length is increased. The Mach number first increases along the suction side of the vehicle airfoil – typically to a value that is transonic – and then decreases on the aft end of the aircraft after about 60% of the chord line due to the presence of the adverse static pressure gradient. Analyzing figure 7 and the equations for the power balance of the aircraft, it is clear that the BLI benefit terms in the power balance equation, as well as in the propulsive efficiency equation are increased as the engine is moved farther aft, since the momentum and kinetic energy defects are increased as the length along the aircraft is increased. It is also worth noting that the engines placed outboard of this position may be subject to a different pressure gradient, Reynolds length, and fundamentally different intake aerodynamics than the center line engine and will thus have differences in the installation BLI impacts on engine performance. This has yet

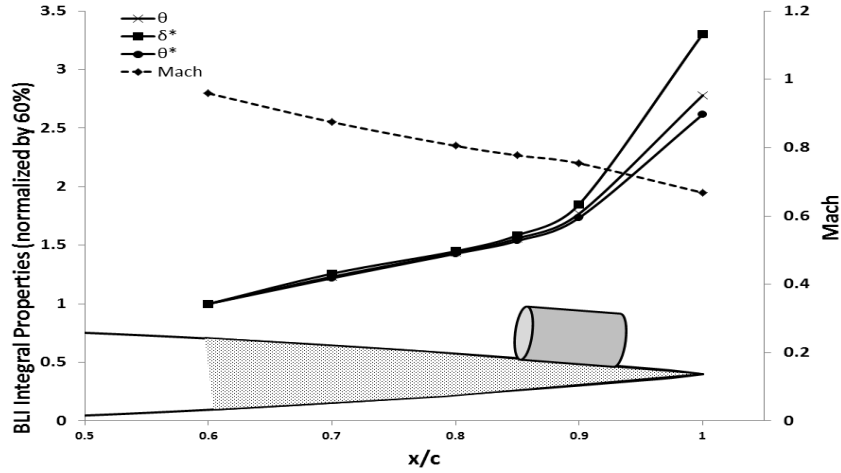


Figure 7: Plot of Mach number, displacement, momentum, and kinetic energy defects vs. the axial length along the HWB centerline based on the Boeing CFD data.

to be sufficiently addressed in the current literature. Another important point to be made is that for each flight condition, the angle of attack of the aircraft (typically set by lift and trim requirements) will have a strong impact on the flow entering the inlet. It is thus necessary to map these boundary layer profiles as a function of this variable as well, which is not typically done.

2.5.3 Observations

Observation 1: Existing system studies use either a simple 1-D boundary layer assumption or use tabular CFD data.

2.6 BLI Inlet Modeling

Figure 8 outlines the various regions of the flow field leading up to the fan face of the embedded engine. The pre-entry boundary layer region was described in the previous section along with the models that are typically employed for conceptual level studies. Additionally, there is the "pre-compression" region which is described by Plas in [45].

This is the region in which the streamtube is affected by the presence of the engine and the flow is compressed into the inlet capture area. Flow that is not ingested into the engine passes over the external cowl region which may typically induce some drag due to wall pressure or shock wave generation. Inside the inlet, the Mach number

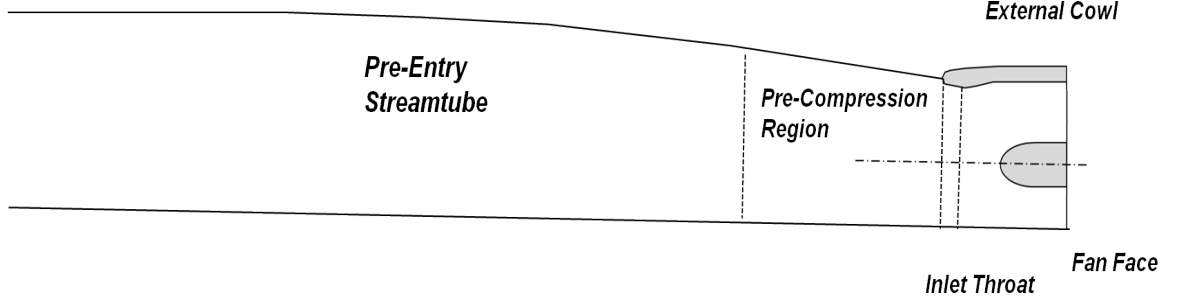


Figure 8: Notional picture of the regions of the flow field before the fan face.

decreases as the flow is diffused inside the inlet until it reaches the fan face. The fan face Mach number is typically a function of the fan design specific flow capability.

2.6.1 Pre-compression region

Most of the system studies ignore the effect of the pre-compression region. This includes [31] [26]. Plas [45] included a model of the pre-compression region using the integral boundary layer theory and modeling the static pressure distribution as an exponential and linear distribution within the region. This approach yields a physics-based method for determining the evolution of the boundary layer properties and thicknesses within the pre-compression region.

2.6.2 Inlet Sizing

With the presence of the boundary layer, the mass flow entering the inlet can be described in terms of the displacement thickness as follows:

$$\frac{\dot{m}}{\rho_e u_e} = (A - b\delta^*) \quad (6)$$

Here b is the width of the inlet assuming a constant width over the height of the boundary layer. If the displacement thickness is known along with the inlet capture area geometry, then the required capture height of the stream tube prior to pre-compression can be calculated to satisfy the mass flow demand of the engine. This was the approach used by Plas [45] to size the inlet capture area. Other authors including [?] have simply ignored the pre-compression region and used the boundary layer profiles from the CFD data for the purpose of direct integration to determine the necessary capture height.

With the capture height calculation, one can mass average the total pressures and temperatures from the wall to the capture height to determine an average recovery. Felder showed representative curves of mass-averaged total properties vs. capture height which are reproduced in figure 9. This data is again based upon the Boeing HWB design CFD analysis.

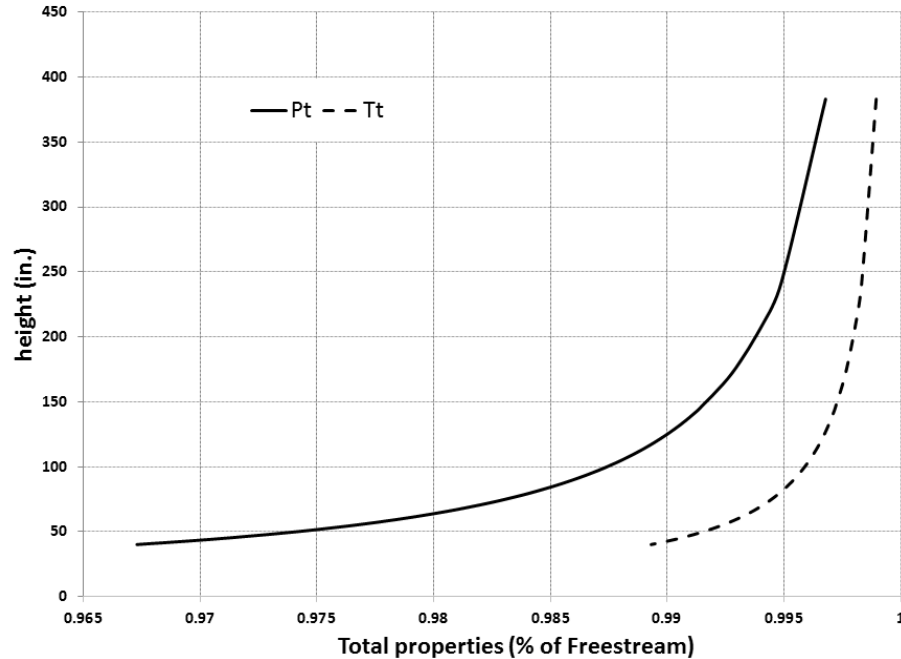


Figure 9: Mass averaged total pressure and temperature prior to the pre-compression region for the Boeing HWB design.

2.6.3 Inlet Duct Recovery

Finally, the last component of the aerodynamic analysis prior to the fan face is the performance of the inlet duct. The necessary output of this analysis depends upon the fidelity of the fan model used. If the fan model requires more detailed fan face profiles, then a higher fidelity analysis must be used. If the fan model requires only a characterization of the "dirty" or distorted region, then a simple 1-D type analysis might suffice, such as the integral boundary layer method [45]. By far the most common approach, however, is the use of a simple inlet recovery parameter or inlet efficiency as is used in standard cycle analysis techniques. This means that the BLI losses are essentially passed as a lower mass averaged pressure recovery to the standard fan analysis. This approach is used in [31] [52] [26] [42] with various values assumed for the pressure loss, which tends to have a significant impact on BLI performance.

2.7 Fan Modeling

At the conceptual, system study level, the fan modeling approach taken is typically a simple efficiency hit. This approach was used in [31] [52] [26] [42]. Although simple, it does provide a basic parametric way to understand the impact of the fan performance relative to the BLI propulsive efficiency benefits to understand technology targets for a BLI fan design. Table 3 shows the differences in assumptions used for the fan efficiency for some of the important system studies mentioned earlier. It is common to assume that the efficiency penalty will be small, however recent work conducted by Pratt and Whitney [21] shows that there is a likely efficiency penalty relative to a clean fan on the order of 0-1.5%.

As discussed previously, Plas [46] conducted a study on 3 different levels of modeling fidelity for a ducted fan. For brevity, the details of each model will not be discussed here, but rather some of the key conclusions from the study will be summarized and

Table 3: Fan efficiency assumption used for several system studies.

Reference	η duct
Dagget, 2003	0%
Kawai, 2006	0%
Nickols, 2009	0%
Felder, 2011	1%
Hardin, 2012	0-8%

some observations will be made that are relevant for the current work.

2.7.1 Parallel Compressor Model

The basics of the parallel compressor model is to model the fan component as separate compressors with different total pressure, axial velocity, and mass flow but with the same speed and characteristic line (PR vs. corrected mass flow). This model is useful because it creates a coupling between the nature of the distorted flow field (i.e. the magnitude of the P_t deficit), the fan design via the characteristic, and the final efficiency and pressure ratio. Figure 10 shows a simple illustration of the model on a fan map of PR vs. corrected mass flow.

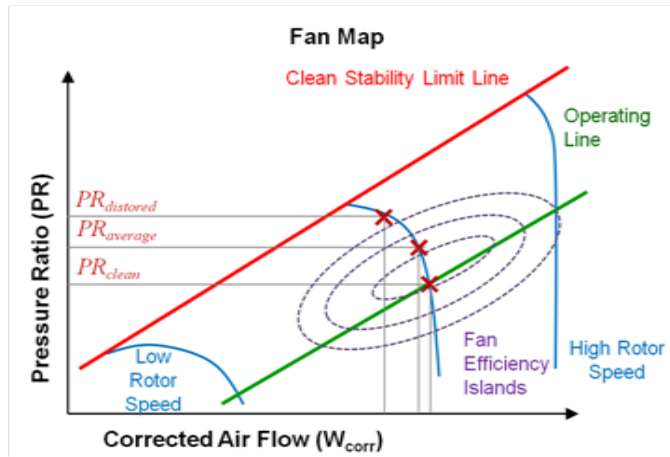


Figure 10: Illustration of the parallel compressor model on a notional fan map.

The parallel compressor model used by Plas is essentially the simplest possible

model because it employs a "2-segment" approach, with one dirty and one clean sector. It is possible to include more sectors should the flow coming into the fan be proven to be more complex [38]. The parallel compressor model has been successfully used for performance prediction in the gas turbine industry and can also be used for operability prediction in certain cases. Recent work has shown its effectiveness for different types of inlet distortion in comparison to experimental rig data [11].

2.7.2 Higher Fidelity Models

Plus additionally employed two other higher fidelity models: an integral boundary layer method and a 3-D body force model. Both models showed differences from the PC approach ranging from 10-40%, and more importantly, these approaches show the importance of the distortion attenuation and nozzle losses in determining the performance of the unducted propulsor. This study shows that the attenuation must be modeled in some way and viewed parametrically, and also that the fidelity of simpler models can have significant impact on the viability of a BLI system. The difficulty with the 3-D models is that it requires computationally expensive high-fidelity physics calculations, meaning that it is difficult to make the approach parametric for large design space explorations. Additionally, a designer would ideally like to have a map for off-design performance calculations, so for each design a separate 3-D map would need to be created. This makes the 3-D approaches somewhat less appealing in the context of conceptual design.

2.7.3 Fan Distortion

As shown by the parallel compressor model, the performance of the fan can be impacted by the presence of inlet distortion. However, perhaps more significantly is the impact on the fan stall margin. Figure 10 shows that the dirty sector of the distortion is closer to the stall margin because the PR is more and the mass flow

less in that region. SAE ARP1420 [10] provides parameters that can describe a total pressure distortion for an inlet aerodynamic interface plane (AIP). Figure 11 illustrates a circumferential variation in the total pressure at a particular radial location for a single-per-rev type distortion (one continuous dirty sector). The circumferential

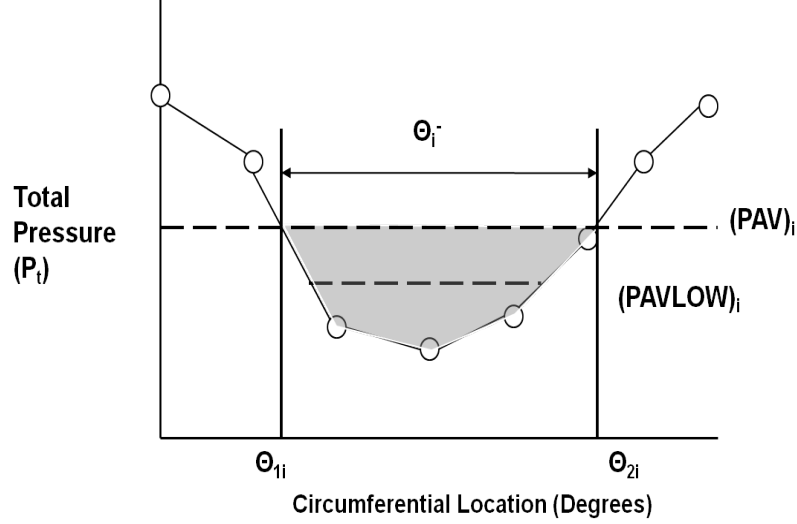


Figure 11: Typical circumferential distortion distribution for a single-per-rev type distortion profile at the i_{th} radial ring.

distortion prescribed by ARP1420 guidelines is given by equation 7, where the terms in the equations are defined by equations 68 and 69.

$$\left(\frac{\Delta PC}{P}\right)_i = \left(\frac{PAV - PAVLOW}{PAV}\right)_i \quad (7)$$

$$PAV_i = \frac{1}{360} \int_0^{360} P(\theta)_i d\theta \quad (8)$$

$$PAVLOW_i = \frac{1}{\theta_i} \int_{\theta_{1i}}^{\theta_{2i}} P(\theta)_i d\theta \quad (9)$$

Finally, the radial distortion prescribed by ARP1420 is shown in equation 73, where PFAV is given by equation 74 and is the averaged over the i radial rings.

$$\left(\frac{\Delta PR}{P}\right)_i = \frac{PFAV - PAV_i}{PFAV} \quad (10)$$

$$PFAV = \frac{1}{N} \sum_{i=1}^N PAV_i \quad (11)$$

Analyzing the above equations, one point seems salient, namely that the lower the average pressure, the higher the circumferential and radial distortion descriptors. This means that if the stall margin reduction is correlated with the descriptor, as is typically done, then lowering the heights of the inlet using smaller inlet heights and more engines should tend to move the fan closer to the stall line. Thus, there may be, depending on the fan characteristic and quality of the fan inlet flow, a point where smaller engines are simply limited by the operability constraint.

To date there have been no significant efforts to incorporate the operability concerns into the boundary layer ingestion modeling approaches at the conceptual level. Perhaps the closest attempt to do so was done by Rodriguez for the case of the 3 engine BWB configuration. His approach was to simply use distortion descriptors as a constraint on the inlet design, so that the optimization would maintain sufficiently low distortion while maximizing efficiency. This may, in fact, prove useful in the preliminary design phase of the inlet, but remains difficult at the conceptual level when the general propulsion system layout has yet to be determined and is perhaps even more difficult for engine designers who may need to make decision before such high fidelity modeling is available.

Observation 2: None of the system studies to date have considered operability within the context of engine sizing for boundary layer ingesting engines.

2.7.4 Gap Analysis

2.8 Towards A Solution

2.8.1 Multi-Design Point Methodology Background

The preceeding section established that although cruise is the primary condition where the performance of the engine is most consequential in terms of fuel burn, that there are several other "off-design" conditions where the engine thrust capability must be sufficient and might therefore be candidates for inclusion into the engine cycle selection process. The traditional engine design process has been performed at a single design point to set the cycle. Performance at other operating conditions is then evaluated in off-design analysis. Though this standard approach provides a good basis for understanding the trends of gas turbine performance, it does not provide a practical approach for a designer to match an engine and performance requirements for a particular airframe.

Schutte [54] designed and analyzed a methodology called simultaneous "multi-point design", in which modern computational tools are used in an engine sizing process which simultaneously satisfies engine requirements and constraints at multiple flight conditions. This is done by linking engine "On-Design" and "Off-Design" within a modified Newton-Raphson solver to satisfy the thrust constraints at all conditions. The process is necessary because it allows the formation of an engine cycle design space where each candidate cycle design is inherently feasible so long as the technology assumptions are physically achievable. This eliminates needless manual iteration between the single point engine "On-Design" solutions and other off-design solutions. The MDP concept is shown graphically in figure 12. The design points are linked via the simultaneous solution of a system of equations. The MDP process is broken down into 3 parts: the requirements and technology definition phase; the MDP setup phase; and the MDP execution phase. The data flow chart for this process is shown in figure

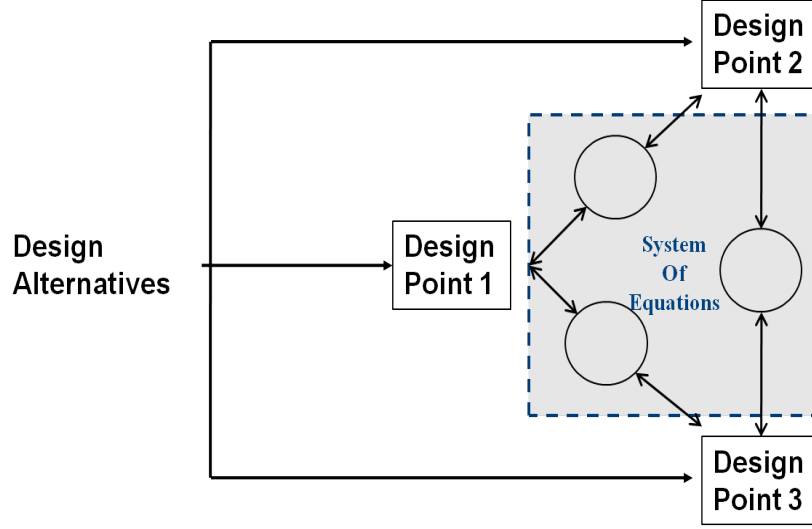


Figure 12: Simultaneous multi-design point cycle analysis equation setup [54]

13. The requirements and technology definition phase is general enough to handle any arbitrary operating (design) condition, which is one of the fundamental gaps in the current BLI literature. Furthermore, it is also able to impose certain flight conditions as a cycle "constraint" condition. If a condition is a critical distortion pinch point in the flight envelope, it could be used as a cycle constraint condition within an MDP analysis. Technology rules for how the distortion is handled or how much is allowable can then be specified to affect the operating point of the engine to move sufficiently away from the fan stall line. Impacts of the distortion related technology rules on the performance of the engine at the other sizing conditions would then be automatically known to the designer. For these reasons, the MDP design process will be the starting point for moving towards a new paradigm for BLI cycle analysis.

2.8.2 Short-Comings of the MDP Process for BLI

Though the MDP process is an appealing starting point for moving towards a proper BLI propulsion system sizing approach, there are a few areas where doing MDP alone is not sufficient for filling in the gaps described above.

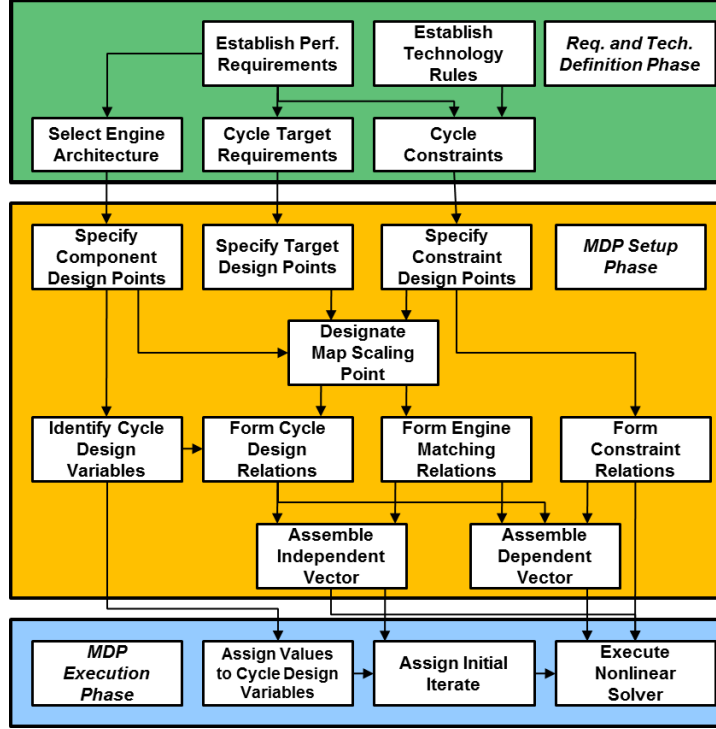


Figure 13: MDP Methodology Data Flow Chart

- MDP does not describe how the installation effects of BLI are to be modeled or mapped across the different flight conditions. It merely assumes that the designer has constructed a proper mapping of the installation effects a-priori. The same goes for the modeling of distortion and how that is achieved.
- MDP does not deal with the problem of distributed architectures, in which the inlet conditions are different across a propulsor array. Rather, it is designed specifically for typical gas turbine arrangement on current tube and wing aircraft.
- The designer using an MDP may not know the flight conditions which are most critical for new concepts such as BLI, where installation effects could have a significant impact on the location of the critical sizing and operability conditions in the flight envelope.

2.8.3 Research Objective

From the above considerations, a research objective has been formulated and is stated as follows:

Research Objective: Develop a methodology for conceptual system level sizing and analysis of BLI propulsion systems which can quantify BLI performance impacts over a range of system operating conditions, determine the impact of architecture and cycle choices on performance and operability, determine critical design conditions for the system, and allow for simultaneous satisfaction of system requirements and constraints at multiple design conditions.

CHAPTER III

A GENERAL METHOD FOR BLI PROPULSION SYSTEM SIZING (BLIPSS)

THE gap analysis of the BLI cycle design literature from the previous chapter highlighted some key areas within this domain that are in need of further investigation. The subject of this chapter is to outline and describe, in detail, an overall methodology for resolving these issues for establishing a proper design space for a boundary layer ingesting propulsion system. The chapter will first give an introduction to the method and will show the overall logic behind the development of the method, a brief introduction to the prior work from which it is derived, and a description of its parts and their intended function. The rest of the chapter will be devoted to identifying key research questions and hypotheses related to each part of the method which will be investigated in later chapters to further develop an understanding of how to use the method in the context of a BLI sizing problem.

3.1 BLIPSS Methodology Overview

The BLIPSS methodology is developed out of a need to fill in the gaps for a propulsion system sizing method described in chapter 2. For reasons stated there, the "Multi-Design Point" method is used as a starting point. There are three main areas which need to be added to the MDP method in order to achieve the stated research objective. First, the proper method for modeling boundary layer ingestion, including both benefits, losses, and operability needs to be included. This will be done in an additional phase added on to the MDP method called the BLI Modeling Phase. The second part of the method addresses the fact that different architectures may have

differing non-symmetric intake conditions at the entrance point of the engine. This leads to disparities in inlet recovery, fan losses, and the amount of boundary layer ingested and recovered by the system. This phase is called the vehicle matching phase, and attempts to modify MDP in order to allow for the use of different inlet conditions, and potentially different propulsor sizes to optimize the amount of BLI that is ingested. The third part of the method deals with the fact that the BLI critical flight conditions may not be known prior to the propulsion system analysis – meaning that they may, in fact, be system dependent variables and would change within the design space. This phase is intended to provide a framework for determining the flight conditions prior to running a design optimization or design of experiments, in order to reduce the run time of the BLIPSS method.

The data flow chart for the methodology is shown in figure 14. Again, this methodology is not intended to represent an entire propulsion system development framework, but rather it is a piece of the puzzle for highly integrated BLI systems which allows for propulsion system sizing of different architectures and the matching of that system to a specific airframe.

3.1.1 BLI Modeling Phase Overview

The BLI modeling phase is the phase of analysis in which the components of the engine cycle analysis which are impacted by BLI – in terms of both performance and operability – are modified to account for these affects. It is clear that this at least requires the definition of a baseline vehicle and engine for a point comparison. The baseline engine can either be defined in terms of an already design fixed engine or it could be a competitive architecture, such as a standard podded turbofan engine. The vehicle definition should be sufficient to define the boundary layer models required in this phase. This could be given in terms of boundary layer data at necessary flight conditions or vehicle geometry on which analysis is to be conducted in the BLI

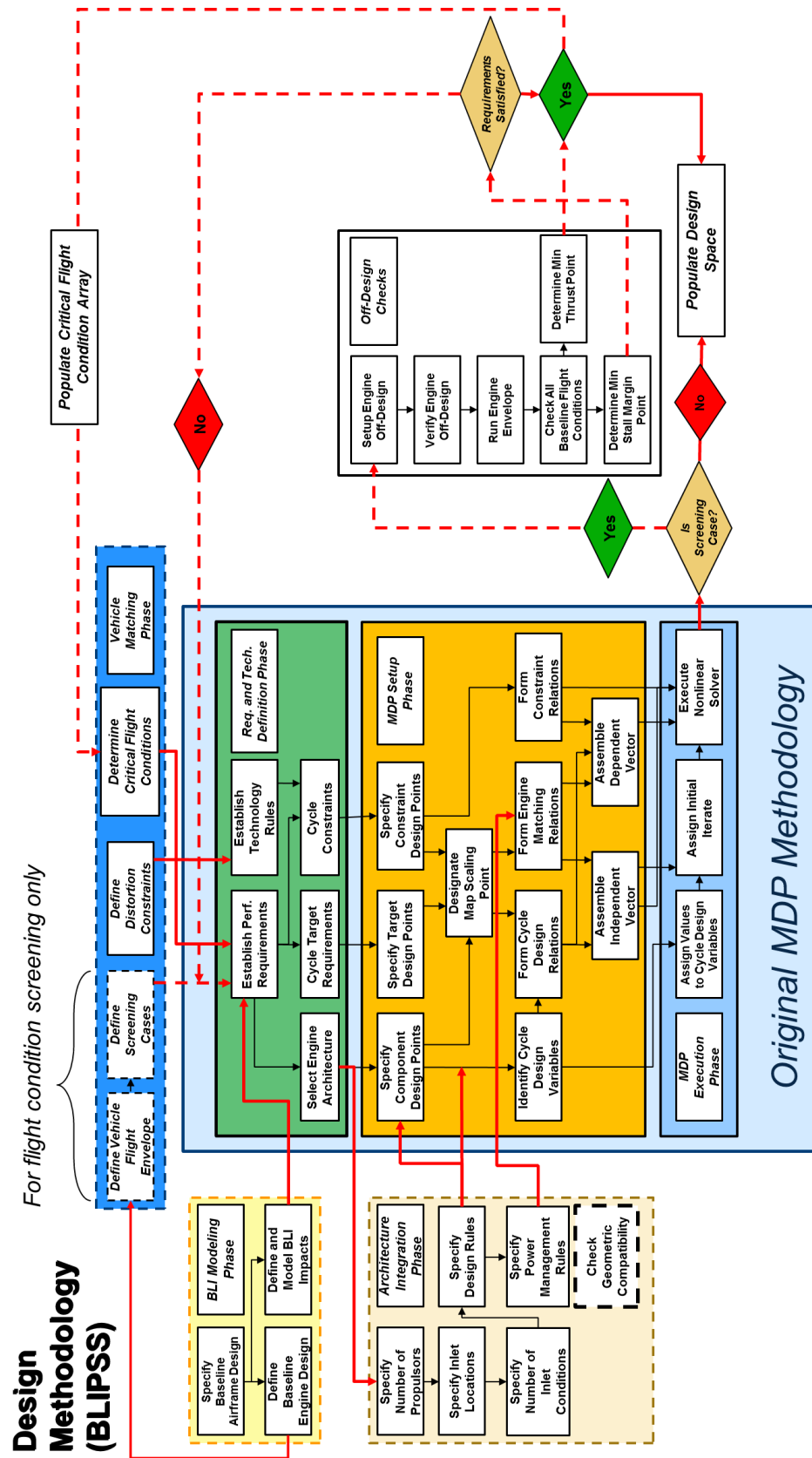


Figure 14: BLIPSS Methodology Data Flow Chart

modeling phase.

3.1.2 Architecture Integration Phase Overview

The architecture integration phase is the phase of the analysis in which the particular architecture which is chosen during the requirements and technology definition phase is defined in terms of the number of propulsors and their locations on the vehicle. The phase requires the specification of a number of propulsors and a location of each propulsor. From this, the number of unique inlet conditions and propulsors can be determined and a model for each unique propulsor can be defined within the MDP setup phase. The design strategy choices made during the architecture integration phase affects the number of turbo-machinery design points and the flight conditions which are chosen for them. The power management strategy are choices made by the designer to determine how different propulsors are power managed. These choices, as well as the architecture itself, determines the overall engine matching relation for the system, which will be different than for a traditional, single-inlet, MDP setup phase.

3.1.3 Vehicle Matching Phase Overview

The vehicle matching phase is the phase in which the critical flight conditions for which the system must be sized are determined for the BLIPSS process. A set of requirements for the distortion constraint must be specified in this phase, along with a series of flight conditions which are to be evaluated. In order to reduce the run-time of the design study, an initial screening exercise is conducted to determine which flight conditions are most critical. This is done for a sub-set of the overall design space, and the results are used to determine the most likely flight conditions which will dominate the sizing of the engine. The flight conditions which are determined to be critical are then included for all non-screening cases going forward within the DoE. This is done to both limit the amount of cases for which a full off-design check must

be done and also limiting the amount of flight conditions which are added to the MDP requirements definitions phase, since adding too many points can make convergence more difficult and also makes programming the MDP process much more difficult.

3.2 Methodology Development: Research Questions and Hypotheses

3.2.1 BLI Modeling Phase

The history of the analysis of boundary layer ingesting engines, much as the history of any analysis, is littered with varying levels of modeling fidelity and assumptions with often quite disparate results. The complicated nature of the question – viscous and turbulent airframe-propulsion interaction – often lends itself to convenient simplifications for the sake of expediency in order to draw some initial conclusion about potential net benefits and viable configurations. Once such decisions have been made, engineers are free to move on to the difficult work of determining the validity of the assumptions and analysis via higher order toolsets such as modern Navier-Stokes codes and the like. This is all very typical of a usual design process, in which conceptual design begins with some crude assumption and is refined by later analysis and optimization. However, the point of this thesis is to try to get closer to a feasible answer – at least for the basic propulsion system cycle design and sizing – before the aerodynamicists embark on refining the assumptions that went into making that decision. Furthermore, it is intended to guide the aerodynamicist and experimentalist in appropriately directing finite resources for their efforts in the most productive directions (correct flight conditions, configurations, initial geometry, etc), and providing sufficient data back to the propulsion engineer in an iterative process which eventually converges on a solution. It is with this basic project in mind that research question 1 is formulated and stated simply as follows:

Research Question 1: What are the minimum requirements for conceptual level modeling of a boundary layer ingesting cycle model in order to reasonably construct the architecture and cycle design space of a BLI propulsion system?

Note that the question asks for the "minimum" modeling requirements for conceptual design. In a sense, this is asking "what can we get away with" or "what is good enough" at the conceptual level, since obviously the best case scenario is to build a complicated fluid dynamics model, allow it to run on an infinitely powerful computer, and come back with a high-fidelity answer. Unfortunately, no such computer exists and even if it did, the designer would still have to know which design to model.

In attempting to answer this question, we first take on some components of the answer as being trivial and therefore not worth further investigation; one needs a reasonable engine cycle model to begin with, as well as thermodynamic component models for the constituent machinery and ducting; one also needs some approximation of the vehicle flow field at the points where it interacts with the engine and a total clean vehicle drag which translates to a thrust requirement. These are the first few blocks of the "BLI modeling phase" and it is somewhat obvious that they must be known to complete any analysis of the system.

The component of the question which is far more interesting, however, is in quantifying the interaction between the flow field and propulsion system and its impact on system performance. These interactions can broadly be classified into 3 regimes: power balance (or thrust balance), turbomachinery performance and efficiency, and engine stability. The first two have been looked at by almost every author on the subject, while the latter has been studied by some component designers, aerodynamic engineers, and a few others INSERT REFERENCE HERE. Stability, though it is certainly a dominant concern among technologists, planners INSERT REFERENCE HERE, and experimentalists INSERT REFERENCE HERE, has tended to take a

”back seat” at the cycle analysis level, in part because it is a difficult subject to analyze, but also because it is often assumed that modern aerodynamic methods will solve the problem after the fact INSERT REFERENCE HERE. For this reason, we will begin the analysis by ignoring the stall margin question and returning to it later to analyze this dubious partitioning of the problem.

THE BLIPPS methodology considers the possibility that flight conditions which may normally be analyzed in engine off-design mode might actually be a sizing point required for the MDP on-design analysis. Therefore, the analysis will also be separated into two different operational modes: engine on-design and off-design. On-design is the analysis which typically sets the size of the engine, while off-design is any operational condition which deviates from those conditions, including variations in flight Mach number, altitude, or throttle setting (”part power”). On-design analysis essentially sets the level of thrust production and efficiency that the system is capable of providing, while the off-design analysis determines the variation of those quantities over a range of operating conditions including system power setting (mass flow ratio). It is thus necessary to consider both modes of operation, but we will begin with the subject of engine on-design analysis.

On Design Analysis with BLI

In order to conduct engine sizing during on-design analysis, it is necessary to augment the basic thrust or power balance relations which match the vehicle requirement with the propulsion system. For example, the basic textbook thrust equation for a podded engine $F = \dot{m}(U_j - U_\infty)$ must be modified to include the effect of BLI on the system. The following analysis establishes the basic power balance relations for boundary layer ingesting according to the most current literature, predominantly produced by MIT in theoretical form [15].

We begin with defining the basic power balance equation for any vehicle in an

aerodynamic flow which follows from the analysis of Drela:

$$P_s + P_v + P_k = W\dot{h} + \dot{E} + \Phi \quad (12)$$

Here, the term P_s represents the net propulsor shaft power or wing flapping power input to the control volume. Since here we are only considering the case where the turbomachinery are outside of the CV, the P_s is considered to be 0, and the effect of the work done by the turbomachinery is included in the net flow of propulsor mechanical energy into the CV represented by P_k . The P_v term represents the net pressure-volume power provided by the fluid expanding to atmospheric pressure and can be non-zero in this case, depending on the character of the nozzles.

The terms on the right hand-side of the equation represent the potential energy change due to climbing ($W\dot{h}$), the total flow-rate of mechanical energy out of the control volume (\dot{E}), and the total rate at which kinetic energy is converted into heat inside of the CV (Φ). The \dot{E} term can be decomposed into various components, but the primary term to consider for subsonic transports of the type considered here is the rate of wake transverse kinetic energy deposition \dot{E}_v . For the case of a relatively close trefftz-plane, where trailing vortices have not dissipated, this term is essentially the equivalent of V_∞ times the induced drag D_i INSERT REFERENCE HERE (Drela).

The dissipation rate Φ can be broken down into three components: surface and wake dissipation due to the presence of the boundary layer, and dissipation in the jet stream aft of the propulsors. Re-writing Eq. 12 according to this decomposition and the assumptions described above, we have the following:

$$P_k + P_v = W\dot{h} + \dot{E}_v + \Phi_{surf} + \Phi_{wake} + \Phi_{jet} \quad (13)$$

This equation describes the basic power balance relation for the case of an aircraft with a propulsor whose internal volume is not considered part of the control volume analysis and for the case of a subsonic transport aircraft. It is valid for both isolated propulsors and the BLI case. The following sections will describe both of these cases,

their differences, and identify key observations from the analysis that are relevant to the research question.

Podded Case

The basic configuration for the podded case – shown in figure 15 – illustrates the fact that the propulsor is (at least to first order) separated from the airframe. Equation 13 can therefore be simplified into terms that are more familiar to an aerodynamicist using standard momentum-based techniques. First, the drag of the aircraft is

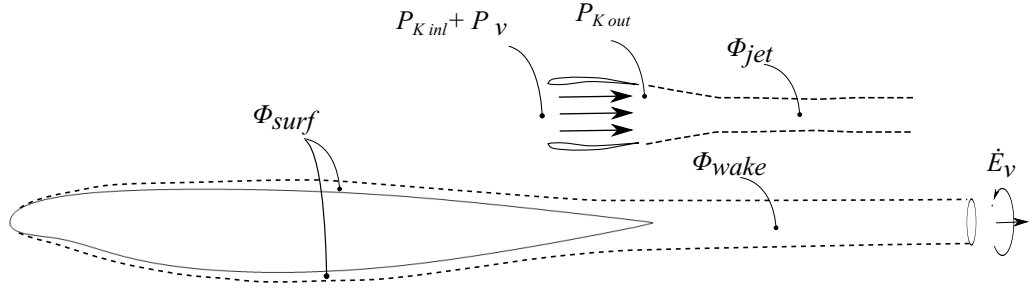


Figure 15: Diagram of the podded case illustrating the various components of the power balance equation.

normally divided broadly into profile drag (due to friction) and "lift-dependent drag" (due to trailing vortices). The first is manifested in the dissipation terms (Φ_{surf} and Φ_{wake}) and is the sum of the surface and wake dissipation, and the second is represented by \dot{E}_v . These power based terms can be translated into an equivalent drag by dividing them by the free-stream velocity V_∞ . The left-hand side of the equation has to do with the engine kinetic energy flux into and out of the control volume and the volumetric mechanical power integral P_v . Writing the equation for

P_k :

$$P_k = \oint -[(p - p_\infty) + \frac{1}{2}\rho(V^2 - V_\infty^2)]V \cdot \hat{n}dA \quad (14)$$

Taking this equation and separating out the integral into that over the inlet and exit as shown in figure 15 and also assuming that the nozzle is not significantly over or under expanded ($p \simeq p_\infty$) gives:

$$P_{k_{out}} = \oint -[\frac{1}{2}\rho(V_j^2 - V_\infty^2)]V \cdot \hat{n}dA_{nozzle} \quad (15)$$

simplifying, we get:

$$P_{k_{out}} = \frac{1}{2}F_n(V_j + V_\infty) \quad (16)$$

Where the net thrust, F_n is as normally defined from the simple jet equation. From the same assumptions as above,

$$P_{k_{inl}} + P_v = 0 \quad (17)$$

Now, the dissipation in the jet stream Φ_{jet} is essentially the wasted kinetic energy of the stream which is eventually converted back into heat after it has been dissipated in the jet. This can be calculated as follows:

$$\begin{aligned} \Phi_{jet} &= \iint \frac{1}{2}(V_\infty - V_j)^2 \rho V_j dA_{nozzle} \\ &= -\frac{1}{2}F_n(V_\infty - V_j) \end{aligned} \quad (18)$$

From 16 and 18, we get:

$$P_{k_{out}} - \Phi_{jet} = V_\infty F_n \quad (19)$$

So, the power contribution of the propulsor is essentially the net kinetic energy flux that the propulsor provides to the total aircraft control volume minus the rate at which energy is dissipated in the jet stream wake. Now that all of the terms of the power balance equation have been defined, we can re-write the equation to be in terms more familiar to the aerodynamicist:

$$\begin{aligned} V_\infty F_n &= W\dot{h} + V_\infty D_i + V_\infty D_p \\ &= W\dot{h} + V_\infty D \end{aligned} \quad (20)$$

Other terms, such as an acceleration term or friction forces during ground roll could be added, but this is sufficient for steady-state flight with a constant climb or descent rate.

BLI Case

The BLI case, illustrated in figure 16, is clearly different in two ways: first, there is an inlet defect due to the presence of the boundary layer, such that P_{kinl} is non-zero; second, there is a component of the wake dissipation which is not present since it is ingested into the propulsor and replaced by the jet stream. The following analysis will develop a mathematical comparison between this case and the original podded case.

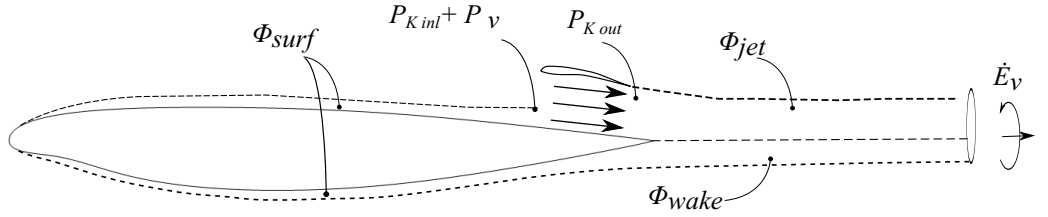


Figure 16: Diagram of the BLI case illustrating the various components of the power balance equation.

First, it is necessary to define a relationship between the podded (clean vehicle) case and the BLI case. This is done by defining a parameter β , which represents the ratio of the wake dissipation in the BLI case to the podded case:

$$\Phi_{wake_{BLI}} = (1 - \beta)\Phi_{wake} = (1 - \beta)(\Phi_{\infty} - \Phi_{TE}) \quad (21)$$

The inlet defect P_{kinl} is equivalent to the surface dissipation ingested into the propulsor at the inlet location of the propulsor:

$$P_{kinl} = \Phi_{Inl} = \gamma\Phi_{surf} = \gamma\Phi_{TE} \quad (22)$$

The parameter γ is defined in Eq. 22 as the ratio of the surface defect at the point of ingestion as normalized by the defect in the podded case at the trailing edge.

In general the surface dissipation is not changed much by the presence of the propulsor, except for the fact that the wetted area of the fuselage upper surface is decreased. Given the parameters defined above, the following derivation for the surface dissipation in the BLI case is made:

$$\Phi_{surf,BLI} = \Phi_{surf} - \beta\Phi_{surf} + \gamma\Phi_{surf} \quad (23)$$

The assumption being made here is that the proportion of the wake kinetic energy which is recovered is the same as the proportion of the trailing edge dissipation in the BLI case to the total TE (surface) dissipation in the podded case. Equation 23 then states that the total surface dissipation in the case of BLI is the podded value, minus the trailing edge ingested value, plus the value of the dissipation at the inlet. Therefore, the term $(\beta - \gamma)$ represents the percent change in the surface dissipation integral.

$$\Phi_{surf,BLI} = (1 - \beta + \gamma)\Phi_{surf} \quad (24)$$

In the case where the propulsor is assumed mounted on the trailing edge of the vehicle, γ and β are equal and the surface dissipation between the two cases is assumed identical unless the propulsor affects the upstream dissipation in the pre-entry region. Moving the propulsor far forward would tend γ and $P_{k,inl}$ towards zero and would also have an impact on the actual value of β , as it would be unclear how the jet stream would interact with the surface aerodynamics. In any case, this would be undesirable and so the case is not considered.

Finally, we define a similar ratio between the induced drag in the BLI case and the podded case:

$$\dot{E}_{v,BLI} = \zeta\dot{E}_v \quad (25)$$

The above definitions can be used in conjunction with Eq. 12 to write the final power balance equation for the BLI case:

$$(P_{kout} - \Phi_{jet}) + \gamma\Phi_{surf} = (1 - \beta + \gamma)\Phi_{surf} + (1 - \beta)\Phi_{wake} + \zeta\dot{E}_v + W\dot{h} \quad (26)$$

Rearranging and simplifying:

$$(P_{k_{out}} - \Phi_{jet}) + \beta(\Phi_{surf} + \Phi_{wake}) = \Phi_{surf} + \Phi_{wake} + \zeta \dot{E}_v + W \dot{h} \quad (27)$$

Using the results from the podded analysis, we get:

$$\underbrace{V_{\infty} F_n + \beta \Phi - \zeta \dot{E}_v}_{\text{Total Net Thrust}} = \underbrace{V_{\infty} D + W \dot{h}}_{\text{Podded Vehicle Drag}} \quad (28)$$

Here, the term β represents all changes to the viscous wake profile in relation to the podded case for an aft-mounted propulsor. This includes the recovery of the wake dissipation, which is now replaced with the jet stream, and another term that essentially represents a reduction in the flux of kinetic energy into the propulsor control volume (ram drag reduction). This equation is generally simplified, at this level of analysis, by assuming that ζ is also zero and therefore the vortex drag is not altered in the case of BLI. We will see in later sections that this is most likely an inappropriate assumption for very high or low engine power levels, where the surface static pressure distribution is modified significantly by the pre-entry flow. This creates an awkward scenario where the actual drag polar, lift, and pitching moment of the vehicle would be throttle dependent, totally throwing asunder all notions of the book-keeping separability of thrust and drag. At the level of conceptual design and cycle analysis, it is essentially necessary to ignore the effect of the engine on the lift distribution since to model this would be cumbersome and is unlikely to have much effect on the sizing of the engine, which is typically done at normal power levels where pre-entry flow pressure gradients are small.

Performance Parameters

It is now useful to define some performance parameters based on this analysis to determine how this might affect the system in relation to the podded case. The thrust saving coefficient is defined as the proportion of the total net thrust of the

propulsor which is related to the BLI wake-recovery effect.

$$TSC = \frac{\beta \cdot \Phi}{\left(V_\infty F_n + \beta \Phi - \zeta \dot{E}_v\right)} = \frac{\beta \cdot \Phi}{\left(V_\infty D + W \dot{h}\right)} \quad (29)$$

Where again, F_n is defined as above. At times, others define the slightly less useful parameter (%BLI) is used and defined as the ratio of the wake recovery term to the total drag (ratio of ingested drag to uningested drag). Assuming that ζ is zero and that there is no excess power required for climb or acceleration, the thrust saving coefficient and %BLI are the same for the vehicle as a whole.

The "BLI" efficiency was defined by Sato INSERT REFERENCE HERE and includes the contribution from both the wake recovery and the propulsive efficiency increase of the engine due to the kinetic energy defect at its inlet.

$$\eta_{BLI} = \frac{\left(T \cdot V_\infty\right)_{Podded}}{\left(\Delta KE\right)_{BLI}} = C_{BLI} \cdot \eta_{pr_{BLI}} \quad (30)$$

With C_{BLI} defined as the ratio of the dissipation and vortex loss terms (rhs of power balance):

$$C_{BLI} = \frac{\dot{E}_v + \Phi}{\dot{E}_v + (1 - \beta)\Phi + \gamma\Phi_{surf}} \quad (31)$$

C_{BLI} is generally greater than unity for non-zero BLI so that it has the effect of increasing the overall value of η_{BLI} . Higher values of β obviously tend to give more benefit.

The propulsive efficiency for a BLI propulsor is calculated according to its definition:

$$\eta_{pr} = \frac{P_k - \Phi_{jet}}{P_k} = \frac{P_{k,out} - \Phi_{jet} + P_{k,inl}}{P_{k,out} + P_{k,inl}} \quad (32)$$

This can be rewritten by using Eq. 22 to compute the inlet defect.

$$\eta_{pr} = \frac{P_{k,out} - \Phi_{jet} + \gamma\Phi_{surf}}{P_{k,out} + \gamma\Phi_{surf}} \quad (33)$$

In the case of no BLI (no $P_{k,inl}$), then Eq. 33 simplifies to the normal Froude propulsive efficiency equation. With ($\gamma > 0$), $\eta_{pr,BLI} > \eta_{pr,Podded}$, meaning there is

a propulsive efficiency benefit for ingesting BLI, along with the general reduction in the amount of power required to propel the aircraft (represented by C_{BLI}).

The overall efficiency of the podded (non-BLI) propulsion system is defined as follows:

$$\eta_o = \frac{F_n \cdot V_\infty}{\dot{m}_f \cdot h_{LHV}} = \frac{V_\infty}{TSFC \cdot h_{lhv}} \quad (34)$$

For the BLI case,

$$\eta_o = \underbrace{\left[\frac{(F_n \cdot V_\infty)_{Podded}}{(F_n \cdot V_\infty)_{BLI}} \right]}_{C_{BLI}} \underbrace{\left[\frac{(F_n \cdot V_\infty)_{BLI}}{(\Delta KE)_{BLI}} \right]}_{Prop.Efficiency} \underbrace{\left[\frac{(\Delta KE)_{BLI}}{(\dot{m}_f \cdot h_{lhv})} \right]}_{Thermal.Efficiency} \quad (35)$$

Therefore, the benefit is seen to be a function of two phenomena: 1.) the reduction in the wake dissipation which is no longer present; 2.) An increase in the propulsive efficiency because of the non-zero kinetic energy defect entering the propulsor (ram drag reduction). Both of these are also found to be strong functions of the amount of BLI ingested, with the final power balance being mainly a function of β . This standard observation from the BLI literature is therefore formulated as follows:

Observation 1: The performance benefit of boundary layer ingestion systems is generally a function of the ratio of the amount of equivalent viscous drag ingested by the propulsor to the total drag in the podded case.

Finally, the use of the thrust saving coefficient can combine the above effects into the thrust specific fuel consumption variable:

$$TSFC = \frac{\dot{m}_f \cdot (1 - TSC)}{F_n} \quad (36)$$

Changes in propulsive efficiency are then wrapped up into the calculation of the thrust saving coefficient and any changes in thermal efficiency would arise from the calculation of the fuel flow \dot{m}_f from the thermodynamic cycle model. For this reason, the modified TSFC metric described in Eq. 36 will be used to describe the benefit of the system going forward.

Calculation of BLI Benefit

Now that the basic power balance equations for a vehicle with BLI have been established as well as the important parameters contributing to the overall benefit of the system, it is now necessary to define how these quantities can, in theory, be computed. First, some useful boundary layer quantities are defined INSERT REFERENCE SATO:

Mass Defect:

$$\mathbf{M} \equiv \rho_e u_e \delta^* = \int_0^\delta (\rho_e u_e - \rho u) dy \quad (37)$$

Momentum Defect:

$$\mathbf{P} \equiv \rho_e u_e^2 \theta = \int_0^\delta (u_e - u) \rho u dy \quad (38)$$

Kinetic Energy Defect:

$$\mathbf{K} \equiv \frac{1}{2} \rho_e u_e^3 \theta^* = \frac{1}{2} \int_0^\delta (u_e^2 - u^2) \rho u dy \quad (39)$$

Density-flux Defect:

$$\mathbf{D} \equiv \rho_e u_e \Delta^{**} = \int_0^\delta (\rho_e - \rho) u dy \quad (40)$$

The above equations relate the conditions in the boundary flow gradient region to the external inviscid flow (EIF) integrated in the “y-direction” normal to the wall. Note that in the case of turbulence, the definitions above apply only to the mean (time-averaged) quantities but the notation is kept the same for convenience and any reference to a flow-field quantity is referring to the mean value.

Sato INSERT REFERENCE HERE gives a derivation for the evolution of the kinetic energy defect in relation to the profile mechanical loss coefficient Φ_p shown in Eq. 41. This is effectively conservation of energy in integral form:

$$\int_{out} \mathbf{K} \cdot \hat{n} dl_{out} = \Phi_p - \Pi_V \quad (41)$$

The above equation is valid for a control volume which has its inlet and side planes sufficiently far from the vehicle such that the integral of the kinetic energy deficit is zero and the “*out*” plane is the location of the exiting plane which can be placed at some axial location along the aerodynamic body. The first term on the right-hand side of Eq. 41 is the viscous dissipation term:

$$\Phi_p = \iint D \, dS = \iint \rho_e u_e^3 c_D \, dS \quad (42)$$

The second term is the so-called “baroclinic” term (Eq. 43), which represents the change in mechanical energy flux due to the pressure gradient acting on the boundary layer flow at a different density than the inviscid flow. The value of this typically scales with M_e^2 and is approximately 5% for high subsonic flows INSERT REFERENCE HERE.

$$\Pi_V = \iint \mathbf{D} \cdot \nabla \frac{1}{2} u_e^2 \, dS = \iint \mathbf{D} \cdot u_e \frac{\partial u_e}{\partial x} \, dS \quad (43)$$

Placing this plane far down-stream of the body at the Trefftz plane (A_∞), the total mechanical dissipation coefficient is given in equation 44 and represents the total dissipative profile drag for the body on the right hand side of the general power balance (Eq. 12):

$$\Phi_p^* = \int_{A_\infty} \mathbf{K} \cdot \hat{n} \, dl_{out} = \Phi_p - \Pi_V \quad (44)$$

The dissipation term from the power balance equation is then computed by integrating the axial 2-D kinetic energy defect \mathbf{K} over the exit plane area. We now consider this integral for two types of aerodynamic wake profiles.

“Class 1” Aerodynamic Body

There are two fundamental aerodynamic body shapes, as defined by Kulfan INSERT REFERENCE HERE. The first is type “Class 1”, which represents wing airfoil type shapes with a distribution along a stacking axis (Fig. 17). Something like a hybrid wing body design falls into this class of aerodynamic bodies. Fig. 18 illustrates the

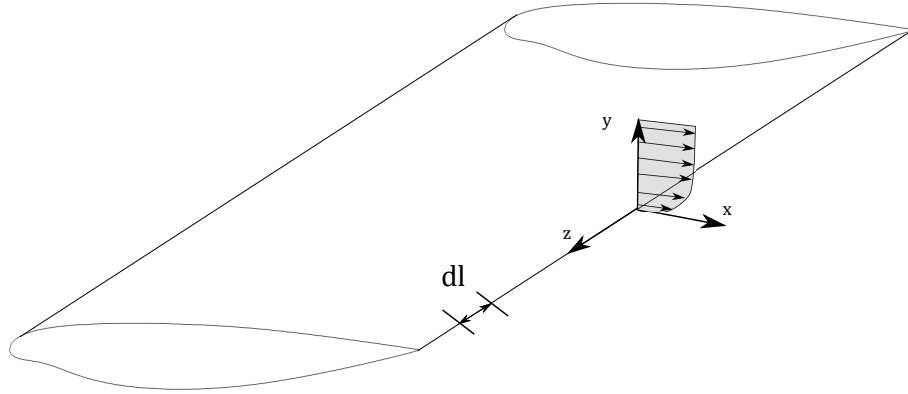


Figure 17: Diagram of a class 1 geometry type with trailing edge boundary layer shown. The dissipation integral is performed along the z -direction.

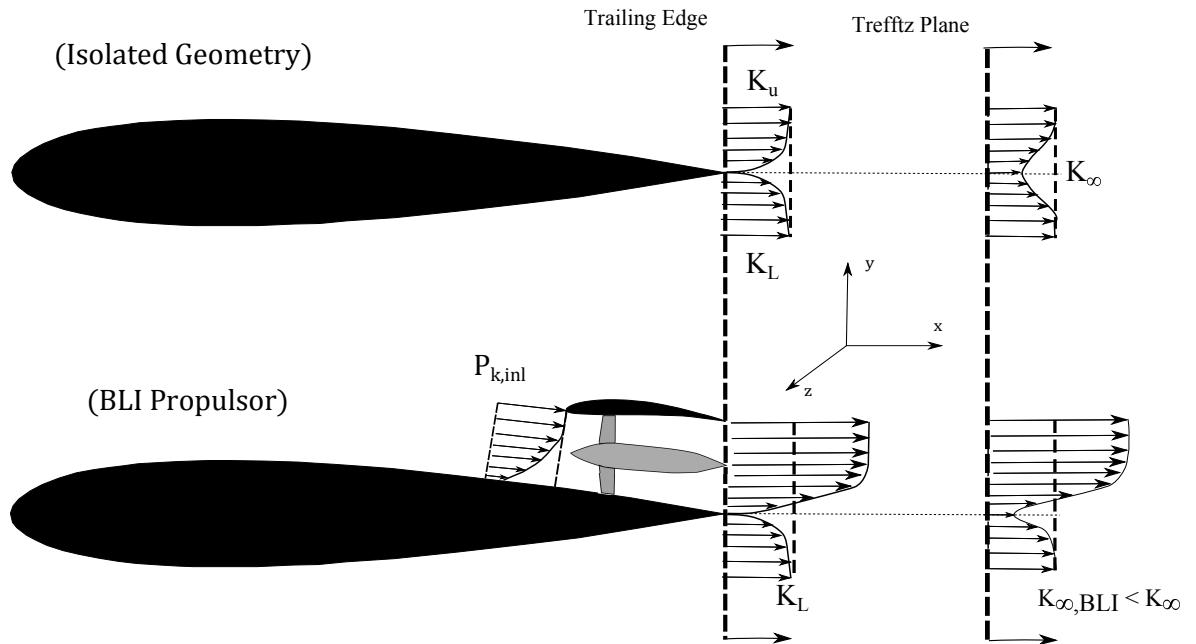


Figure 18: Illustration of a class 1 geometry aerodynamic wake for the isolated airfoil and case with a BLI propulsor.

type of wake which develops for a BLI propulsor on a class 1 type aerodynamic body. The wake dissipation factor for the isolated geometry case is:

$$\Phi_p^* = \int K_\infty \cdot \hat{n} \, dl = \underbrace{\int (K_L + K_u)}_{\text{Trailing Edge}} + \underbrace{\Phi_{wake}^*}_{\text{Wake dissipation}} \quad (45)$$

The wake for the ingesting propulsor case is $K_{\infty,BLI}$ and the parameter $\nu = K_{\infty,BLI}/K_\infty$ is defined to form a relation between the BLI and isolated case. For $\nu = 1$, there is no boundary layer ingested at that z-location, while $\nu = 0$ represents the case where all of the defect is ingested (lower and upper surface). An approximation for ν can be made by assuming that only the contribution of the upper portion of the wake is removed:

$$\Phi_{p,BLI}^* = \int \nu \mathbf{K}_\infty \cdot \hat{n} \, dl = \int \frac{K_L}{(K_L + K_u)_{TE}} \cdot (\mathbf{K}_\infty \cdot \hat{n}) \, dl \quad (46)$$

The next step is to carry out the integration over the length of the wake at the trefftz plane to compute the mechanical energy flux for the BLI case in relation to the isolated body case. Fig. 19 shows an example “Class 1” body with constant cross section and chord length.

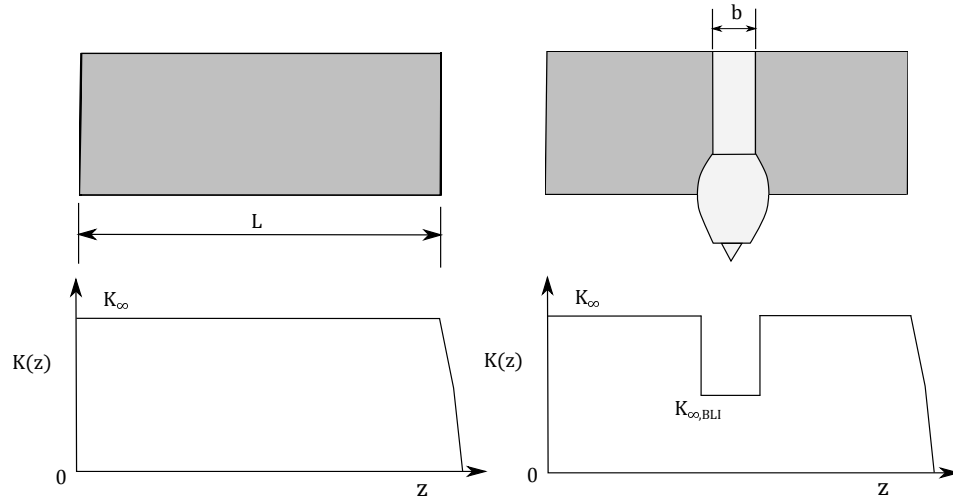


Figure 19: Illustration of the distribution of the kinetic energy defect over the length of a notional “class 1” aerodynamic body.

The variable “b” here is a term representing the “span”, or width, of the ingested boundary layer. The dissipation integral (Eq. 46) is the area under the curve of

this distribution. From this, and by using the definition of β in Eq. 21, we get the following general relation for a class 1 vehicle:

$$1 - \beta = \frac{\Phi_{p,BLI}^*}{\Phi_p^*} = \frac{\int_{x=\infty} \nu(z) K_\infty(z) dz}{\int_{x=\infty} K_\infty(z) dz} \quad (47)$$

From fig. 19, and carrying out the integration for this notional class 1 body, an approximation of β is thus:

$$\begin{aligned} 1 - \beta = \frac{\Phi_{p,BLI}^*}{\Phi_p^*} &= \frac{K_\infty(L - b) + b\nu K_\infty}{LK_\infty} \\ &= \left(1 - (1 - \nu)\frac{b}{L}\right) \end{aligned} \quad (48)$$

Again, Eq. 48 is an approximation, but is at least useful for simple cases and understanding the overall parameters involved in the analysis for the class 1 type. From Eq. 48, the relationship for the thrust saving coefficient is as follows:

$$TSC = \frac{\beta \cdot \Phi_p^*}{DV_\infty + W\dot{h}} = \frac{(1 - \nu)bK_\infty}{DV_\infty + W\dot{h}} \quad (49)$$

Observation 2: For class 1 aerodynamic bodies with BLI, the ratio of ingested drag to net thrust depends on both the value of the recovered boundary layer kinetic energy defect at the trefftz plane and the total span of the boundary layer defect ingested by the engine stream-tube.

“Class 2” Aerodynamic Body

The “class 2” aerodynamic body, as defined by Kulfan INSERT REFERENCE, is the type where the cross-sectional stacking axis is along the “x-axis”. These types of bodies are generally things like fuselages, nacelles, missile or payload pods, etc. These can generally be specified by either having a set of cross-sections which are rotated around some center-line axis or can also be represented by stacking along a vehicle

station-line. For BLI, the important aspect of the class 2 type problem is that the trailing edge and downstream wakes are of a fundamentally different character. An illustration of this is shown in fig. 20 with a notional tube and wing aircraft. The fuselage tail-cone has a wake at the trailing edge of the vehicle with a circumferential distribution around the body which is roughly uniform. The gradient in the boundary layer is in the radial or “y” direction.

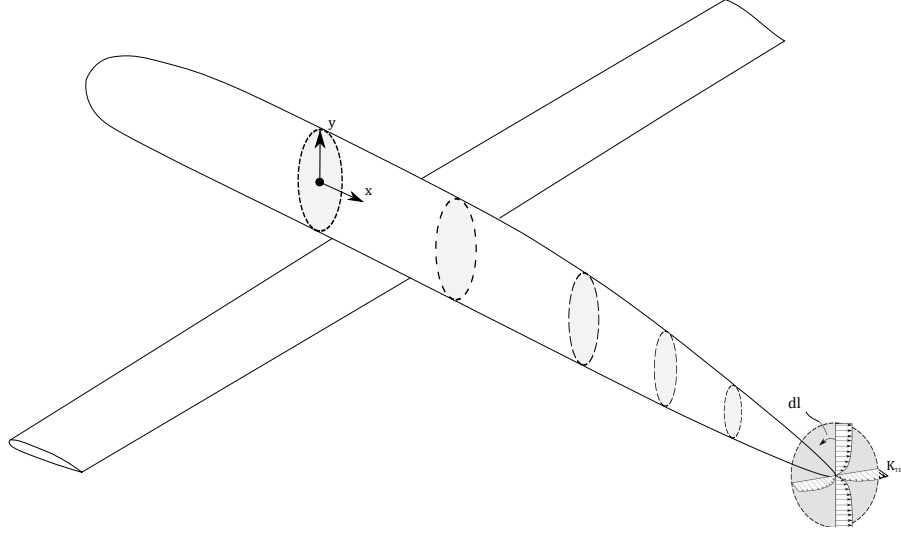


Figure 20: Illustration of the distribution of the kinetic energy defect over the length of a notional “class 1” aerodynamic body.

The wake integral from equation 44 can be computed by integrating the boundary layer kinetic energy defect over the circumference of the wake and assuming $dl = \delta d\theta$, where δ is the boundary layer thickness (distance from wall to “edge”).

$$\Phi_p^* = \int_{T_{efftz}} K_\infty(\theta) \delta d\theta \quad (50)$$

and the equation for β , similar to Eq. 47, is the following:

$$1 - \beta = \frac{\int_0^{2\pi} K_\infty(\theta) \nu(\theta) \delta(\theta) d\theta}{\int_0^{2\pi} K_\infty(\theta) \delta(\theta) d\theta} \quad (51)$$

If we assume circumferential uniformity, then the K_∞ and δ can be pulled out of the integration. The BLI benefit term (β), then, is only a function of the fraction

(ν) of the isolated wake which is recovered in the BLI case. For most aerodynamic bodies of practical concern, the wake will be small enough to entirely ingest it inside of an aft mounted propulsor so that $\nu(\theta) = 0$ at every θ and the wake is entirely recovered, as shown in fig. 21. With ν everywhere zero at the trefftz plane, then β is precisely equal to one, unless the wake from other bodies, such as a wing, is included. It is likely that the entire wake will not be recovered, as illustrated in fig.

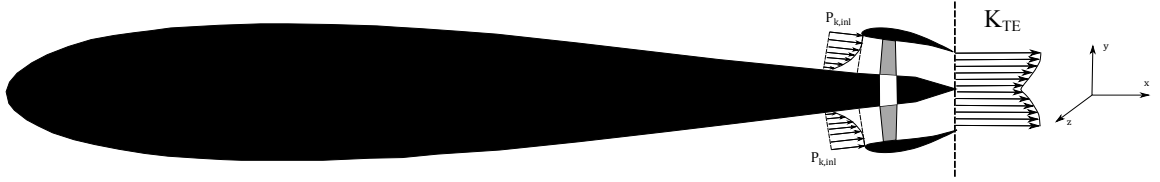


Figure 21: Illustration of the the wake defect for a class 2 body with BLI.

21, and that there will be some residual kinetic energy defect in the jet stream of the BLI propulsor. This can be captured either by modeling the jet stream with an overall gross-thrust coefficient or by including a recovery factor, such as that defined by Smith [INSERT REFERENCE HERE](#), and include the defect in the calculation of $P_{k,out}$ in the power balance equation (Eq. 27). These approaches are equivalent assuming the nozzle gross thrust coefficient is calculated accordingly.

The primary difference between the “Class 1” and “Class 2” type vehicle with boundary layer ingestion is that a single propulsor can be designed to ingest the entire trailing edge wake defect for the class 2 designs. As such, observation 2 does not apply for these types of designs. Furthermore, if the entire wake is ingested by a propulsor which surrounds a class 2 type body, then the distortion will be primarily radial, rather than being a combined radial/circumferential complex distortion profile. This leads to a natural classification for BLI propulsion systems:

- Class 1 BLI Systems: Laterally distributed boundary layer, for which the calculation of the dissipation integral (wake recovery term) is dependent on the width of the engine ingested stream-tube.

- Class 2 BLI Systems: Circumferentially distributed boundary layer, for which the dissipation integral is not dependent on the width of the ingested stream-tube, but only on the radius.

Propulsor Sizing: Class 1 BLI

Consider the case of a general cross-section with area “A” (fig. 22) with some velocity distribution over its surface. The general equation for the mass flux through this cross section is from Eq. 52.

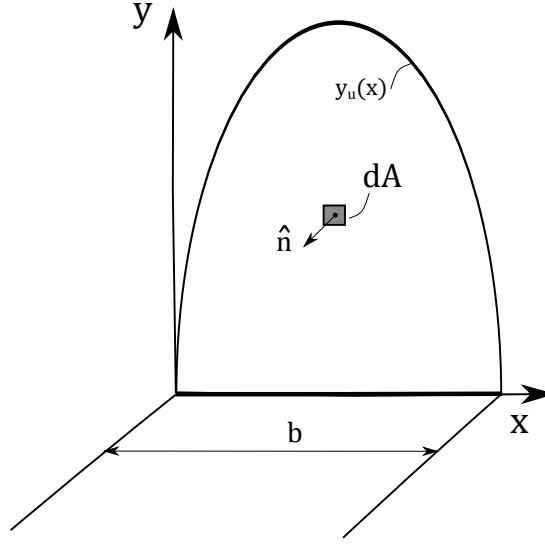


Figure 22: General cross-section diagram.

$$\dot{m} = \iint_A \rho(\mathbf{u} \cdot \hat{n}) dA = \int_0^b \int_0^{y_u(x)} \rho u_x dy dx \quad (52)$$

From Eq. 37,

$$\int \rho u dy = \int \rho_e u_e dy - \mathbf{M} \quad (53)$$

Then:

$$\begin{aligned} \dot{m} &= \int_0^b \left[\rho_e u_e y_u(x) - \mathbf{M}(\mathbf{x}) \right] dx \\ &= \int_0^b \rho_e u_e \left(y_u(x) - \delta^*(x) \right) dx \end{aligned} \quad (54)$$

Here, the edge velocity and density are set by the incoming local properties which are a function of the vehicle aerodynamic shape and free-stream conditions. Therefore,

if the designer desires a specified mass flow, then the width or height of the inlet can be adjusted to achieve the desired mass flow, and the integration of Eq. 54 is computed to do so. If the cross-section shape is known (fixed b and h), the mass flow through that cross-section can be calculated from this relation. To demonstrate this in a simple way, the assumption is made that the 1-D mass defect δ^* and edge velocity and density are constant in the x -direction over the length of the inlet. From this assumption,

$$\dot{m} = \rho_e u_e \int_0^b y_u(x) dx - \rho_e u_e \delta^* b \quad (55)$$

Defining $h = \max(y(x))$, and recognizing that $\int y(x) dx = A$, the following definition is useful:

$$r^* = \frac{A}{b \cdot h} \quad (56)$$

Here, r^* is a measure of how closely the inlet shape matches to a rectangular shape, with a value of unity representing a rectangle with width “ b ” and height “ h ”. Defining the inlet aspect ratio to be $AR = b/h$, then Eq. 55 becomes:

$$\dot{m} = \rho_e u_e \frac{r^* b^2}{AR} - \rho_e u_e \delta^* b \quad (57)$$

Then, the above quadratic equation can be solved for the cross-section width, which directly multiplies the thrust saving coefficient from Eq. 49.

$$b = \frac{\delta^* AR}{2r^*} + \sqrt{\left(\frac{\delta^* AR}{2r^*}\right)^2 + \frac{\dot{m}}{\rho_e u_e} \frac{AR}{r^*}} \quad (58)$$

It is now worth considering what design choices are available to the designer to affect the size of the ingested engine stream-tube and therefore the overall amount of ingested boundary layer (drag).

In general, anything that affects the engine mass flow demand will affect the ingested stream-tube size. The first obvious choice is the selection of the engine fan pressure ratio, which will have a very large impact on the bypass-ratio of the engine and the ingested mass flow (INSERT REFERENCE). Figure XXX shows a notional

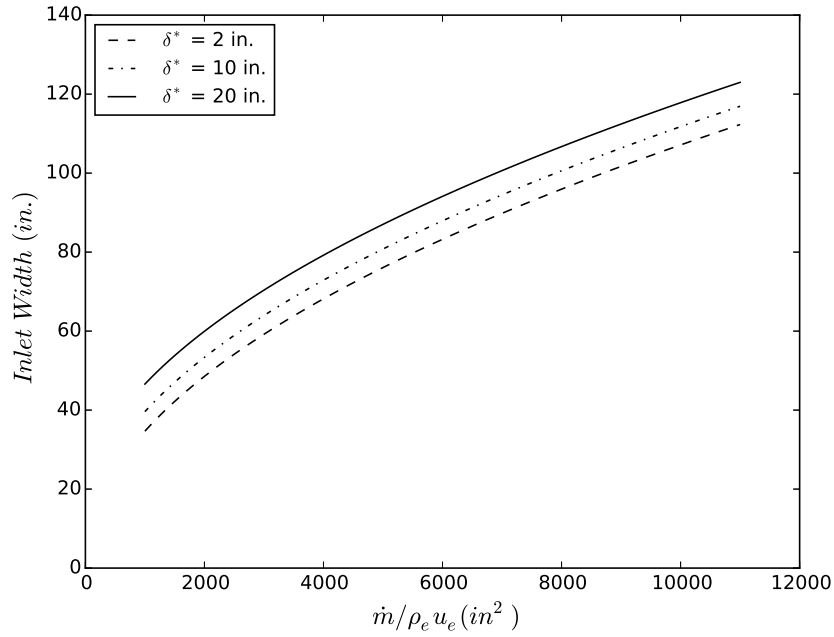


Figure 23: Influence of mass flow on the cross-section width solution.

plot of the ingested mass flow vs. fan pressure ratio for a typical modern hi-bypass ratio turbofan engine. For architectures without traditional turbofan engines, such as a distributed propulsion system, the fan pressure ratio will still have a large impact on the sizing of the fan and the required ingested mass flow (INSERT FELDER REFERENCE /Others?).

Secondary cycle variables and technology factors additionally affect the mass flow demand of the engine. For instance, the maximum temperature that the engine can burn at, typically limited by the turbine materials and cooling requirements, will have a significant impact on the available thrust of the propulsion system. Other less important factors are things like the component efficiencies of the fan, low and high pressure compressors, and the burn efficiency and pressure drop of the combustor. Anything that ultimately affects the ideal or actual cycle of the engine will have some impact on the desired mass flow and therefore the width of the ingested stream-tube.

Another design feature which has a significant impact on the ingested stream-tube

width is the aspect ratio of the inlet aperture area. If the inlet's width is much larger than it's height, then the amount of captured boundary layer will be greater than the case where the width is equal to the height (aspect ratio = 1), as shown in fig. 24. The designer can therefore increase the aspect ratio of the inlet shape in order to achieve higher levels of ingested boundary layer. Higher mass flows make the inlet width even more sensitive to the aspect ratio of the inlet for a fixed boundary layer size, as demonstrated in fig. 24.

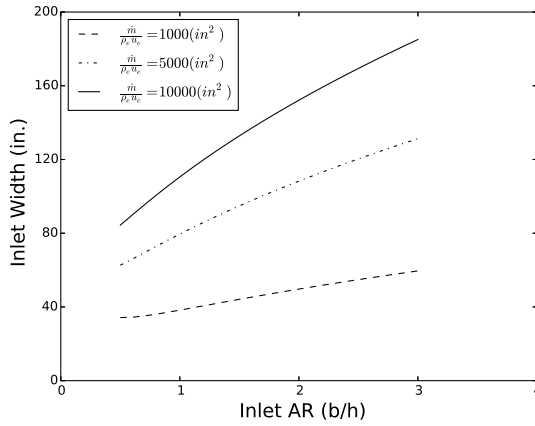


Figure 24: Influence of inlet aspect ratio on inlet width sizing.

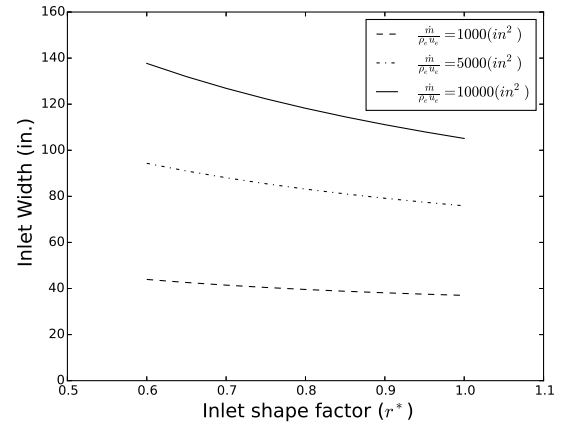


Figure 25: Influence of inlet aperture shape on inlet width sizing.

The choice of inlet aperture shape also has a relatively weak influence on the inlet width sizing as shown in fig. 25. As the inlet is tapered at the top, the width at the bottom of the inlet near the boundary layer must increase to capture more flow. Table 4 shows several typical BLI inlet shapes for class 2 type BLI with values of r^* and $y(x)$ shown.

Finally, a fundamental choice with regard to determining the overall system β is the location of each propulsor on the upper surface of the airframe. This involves both the selection of the number of propulsors (something that would effect the engine stream-tube size) and the location of each propulsor both span-wise and chord-wise. This last choice will affect the size of the boundary layer thickness, as well as the


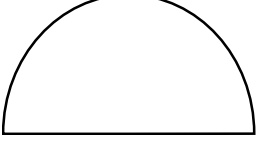
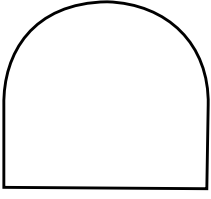
Shape	$y(x)$	r^*
	$y(x) = h$	$r^* = 1$
	$y(x) = h \cdot \sqrt{1 - 4 \frac{(x - b/2)^2}{b^2}}$	$r^* = \pi/4$
	$y(x) = \frac{h}{2} + \frac{h}{2} \cdot \sqrt{1 - 4 \frac{(x - b/2)^2}{b^2}}$	$r^* = 1/2 + \pi/8$

Table 4: Table showing inlet shapes, $y(x)$, and r^*

local velocity and static pressure at the inlet. This has an impact on both the total amount of drag ingested and the overall losses in the inlet and fan due to distortion (REFERENCE). All of the above discussion leads to the following observation 3:

Observation 3: The engine mass flow size, inlet aperture shape, and location on the vehicle affect the ratio of the ingested drag to uningested drag for class 1 BLI systems.

Propulsor Sizing: Class 2 BLI

For class 2 BLI systems, the distortion is primarily radial, but the fundamental equation still applies from Eq. 54, except that the integration is different because of the way that the boundary layer is distributed. Furthermore, the calculation of the stream-tube width is irrelevant (even meaningless). Rather, the primary variable is the radius of the propulsor which determines how much mass is ingested. Consider a general flow annulus for a class 2 BLI problem with inner radius r_i and outer radius

r_o . The equation for mass flow is then:

$$\dot{m} = \int_0^{2\pi} \int_{r_i}^{r_o} \rho u_x r dr d\theta \quad (59)$$

The definition of \mathbf{M} here is slightly different than Eq. 37, since it must account for the effect of radius on the area averaging of the velocity:

$$M_r(\theta) = \int_{r_i}^{r_o} (\rho_e u_e - \rho u) r dr \quad (60)$$

From Eq. 60, the final equation for the mass flow of a class 2 BLI propulsor is:

$$\dot{m} = \int_0^{2\pi} \left[\frac{r_o^2 - r_i^2}{2} \rho_e u_e - M_r(\theta) \right] d\theta = \rho_e u_e A - \int_0^{2\pi} M_r(\theta) d\theta \quad (61)$$

With the second part of Eq. 61 recognizing $A = \pi(r_o^2 - r_i^2)$. If the propulsor is sized with a radius greater than the boundary layer thickness, then the above can be simplified to solve for the required outer radius for a given desired mass flow. The net result is that the propulsor has to be a little bit bigger for a specified mass flow, however if the amount of BLI ingested is large, then the propulsive efficiency improves and the specific thrust increases requiring less mass flow.

The analysis of Smith [57] showed that a wake ingesting propeller with class 2 BLI will have significantly improved propulsive efficiency if the wake comprises a large portion of the total vehicle required drag. In general, for better propulsive efficiency, larger mass flow designs are desirable, since they require less jet velocity to produce the same thrust. However, Smith notes:

...when a large part of the craft's wake is ingested by the propulsor, there is much less incentive to keep the propulsor large. The message here is that, for best efficiency the propulsor should be positioned and sized to ingest as much wake fluid as possible (increase D/T), but after that, making it still larger does not pay off in propulsive efficiency and would have other adverse effects such as increased weight.

For the case of class 2 BLI, this amounts to sizing the propulsor with a large enough radius to consume the entire wake, while for class 1 BLI, there is a more significant design trade-off since larger mass flows imply larger levels of BLI.

Distortion Effects on the Engine

We now turn to the question of how the losses induced by the boundary layer ingestion are developed and also the question of model fidelity requirement with respect to these losses. Generally, the primary determining factor for the losses of the engine will come from the loss of total pressure due to the presence of the distortion. This pressure drop can be approximated by integrating the boundary layer velocity profile over the fan face area. Appendix A describes a mathematical development of the inlet model to be used later in this thesis but also contains an integral formulation showing that the total pressure loss can be approximated by using the kinetic energy defect property defined in Eq. ??, assuming that the density thickness is negligible and a uniform static pressure.

$$\bar{P}_t = P_s + \frac{1}{2}\rho_e u_e^2 \frac{(A - \delta^* - \theta^*)}{(A - \delta^*)} \quad (62)$$

Equation 62 shows that the total pressure loss is proportional to the size of both the boundary layer blockage represented by δ^*/A and the kinetic energy thickness to area ratio θ^*/A . This means that a bigger ratio of boundary layer to "clean" flow yields a worse total pressure recovery. Note that this is in direct contradiction to the analysis developed previously for the BLI benefit, which dictates that ingesting a larger percentage of the boundary layer into the inlet is more beneficial. The fraction of boundary layer to total flow area is a function of the amount of boundary layer ingested, the value of the 2-D "height averaged" boundary layer thickness and shape, and also the edge velocity of the boundary layer itself – implying faster flows will tend to produce more losses in a shear layer. This observation is also corroborated

in several experimental sets of data including that of INSERT NASA REFERENCE (BERRIER) and (SHEDON). These results show that bigger percentages of boundary layer to total flow area yield worse inlet recoveries implying an essential trade-off involved in designing the amount of BLI to be ingested into a system and the subsequent engine size required. Observation 4 comes from the preceding analysis:

Observation 4: The boundary layer thickness does not scale directly with the propulsor mass flow, but the stream tube does change. Therefore boundary layer related losses will be different for changes in engine stream tube size, since the total inlet recovery is a function of the ratio of the boundary layer flow to the total flow.

Off-Design Analysis

The off-design analysis of BLI engines is something that has not been very extensively researched in the system study literature. Typically, the focus is on the cruise point efficiency and therefore variations in flight Mach and altitude are not considered especially important for the sizing of the vehicle. However, the aerodynamic design point of an engine is not the only point of concern. In fact, the BLIPSS methodology is specifically designed to account for the fact that performance at off-design conditions for highly integrated systems is important to capture. Therefore, understanding the fidelity requirements for a BLI engine model in off-design is nearly as important as quantifying it for the cruise condition.

μ Variation

Shedon [55] defines a simple model for an inlet, in which the inlet duct loss varies with the cube of the inverse of the mass flow ratio defined as follows:

$$\mu = \frac{A_c}{A_\infty} = \frac{\rho_\infty u_\infty}{\rho_c u_c} \quad (63)$$

The parameter μ is effectively a measure of how the stream-tube expands or contracts as it approaches the inlet hi-lite area. The μ^3 variation [55] is defined, in its simplest form, as follows:

$$\frac{\Delta P}{q_c} = IC_{Fd} + JC_{Fa} \cdot \mu^3 \quad (64)$$

Here there are two skin friction coefficients, one for the duct and the other for the region of the vehicle prior to entry (as often seen in military aircraft). The pre-entry flow is the region sensitive to the mass flow ratio variation and is of particular importance for boundary layer ingesting systems. Usually 64 is re-arranged in terms of the free-stream dynamic head rather than the local capture head as follows:

$$\frac{\Delta P}{q_\infty} = \frac{IC_{Fd}}{\mu^2} + JC_{Fa} \cdot \mu \quad (65)$$

An analysis of 65 shows that there are essentially two regimes over which a BLI intake can operate: one in which the flow accelerates prior to entry ($\mu \ll 1$), and one where the flow is retarded prior to entry ($\mu \gg 1$). At extremes of these two regimes, the actual intake recovery varies from 65 because of pre-entry separation and lip flow separation, neither of which are included in the derivation of 65. Pre-entry separation occurs in regions of extreme flow retardation ($\frac{dP}{dx} > 0$, $\mu \gg 1$). This generally happens in very low mass flow demand regions at high-speeds, such as possibly end of cruise or descent. Lip separation occurs in the opposite extreme in the low μ regime where mass flow is very high and velocity is low, which would be of greater concern at the take-off maximum power condition.

The preceeding analysis again shows that, fundamentally, the determination of inlet losses is a function of how the inlet stream-tube varies as it approaches the inlet.

Flight Condition Variation

There has been some experimental data defining variations in inlet recoveries at different flight Mach, Reynold's, and mass flow ratio INSERT REFERENCE HERE

for inlets designed specifically for BLI applications on large transports. This data showed that flight Mach number has a very strong influence on the overall recovery, with the mass flow into the inlet playing a significant secondary role which is in congruence with the μ^3 analysis. The theoretical development by [55] also stressed the importance of the skin friction coefficient which significantly increases with the Mach number of the flow. Furthermore, the 65 gives an expression for duct loss which is normalized by the free-stream head which increases significantly at higher Mach. The expectation, then, is that the size of the boundary layer relative to the size of a fixed capture height inlet will decrease as the free-stream Mach number is decreased along with both benefit and loss. This implies that the thrust saving coefficient at low altitude and speeds, especially at the take-off condition, should be relatively lower – for similar vehicle angles of attack – than that at high speeds, but that distortion concerns would not be as great.

Angle of Attack Variation

In general, subsonic pitot inlet based engines are not generally thought to have much variation in thrust or performance with the angle of attack of the vehicle. In cases where large angle of attack is required, the inlets can typically be scarfed to provide a favorable flow angle into the intake, thereby reducing any distortion and mitigating loss of pressure recovery. In the case of BLI, this is not possible, and we would therefore expect to see significant variation in the performance of the engine as a function of the vehicle angle of attack. Figure 26 shows the variation of boundary layer properties for a NACA 2012 symmetric airfoil at a flight Mach of 0.7 with a Reynolds of 10^5 , as predicted by XFOIL INSERT REFERENCE HERE.

Clearly the boundary layer thickness increases significantly, which will impact the thrust saving coefficient and inlet recovery. Typical top-of-climb angle of attacks for a hybrid wing body vehicle, such as the N2B or N2A, can be as high as 3.5-5 degrees

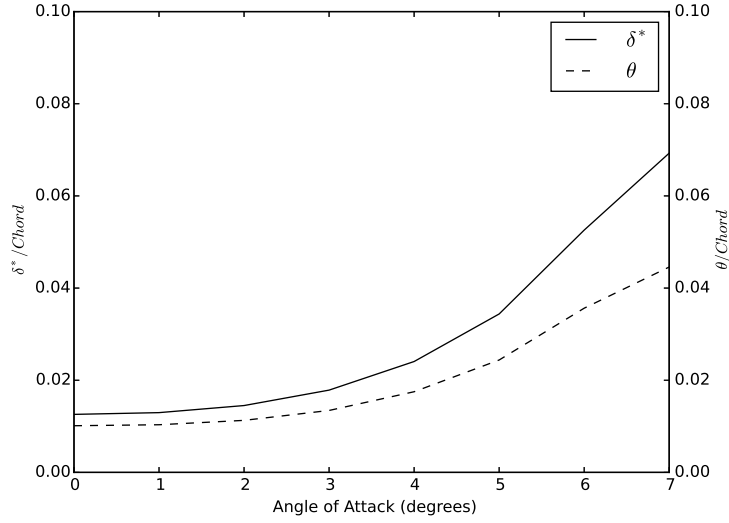


Figure 26: Plot showing trend of boundary layer thicknesses vs. airfoil angle of attack for a NACA 2012 airfoil at Mach = 0.7, $\text{Re} = 10^6$ as predicted by XFOIL

INSERT REFERENCE HERE, and declines as fuel is burned during cruise and lift required is reduced. Therefore the variation in thrust, efficiency, and operability as a function of angle of attack, if found to be significant, would be necessary to include in a model at this level.

Hypothesis 1

Though the discussion above is barely touching the surface in terms of the complexity of an actual boundary layer ingesting flow field, there are some clear basic trends which have arisen from the analysis. First, the benefit of the system is ultimately a balance between drag recovery and distortion losses, which tend to both increase with the ratio of distorted boundary layer flow to clean flow. Second is that, at a given design point, any design choice which impacts the size of the ingested stream-tube will impact the amount of boundary layer that is ingested, though those choices will not have an impact on the vehicle boundary layer. Third, that the boundary layer thickness varies significantly with flight Mach number and angle of attack for a given vehicle. Fourth, that the losses in the inlet duct leading to the propulsor face will vary

significantly with the free-stream mass ratio and the flight condition. Given that the BLIPSS methodology is intended to be able to account for multiple design conditions, it is therefore necessary, if it is to be used, to account for these fundamental variations in benefits and losses. Otherwise, changes in flight conditions and power settings will not appropriately match the actual variation in design point performance even at a first level approximation. From these observations, the following hypothesis is formed:

Hypothesis 1: If multi-design point BLI propulsion system cycle models do not include the physical relationship between the vehicle boundary layer profile, the ingested stream-tube size and its variation, and system powerbalance and engine losses at critical sizing conditions, then a significant portion of the predicted propulsion system design space will be infeasible.

Stall Margin and Stall Constraint

Hypothesis 1 deals with the basic modeling requirements for any BLI system. It is formulated out of a need to appropriately size the system – based on requirements at multiple flight conditions – and thereby appropriately form a design space from which early design choices can be made. The hypothesis is developed in order to properly establish the trade-off between the propulsive efficiency benefit of ingesting more low momentum flow and the losses incurred by doing the same. The other major component of any boundary layer ingesting system, not addressed by Hypothesis 1, is the impact on the operability of the propulsion system incurred by the ingestion of distorted inflow. Clearly this is an important component of the problem, and yet it is not typically addressed at the level of conceptual design.

Operability is considered to be a constraint on a propulsion system, meaning that adding more is not necessarily desirable beyond that which is required. The

major tool for meeting this constraint is the stall margin stack-up INSERT REFERENCE HERE. A fan stall margin stack-up typically comprises some percentage which is dedicated to account for possible distortion exiting the inlet at the fan face. If ingesting boundary layer produces levels or types of distortion which are fundamentally worse than that of typical fan designs, then something must be done in the design to restore normal levels of safe operability. While it is difficult to determine the efficacy of various distortion mitigating actions in the conceptual design phase, it is worth investigating how conceptual design choices – the kinds of which the BLIPSS methodology is intended to facilitate – affect the likely level of stall margin loss due to distortion and therefore the likelihood of being able to restore it to normal levels. Research question 2 is formulated accordingly:

Research Question 2: How does the stall margin constraint affect the BLI propulsion system design space?

Distortion Stall Margin Loss

The stall margin stack-up percentage which is included to account for distortion is usually estimated in design based on prior requirements for existing designs. Testing of fans and compressors then occurs after detail design of the fan is carried out and a test rig can be constructed. The ARP 1420 INSERT REFERENCE HERE guidelines have developed over the years to guide this experimental process to fruition by giving the operability analyst a standard set of tools and experimental setup to appropriately estimate and measure stall margin loss for specific designs. The standard rig setup dictated by ARP 1420 is shown in figure 27 and consists of a set of pressure probes and rings at which the total pressure of the flow is measured. Typical distortion types can be described in terms of per-rev, which gives measurement of how many low pressure circumferential sections is the blade passing through. For BLI systems

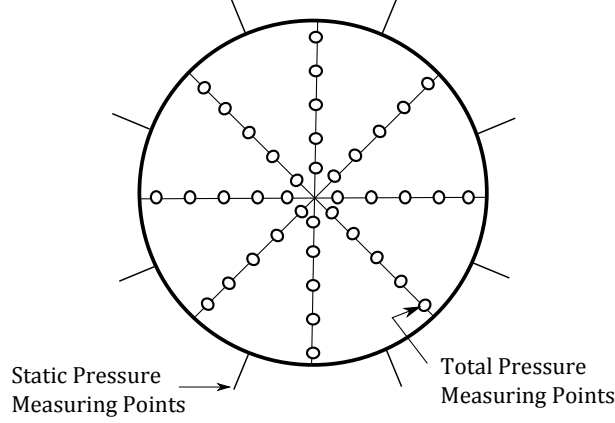


Figure 27: Standard ARP 1420 test rig showing static and total pressure probe locations

which ingest boundary layer from the upper surface of a vehicle, such as that for the typical HWB type configurations, the distortion usually takes on a 1-per-rev circumferential distortion type. This type is illustrated for in figure 28. The extent is defined as in Eq. 66 and is representative of the circumferential extent over which the total pressure is lower than the average.

$$\theta_i^- = \theta_{2i} - \theta_{1i} \quad (66)$$

The circumferential intensity is defined as:

$$\left(\frac{\Delta PC}{P}\right)_i = \frac{(P_{av})_i - (P_{avlow})_i}{(P_{av})_i} \quad (67)$$

$$(P_{AV})_i = \frac{1}{360} \int_0^{360} P(\theta)_i d\theta \quad (68)$$

$$(P_{AVLOW})_i = \frac{1}{\theta_i^-} \int_{\theta_{1i}}^{\theta_{2i}} P(\theta)_i d\theta \quad (69)$$

Then, the total circumferential intensity is the sum of each of the rings.

$$DPCP_{avg} = \frac{1}{N} \sum_{i=1}^N \left(\frac{\Delta PC}{P}\right)_i \quad (70)$$

The stall margin loss is typically defined in terms of ΔPRS defined, which is the difference between the clean and distorted stall pressure ratio at constant flow in percentage of the clean stall pressure ratio which is illustrated also in figure 30.

$$\Delta PRS = \frac{PRS_{Clean} - PRS_{Distorted}}{PRS_{Clean}} \quad (71)$$

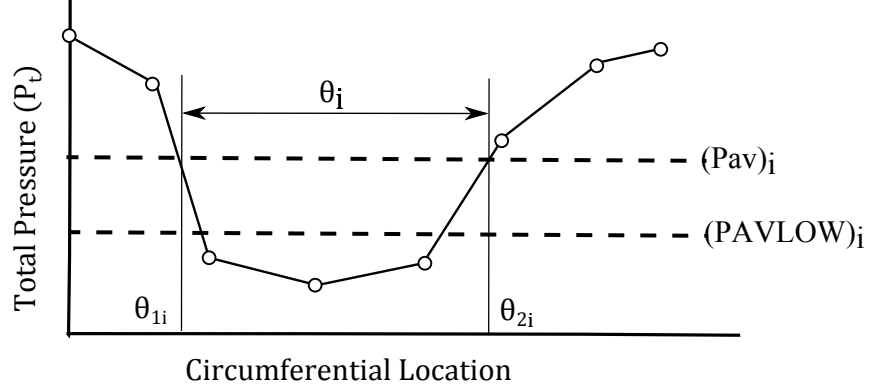


Figure 28: Illustration of a one-per-rev distortion type for a single probe ring.

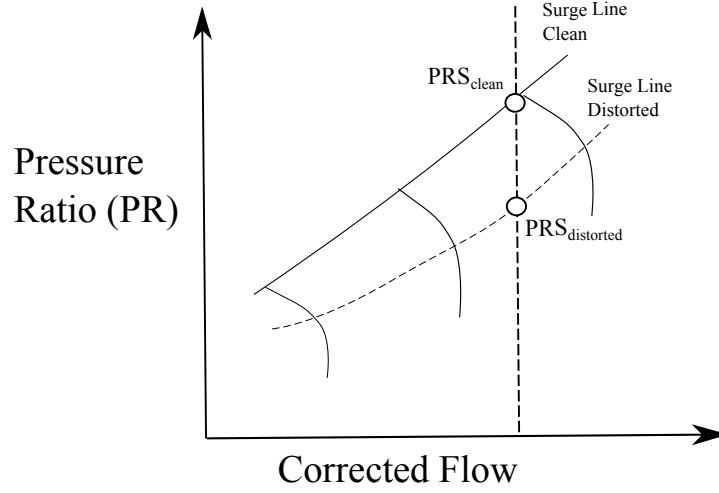


Figure 29: Illustration of the definition of delta PRS with distortion

Typically the ΔPRS is quantified by correlating it with the intensity defined in Eq. 67. An example for classical one-per-rev distortion type would be described in 72 and is represented with a simple linear correlation.

$$\Delta PRS = K_c \cdot DPCP_{avg} \quad (72)$$

The other type of distortion common to BLI systems is radial pressure distortion, which represents a gradient of the total pressure in the radial direction as is common within a viscous boundary layer. Radial pressure gradients can significantly affect the compressor characteristic and the pressure ratio at which stall occurs. The ARP

1420 radial descriptor is defined by Eqs. 73 and 74.

$$\left(\frac{\Delta PR}{P}\right)_i = \frac{PFAV - (P_{AV})_i}{PFAV} \quad (73)$$

Where,

$$PFAV = \frac{1}{N} \sum_{i=1}^N (P_{AV})_i \quad (74)$$

The standard $DC(\theta)$ which represents a descriptor for complex distortion types containing both circumferential and radial is then defined as follows:

$$DC(\theta_E) = \frac{1}{N} \sum_{i=1}^N \left[\left(1 - \frac{\Delta PR}{P}\right)_i \cdot \left(\frac{\theta_i}{\theta_E}\right) \cdot \left(\frac{\Delta PC}{P}\right)_i \right] \cdot PFAV / q_{avg} \quad (75)$$

This descriptor, which combines the types of distortion which can be represent various complex patterns can also be correlated with ΔPRS , which is standard practice for experimental testing and quantification of distortion stall margin loss INSERT REFERENCE HERE.

Canonical Example

Consider now the case of a circular fan aerodynamic interface plane defined in terms of polar coordinates (r, θ) and with a standard ARP 1420 set of rakes applied to it. The hub-to-tip ratio of the fan is fixed at 0.45. The centerline $(\theta = 0)$ is represented by a $1/7^th$ power law velocity distribution typical of turbulent flat-plate boundary layer profiles with a 99% thickness defined as δ . The ratio of the boundary layer thickness to fan blade span is δ/h .

$$\frac{u}{u_e} = \left(\frac{y}{\delta}\right)^{1/7} \quad (76)$$

The circumferential variation in the velocity distribution is assumed to be defined as follows [48]:

$$p_t(r, \theta) = p_{t_l}(r) \cos^{10}(\theta) + p_{t_h}(r) \left[1 - \cos^{10}(\theta)\right] \quad (77)$$

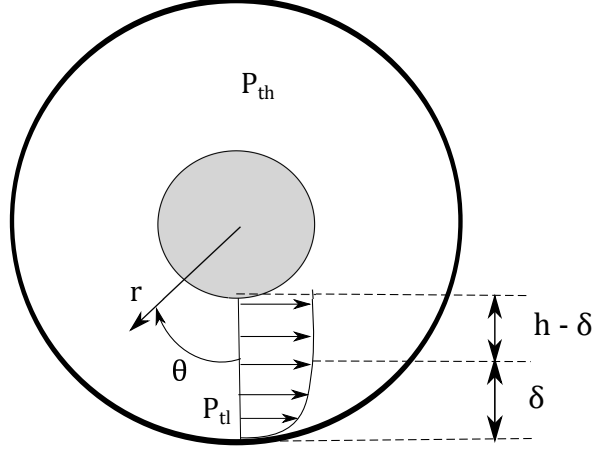


Figure 30: Illustration of the Notional Fan Face AIP

Applying the above parameterizations and assumptions in velocity profile, a 2-D fan face representation can be constructed and the distortion descriptor $DC(\theta_E)$ can be calculated. Some values for the pressures and temperatures assumed in this case are shown in table 5. Figure 31 shows the AIP pressure distributions for 5 typical rakes generated for a boundary layer thickness to blade height ratio of unity. From

Parameter	Value
P_{th}	15 psia
M_e	0.65
r_h/r_t	0.45
r_t	56 in.

Table 5: Distortion Example Parameters

these distributions, the rake data can be used to calculate the distortion descriptors. The boundary layer height to blade height ratio was varied from 0.1 to 2 and the distortion descriptors are calculated. The results – shown in figure 32 illustrate what happens when the thickness of the boundary is increased relative to the size of the clean flow area.

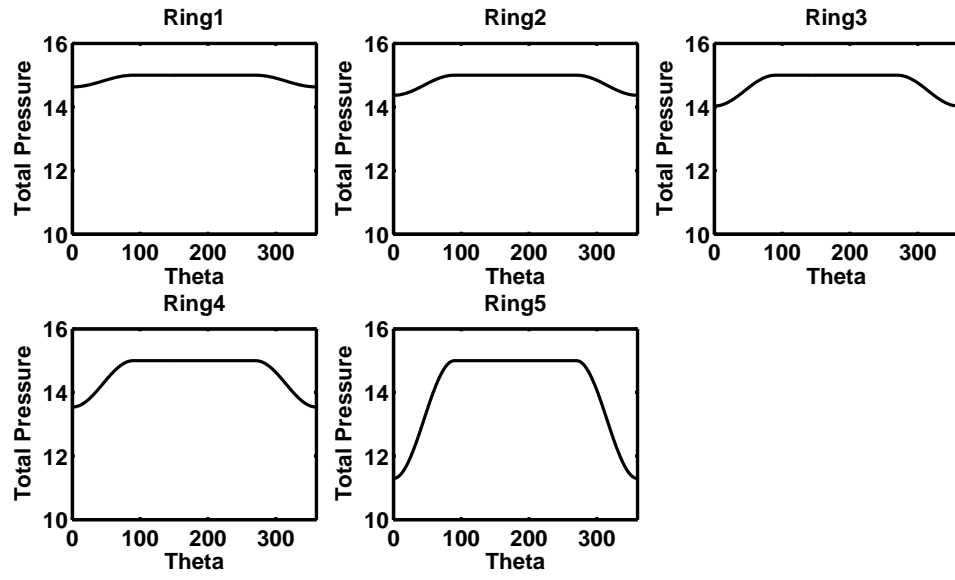


Figure 31: Example fan face ring total pressure distribution.

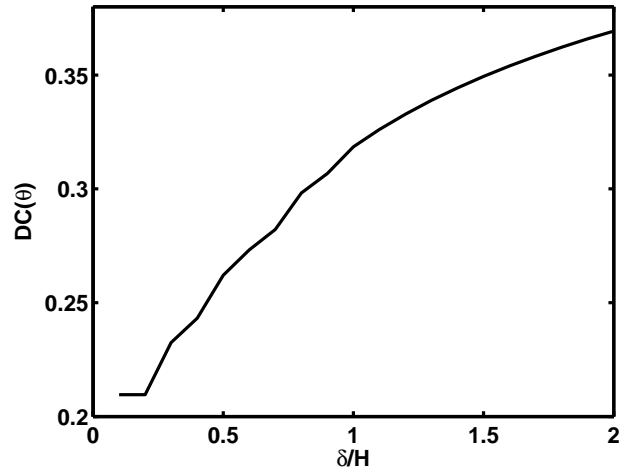


Figure 32: $DC(\theta)$ descriptor plotted vs. boundary layer thickness ratio.)

Hypothesis 2

Since $DC(\theta)$ generally correlates directly with ΔPRS , it stands to reason that increasing the boundary layer thickness to height ratio will harm the stability margin of the fan substantially. This could, in theory, place limits on the size of the propulsor in relation to the size of the boundary layer in order to maintain operability. From observation 2, it has been established that the benefit of BLI is a strong function of the same ratio, implying that operability may limit the cycle designer's ability to ingest more drag within imposing an operability problem on the system. If the cycle designer is given a hard target on what the allowable stall margin loss (ΔPRS) is at the conceptual phase, then this would limit the possible benefit that a BLI propulsion system would give. Hypothesis 2 is therefore derived from this simplified analysis and is stated as follows:

Hypothesis 2: The operability constraint limits the thrust saving coefficient achievable by a given propulsor.

There are a few caveats worth mentioning to clarify the statement of Hypothesis 2. It does not necessarily say that the constraint will be an active constraint on the system. For instance, if something else, such as engine core "size-effect" losses or other practical concerns limit the available amount of ingestion, then the constraint would still be present in the design space but would not affect the design choice made. Also note that the hypothesis is made in terms of a single propulsor, not necessarily an entire system. There may, in fact, be system configurations in which part of the propulsion system ingests boundary layer while another part does not. In this case, increasing the thrust saving coefficient of the BLI propulsor would not necessarily increase the overall β of the system, but it would decrease operability via distortion increase.

BLI Modeling Phase Process

Hypotheses 1 and 2, if substantiated, imply a solution to research question 1: namely that the BLI modeling phase should consist of building models which accurately represent the relationship between the major conceptual design variables determining the level of BLI ingested and losses in performance and operability of the system. The following modeling algorithm for the BLI modeling phase is thus developed from this understanding and the preceeding theoretical analysis:

Prior to Analysis

- ① Establish vehicle airframe geometry
- ② Identify BLI propulsor type: Class 1 or 2
- ③ Establish aerodynamic cross-section stack-up (based on step 1): Lateral for C1; rotational for C2

For each flight condition and propulsor location:

- ④ Compute BL defect property from “clean” airfoil analysis ($\delta^*, \theta, \theta^*$) at $(x, y)_{inl}$, $(x, y)_{TE}$, and $(x, y)_{trf ftz}$
- ⑤ Approximate $\nu = K_{\infty BLI} / K_{\infty}$ based on BLI type.

For each cycle analysis iteration

- ⑥ Compute BLI thrust term ($\beta \cdot \Phi_p^*$) based on BLI type (Eq. 48 for C1, Eq. 51 for C2)
- ⑦ Compute $\frac{A_o}{A_c}$ and inlet losses based on inlet BL properties.
- ⑧ Estimate inlet distortion and compute propulsor operating line
- ⑨ Estimate ΔPRS and $\Delta \eta_F$

3.2.2 Architecture Integration Phase

With advances in aerospace concepts toward more fuel efficient, revolutionary aircraft, such as the HWB, there are many possible types of architectures that could potentially become viable. Varying numbers of BLI engines could be used, such as 2, 3, 4, or 5 engine BLI turbofans INSERT REFERENCE. The concept of turbo-electric distributed propulsion has also been investigated as a possible architecture, in which there are turbo-generators which do not ingest boundary layer but transfer power, via an electrical distribution system, to a propulsor array which spans the upper surface of the vehicle INSERT REFERENCES HERE. Each of these architectures can take advantage of boundary layer ingestion, with some of them ingesting more overall stream-tube than others. Figure 33 shows several of these possible architectures, with varying propulsor numbers and locations on the upper surface of the HWB. All of these potential propulsion system architectures need to be evaluated in comparison to each other, but also need to be properly sized at the conceptual level in order to make legitimate comparisons of overall fuel burn and weight between the systems.

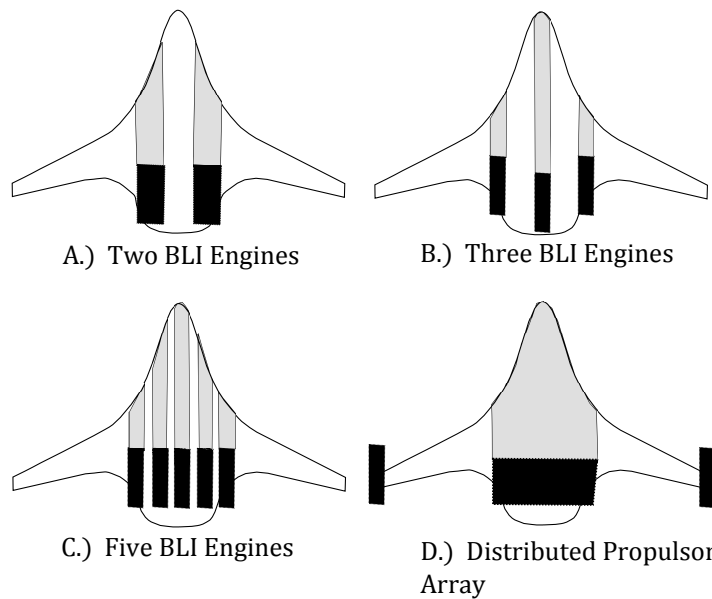


Figure 33: Examples of potential propulsion system architectures for an HWB aircraft.

Observations and Research Question 3

As noted in chapter 2, the problem of integration for BLI systems in relation to the MDP sizing process is that the airframe can impact each propulsor/gas generator in different ways depending on the location of the propulsor on the airframe. This relates to both the nature of the boundary layer at the inlet location, which will significantly impact the recovery, and the overall amount of boundary layer ingested and recovered by the engine. Factors which impact this are mostly related to the airframe geometry, including things such as the airframe airfoil design (thickness-to-chord, camber, etc) and the overall chord length. For example, in general the boundary layer thickness will increase as a function of the axial location along a surface. A simple demonstration is seen in Eq. [?] for a turbulent flat-plate boundary layer – assuming a 1/7th power law – which represents the increase of the boundary layer thickness with axial position
INSERT REFERENCE HERE.

$$\frac{\delta}{x} = \frac{0.3747}{(Re_x)^{0.2}} \quad (78)$$

This means that if chord length of the airfoils tapers, as it clearly does for the HWB, then the boundary layer will decrease as a function of the %Chord, and the amount of wake recovery generated by ingesting the boundary layer will be less. This is also saying that the inner portion of the HWB center body, which is much longer and therefore thicker, will generate more viscous profile drag. Thus, choices of where the propulsors are placed will have an impact on the overall thrust saving coefficient, inlet recovery, and the stall margin loss of the system. To further corroborate the idea that this will significantly impact the system, one need only look read reference
INSERT N2B reference here, in which the boundary layers of the outboard sections of an HWB design (Boeing N2B) were found to be significantly smaller than the outboard (factor or 1/2). Furthermore, the engine aerodynamic interface planes had significantly different levels of distortion and overall recovery between them. The

above considerations illustrate the nature of the integration problem vis a vis the propulsion system cycle analysis, and research question 3 is formulated as a result:

Research Question 3: How can multiple design points, different BLI propulsion system architectures, and variations in inlet properties between propulsors/engines at a given flight condition be accounted for in BLI propulsion system conceptual design?

Methodology Development

To establish a way of dealing with the above research question, it is first necessary to understand how the MDP methodology operates in practice. Figure 34 shows the sequential SDP process. This process is designed for a single engine and design point. The idea is to iterate between the desired off-design conditions to check that the requirements at those conditions are met. The operating thrust at the design condition can be altered to then satisfy the off-design conditions.

Sequential SDP: Single Engine, Single Design Point

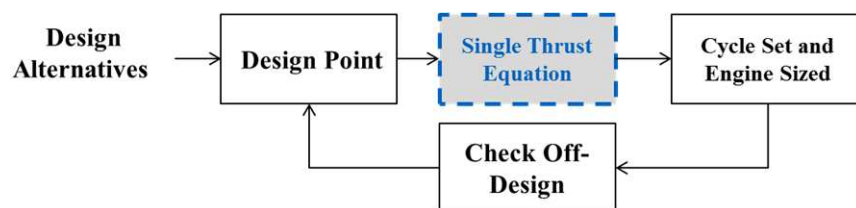


Figure 34: Illustration of Sequential Single Point Design

By comparison, the multi-design point process, illustrated in figure 35, is intended to remove the iteration with the off-design conditions in order to automate the design process to produce a design space with off-design conditions automatically satisfied.

To account for the performance of the engine/propulsor at different inlet conditions, the MDP process from 35 could be iterated with an off-design condition where the inlet conditions are changed. Then, the engine could be rematched according to

Multi-Design Point: Single Engine, Multiple Design Points

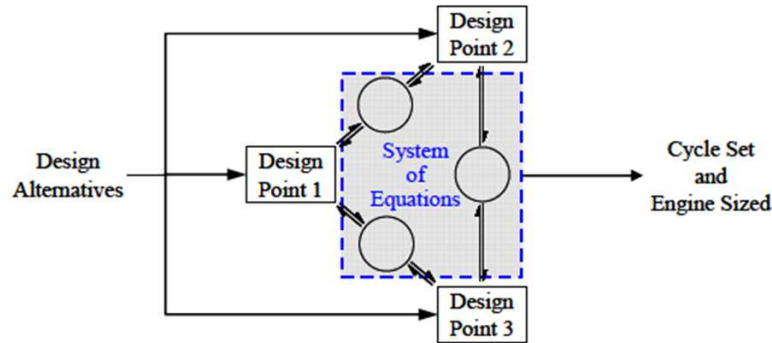


Figure 35: Illustration of Multi-Design Point Process

the change in performance that is calculated. Instead of this manual process, which is analogous to the SDP process, the inlet conditions can be included as "Design Points" in the MDP analysis. To extend this even further, the possibility of having different sized propulsors can be included in this, which would mean that each unique propulsor/inlet combination at each flight condition would be considered a "Design Point" in the automated MDP process. This process is illustrated in figure 36.

There are two major changes which occur from this view of the multi-engine/propulsor MDP process: first there needs to be some set of rules which relate the design and operation of the propulsor at each flight condition; second is that the thrust calculated is now the sum of the separate propulsor thrusts from each "design point" times the number of propulsors included in that design point (since it is possible to have multiple propulsors represented by a single design point). The rules required for the completion of the ME-MDP process are classified into two categories: design rules, and power management rules. These are discussed in more detail in the following section.

BLIPSS : Multi-Engine, Multi-Design Point

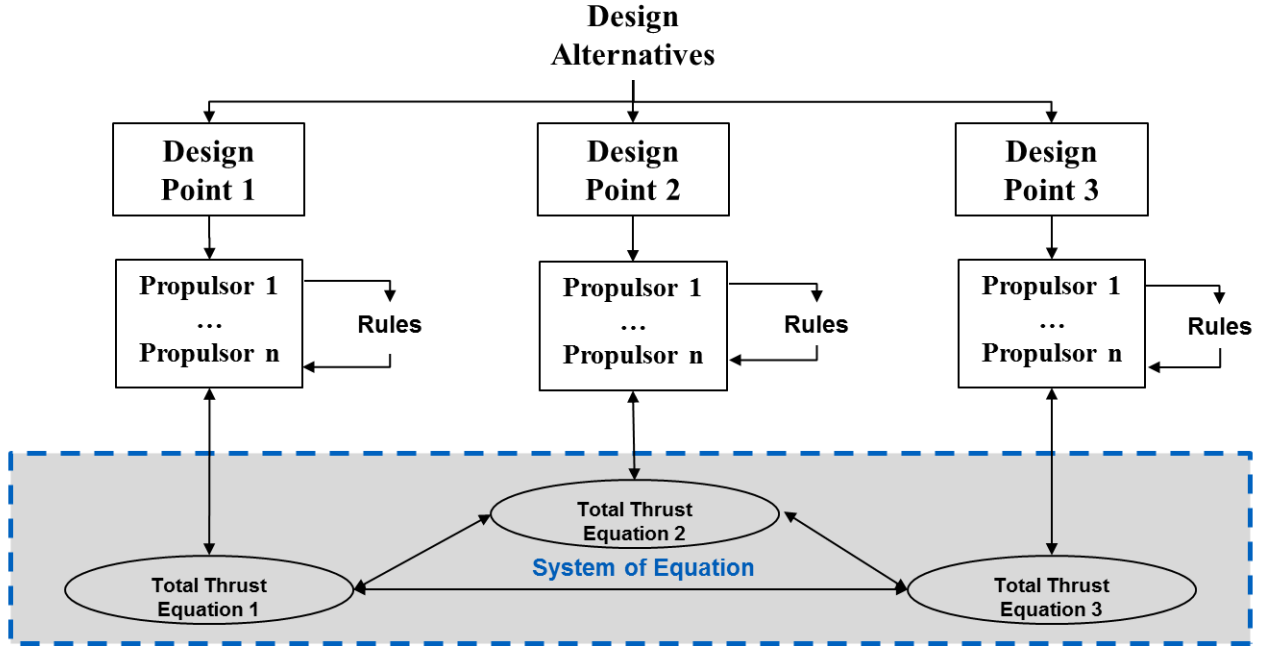


Figure 36: Illustration of Multi-Engine Multi-Design Point Process

Design Rules

Design rules are defined as a mathematical relationship that relates the size of a propulsor or propulsor components at its aerodynamic design point to another uniquely different propulsor at the aerodynamic design original propulsor. If there is only a single engine/propulsor designed, then there is no need to have additional design rules. If "k" unique propulsors are designed, then there can be as many as $\sum_{i=1}^k N_{comp} - 1$ design rules, where N_{comp} is the number of aerodynamic design points for propulsor "i". For example, if 2 different turbo-fan engines were sized for a 3-Engine HWB with BLI (a case to be considered in detail later in this document), then the number of design rules is exactly 1. If there is only a single aerodynamic design point (only 1 propulsor designed), then there is no required design rule. Examples of design rules for each of the propulsor architecture layouts from figure 33 are shown in table XXX. Another interesting aspect of the creation of design rules is that it creates additional

cycle design variables for the system, which may have a significant impact on the amount of BLI ingested by each propulsor and potentially the system as a whole.

Power Management Rules

Power management rules are mathematical relationships that relate the power output of one propulsor **at each design point** to the power output of another. In general, the amount of power provided by a propulsor will be proportional to the speed, meaning the power management scheme will pertain to the speeds of the fans/propellers. Some engine manufacturers use the fan speed (N_1) as the primary power management variable which is measured in the engine, while others use engine pressure ratio (EPR) to correlate thrust INSERT REFERENCE HERE.

Power management rules are specified at each flight condition, except for the aerodynamic design points of the propulsors, since turbo-machinery components are, by definition, at 100% speed at their ADP. If one propulsor is at its aerodynamic design point, and another is not, then the power management rule and the design rule are the same thing at that point, since setting the size of the propulsor will also set the relationship between the power output of the propulsors. Therefore, the number of additional power management rules (on top of the design rules) required can be computed by Eq. 79, where k is the number of unique propulsor/inlet combinations, "P" is the number of design points, and N_{comp} is the number of ADPs for each propulsor.

$$N_{pm} = \underbrace{P(k-1)}_{\text{Design + PM Rules}} - \underbrace{\left(\sum_{i=1}^k N_{comp} \right)}_{\text{Design Rules}} - 1 \quad (79)$$

Engine Matching Relations

The normal engine matching relations are a set of independent variables and dependent relations that are solved by the Newton-Raphson solver in the MDP method.

The independent variables in the engine matching relations are typically the fuel-to-air ratios of the burner, while the dependent relations are equations which set the thrust to a desired level of thrust or the speed of the engine/propulsor to a desired fraction of the design speed (which correlates with thrust). As such, the MEMDP method must necessarily modify the engine matching relations to accomodate the new architectural arrangement.

If a propulsion system has k uniquely defined propulsor/inlet condition combinations and the i^{th} combination contains m_i propulsors, then the total number of propulsors is defined by:

$$n = \sum_{i=1}^k m_i \quad (80)$$

and the total thrust, in the case of BLI is defined by:

$$F_{n_{BLI}} = \sum_{i=1}^k m_i (F_{n_{BLI}})_i \quad (81)$$

As such, the thrust saving coefficient and thrust specific fuel consumption are also computed as the sum.

$$TSC = 1 - \frac{\sum_{i=1}^k m_i F_{n_i}}{\sum_{i=1}^k m_i \frac{F_{n_i}}{(1 - TSC_i)}} \quad (82)$$

$$TSFC = \frac{W_f}{F_{n_{BLI}}} = \frac{\sum_{i=1}^k W_{fi}}{\sum_{i=1}^k (F_{n_{BLI}})_i} \quad (83)$$

Finally, the total amount of engine matching relations is precisely equal to $P + N_{pm}$. These engine matching relations comprise the vector of independent variables which affects the power output of each propulsor and the vector of dependent thrust or power balance relations (power management rules plus P total thrust relations). If k is greater than unity, and the additional $(k-1)$ unique propulsors are allowed their own design points, then the number of engine matching relations is reduced and each replaced with a single cycle design relation for the uniquely designed propulsor.

Alternative Approaches and Hypothesis 3

The major alternative approach to dealing with the problem of inlet condition variation is to add an augmentation term to the boundary layer ingestion term in the power balance. This approach will be called the "augmented power balance approach". This would work by sizing a single propulsor in a traditional manner, but with the wake recovery term for that single propulsor augmented to reflect the difference in wake-recovery between the different propulsors on the vehicle. This approach has the difficulty of not always knowing "a-priori" exactly how much wake recovery will be lost or gained due to that variation and it also does not capture differences in inlet recovery between the propulsors induced by the boundary layer disparity. It also does not allow the new degrees of freedom appropriated by the additional design rules and power management rules in the ME-MDP method. This alternative approach was used in an example system level study of a distributed propulsion architecture by MIT INSERT REFERENCE HERE. A comparison of this approach will be shown in later sections.

With the above description of the proposed ME-MDP approach to be used within the BLIPSS design method, the following hypothesis has been formed in relation to research question 3.

Hypothesis 3: Differing inlet conditions for BLI propulsion systems can be accounted for by using a modified simultaneous MDP approach and specifying the number of engines, inlet conditions, a set of power management rules, design rules, and by modifying the engine engine matching relations to relate to the total vehicle thrust rather than thrust per engine. If the difference in the local inlet properties are large, this approach will yield increasingly different performance predictions than if the traditional single engine or the augmented power balance approach is used.

Canonical Problem and Research Question 4

The test problem for hypotheses 1-3 chosen for this thesis is the N2A boeing HWB design. The selected propulsion architecture to test hypothesis 3 is a 3-engine turbo-fan based architectures. As such, this section will define the architecture integration phase and pose a relevant research question for this canonical problem with regard to the power management and design rules. A diagram of the 3-engine configuration is shown below in figure 37 with some key parameters for the system defined. The propulsion system will, in order to maintain symmetry, always have one "inboard" engine at the aircraft centerline (thicker boundary layer) and an outboard engine which is at some parametric location value. This value will be used to test hypothesis 3 and to determine engineering trades on the system overall.

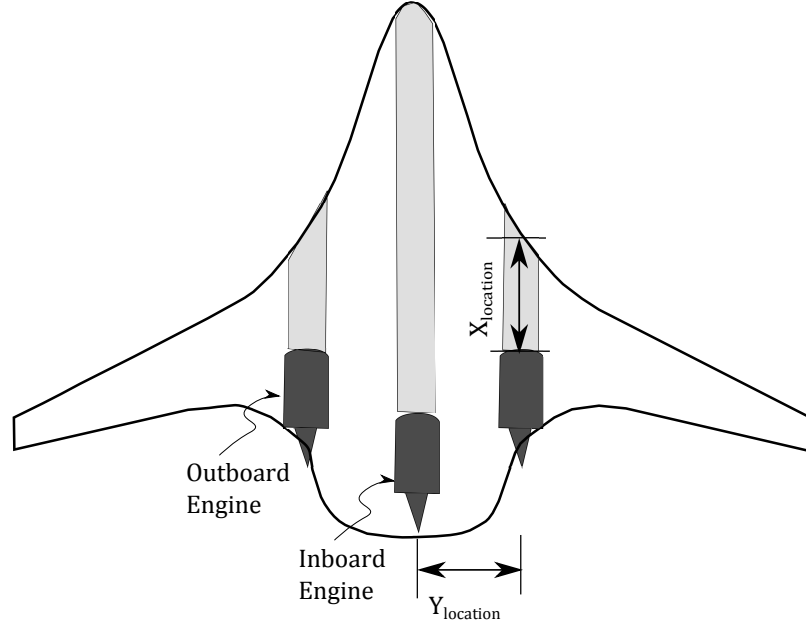


Figure 37: Illustration of 3-Engine Boeing N2A.

Design Options for 3 Engine HWB

The design options for any propulsion system can be specified by showing the design point mapping matrix as defined by Schutte for the MDP process. Different design potential rules can be specified for each design option. These are shown in table 6. The single inlet case is the condition where only the single inlet condition is

considered. This case will be used to test hypothesis 3 and is representative of the standard cycle analysis where only a single propulsor/inlet condition combination is considered. The single engine is the case where there is only a single design point (one-engine designed). For this case, there are two options, either inboard core design point or outboard core design point, which raises the question of which is better to choose. Finally, there are the two design options where the inboard and outboard

	X = Not used D = On-Design O = Off-Design		
Design Option		Core/HP Spool	Fan/LP Spool Design Rule
Single Inlet	Inboard	D	D
	Outboard	X	X
	Inboard	X	X
	Outboard	D	D
Single Engine	Inboard	D	D
	Outboard	O	O
	Inboard	O	O
	Outboard	D	D
Fixed Core	Inboard	D	D
	Outboard	O	D
Double Engine	Inboard	D	D
	Outboard	D	D

Table 6: Design point mapping matrix for the 3 engine architecture highlighting the available design rules.

propulsors are sized independently. The fixed core design assumes that only the bypass and LP spool are re-designed for each, while the core/HP spool are designed at either inboard or outboard and held constant. The double engine is the case where a new engine is sized for both conditions. In each of these cases, there is a design rule required for the analysis because the size of the propulsors with respect to each

other are not fixed. Therefore, a new variable is defined and called the "mass flow ratio" or MFR, which is not to be confused with the ratio of free-stream tube area to capture which is sometimes called the mass flow ratio. The MFR is defined as the ratio of the mass flow of the outboard engine to the inboard engine and is considered a cycle parameter.

$$MFR = \frac{\dot{m}_{outboard}}{\dot{m}_{inboard}} \quad (84)$$

It is worth noting that other design rules could be used, such as the ratio of the thrusts, which would effectively represent the same thing, but it is easier from a practical standpoint to fix the mass flows of the engine, since mass flow demand is typically an independent parameter while thrust is a dependent result of the cycle analysis. By using the MFR as the design rule, the mass flow of one engine can be varied to satisfy the thrust matching relation, and the other engine mass flow can be set to a value for each pass through the model based on the MFR.

The research question for this section of the thesis pertains to which of the above options is preferable for this application. Chapter 5 will discuss the modeling setup and implementation of the 3-Engine N2A cycle analysis, as well as the architecture integration phase setup. From this analysis, general conclusions about choices of design options and design rules for other systems will also be made.

Research Question 4: For BLI propulsion systems, which design options provides the largest benefit?

Observations and Hypothesis 4

A hypothesis in regard to research question 4 can be made by reiterating the conclusion from : namely that the performance of the engine changes significantly with the ratio of the boundary layer to inlet height, and that this can be controlled for each

propulsor by varying the mass flow ratio. Having the extra independent mass flow ratio variable allows the designer to match each propulsor to the appropriate boundary layer to height ratio. However, as discussed previously, there may be countervailing factors that prevent one or more of the propulsors from being sized to a particular level.

One such potential factor is the existence of significant size effects for gas turbine engines, and specifically the gas turbine core. To illustrate these effects, 38 shows the polytropic efficiency of a high pressure compressor plotted against the exit corrected flow – a normalized measure of the "size" of the compressor. Clearly making the gas turbine core very small at its design point by varying the mass flow ratio will have a significant impact on the performance of the core.

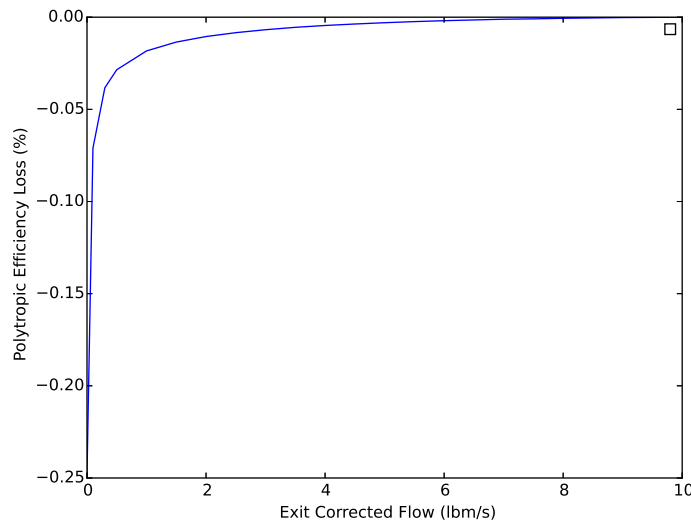


Figure 38: Plot showing size effects of a typical gas turbine axial compressor at very small exit corrected flow INSERT REFERENCE HERE.

Another potential factor which can effect the gas turbine core is flow mis-match which could happen in the case of the fixed core design option. If the outboard and inboard engines are designed to the same bypass ratio, then the core will need to be "over" or "under" sped in relation to the design point. This can have a significant impact on the efficiency of the core and the pressure ratio at which it operates. As

such, the following hypothesis is developed based on the above reasoning.

Hypothesis 4: Sizing a different propulsor for each inlet condition will provide a better fuel burn benefit than the single engine option, unless doing so affects the thermal efficiency of the gas turbine core. As the difference between the engine inlet conditions is increased, so too is the value gained by re-sizing the engine for that inlet condition.

3.2.3 Vehicle Matching Phase

The point of the vehicle matching phase is to determine the flight conditions for which the propulsion system need to be designed and which therefore need to be included in the MDP analysis. This section will outline the basic requirements for including a flight condition within the MDP analysis, and also outline a method for finding the flight conditions in the most efficient way for a given set of requirements. Research question five is formulated with respect to this phase of the analysis:

<p>Research Question 5:: What flight conditions are necessary to include for sizing BLI systems in a MDP cycle analysis?</p>

In general, sizing points need to be included in the MDP analysis if some aspect of the design at that point will constrain or place more demand on the system. For instance, it is common to include both top-of-climb (TOC) and take-off (TKO) conditions in an MDP, since TOC places a significant mass flow demand on the system while TKO (especially for a hot day) is the hottest point of operation and therefore sizes the cooling flow which impacts the overall required mass flow and fuel consumption rate. Looking at the MDP analysis, there are two ways to include flight conditions in the analysis: constraint points or target points. For the latter, thrust or cycle targets are precisely met, while constraint points merely constrain some aspect

of the system at that point. For BLI, the thrust or power balance requirement is precisely the same as for a podded system, though the thrust target point may not necessarily be the same as the typical top-of-climb position. While distortion concerns can be important for podded subsonic inlets, it is not often considered to impact the choice of propulsion system design, but rather impacts the final stall margin stack-up of the fan. The increased inherent distortion for a BLI system places an additional requirement for a BLI system which must be included in the MDP analysis.

Thrust Sizing Condition

Consider the un-installed thrust of an isolated, ducted fan propulsor:

$$T = P_k - \phi_{jet} = \dot{m}(V_j - V_\infty) \quad (85)$$

Now, define the installation losses of a propulsor in relation to the un-installed thrust value:

$$\phi_{inlet} = \frac{F_{loss,inlet}}{T} = \frac{\Phi_{Inlet}}{T \cdot V_\infty} \quad (86)$$

$$\phi_{Nozzle} = \frac{F_{loss,Nozzle}}{T} = \frac{\Phi_{Nozzle}}{T \cdot V_\infty} \quad (87)$$

The installed net thrust of the propulsor is then:

$$F_n = T \cdot (1 - \phi_{Nozzle} - \phi_{Inlet}) = \dot{m}(V_j - V_\infty) \cdot (1 - \phi) \quad (88)$$

Where ϕ is the sum of the inlet and nozzle loss percentages. For a given fan pressure ratio, increased inlet and fan losses will required a larger propulsor mass flow. Setting Eq. 88 equal to the net thrust required of the vehicle, we get:

$$TV_\infty \cdot (1 - \phi) = (DV_\infty + W\dot{h}) \quad (89)$$

and the mass flow required for the engine is then:

$$\dot{m} = \frac{D + W\dot{h}/V_\infty}{(F_n/\dot{m})(1 - \phi)} \quad (90)$$

This can be corrected to sea-level by using the parameter $\delta = P_t/P_{sl}$ and $\theta = T_t/T_{sl}$.

$$\dot{m}_c = \dot{m} \cdot \frac{\sqrt{\theta}}{\delta} = \left(\frac{D + Wh/V_\infty}{\delta} \right) \cdot \left(\frac{1}{1 - \phi} \right) \cdot \left(\frac{1}{ST_c} \right) \quad (91)$$

Where ST_c is the corrected specific thrust given by:

$$ST_c = \frac{F_n}{\dot{m}\sqrt{\theta}} \quad (92)$$

The corrected specific thrust is mainly a function of the engine/propulsor type, cycle parameter choices, and flight condition. The general trend of specific corrected thrust for a commercial turbo-fan engine is shown in figure 39 showing a significant fall at very high Mach numbers such as at the top-of-climb flight condition. The

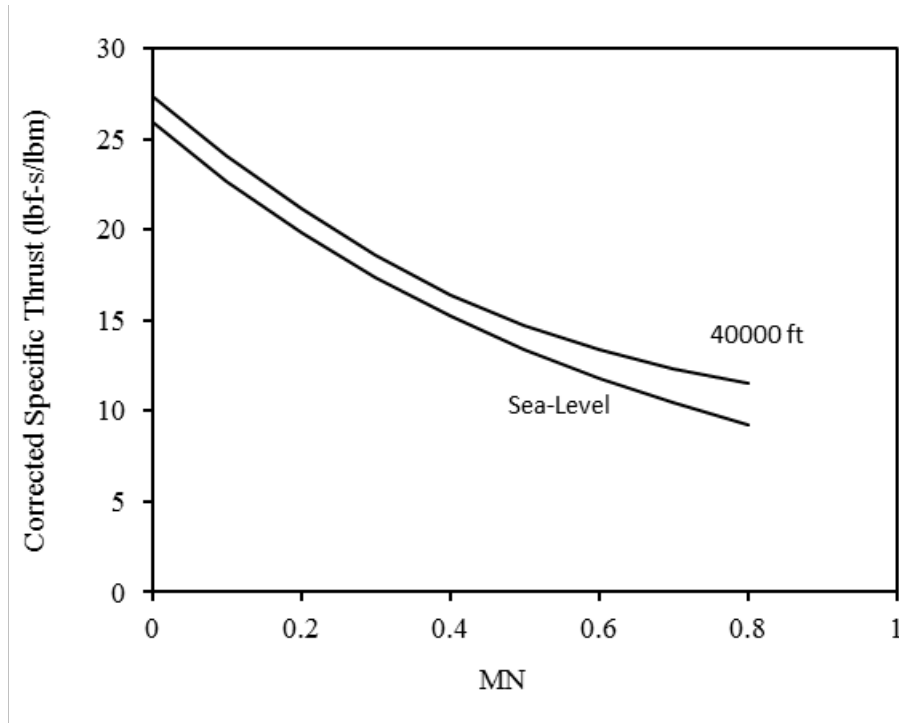


Figure 39: Turbofan specific thrust vs. Mach number for different altitudes.

first term in Eq. 91 represents the corrected thrust required to power the vehicle. Through the course of the mission of a typical commercial vehicle, the Mach number will obviously increase significantly at cruise flight speeds and the lift coefficient will decline significantly as the weight and lift required is decreased. The net result is that

the corrected thrust required changes over the course of the mission and is generally decreased as the engine moves to top-of-climb. However, this is not enough to offset the significant decrease in the thrust per unit mass flow delivered at higher flight velocities. The top of climb condition is therefore typically used to size the mass flow of typical turbofan engines.

The loss term $\frac{1}{1-\phi}$ can also influence this balance. If the losses are significant enough at any flight condition, it's possible that this could offset the loss in specific corrected thrust in the final term.

BLI Case

For BLI, the primary difference is that there is now a benefit term represented by the thrust saving coefficient, as derived previously.

$$F_n = T \frac{(1 - \phi)}{1 - TSC} \quad (93)$$

From the previous analysis, Eq. 91 can be updated to include the thrust saving coefficient due to the boundary layer ingestion.

$$\dot{m}_o = \left(\frac{D + W\dot{h}/V_\infty}{\delta} \right) \cdot \left(\frac{1 - TSC}{1 - \phi} \right) \cdot \left(\frac{1}{ST_c} \right) \quad (94)$$

This means that the critical flight condition may potentially change depending on the ratio of the boundary layer benefit to losses represented by the second term of Eq. 94. It also potentially means that the critical mass flow sizing condition could be dependent the amount of boundary layer ingested, which was seen previously to have a significant impact on the system TSC and losses.

Futhermore, this shows that the BLI engine will have a fundamentally different lapse profile with respect to a podded engine to the change in the amount of wake recovery that occurs as the Mach and Reynolds number is changed during the flight. This could potentially have an impact on the optimal flight path that the vehicle might take, implying that a much tighter coupling between vehicle and propulsion

system designers must take place for commercial BLI systems which ingest significant amounts of boundary layer.

Stall Margin Condition

Consider a fan operating at some pressure ratio (PR) and corrected flow ($W_c = W \cdot \frac{\sqrt{\theta}}{\delta}$) and exhaust area A_e . As the ambient conditions and throttle change, the area must necessarily remain constant. Given this, Eq. 95 shows a relationship between the constant area, the ambient conditions, and the nozzle exit velocity.

$$A_e = \text{constant} = \frac{W}{\rho_e u_e} = W \cdot \frac{\sqrt{\theta}}{\delta} \cdot \frac{1}{M_e} \quad (95)$$

From Mattingly INSERT REFERENCE HERE, the equation for the fan exhaust stream is given by:

$$M_e = \sqrt{\frac{2}{\gamma - 1} \left(\pi_r \pi_d \pi_f \pi_{fn} - 1.0 \right)} \quad (96)$$

Where π_d is the diffuser pressure recovery, π_f is the fan pressure ratio (a.k.a FPR), π_{fn} is the fan nozzle duct pressure drop, π_r is the ram recovery term given in Eq. 97, and γ is the ratio of specific heats.

$$\pi_r = \left(1 + \frac{\gamma - 1}{2} M_o^2 \right)^{\frac{\gamma}{\gamma - 1}} \quad (97)$$

Clearly, two factors are of major importance in determining the flow required for a given nozzle exhaust area, which are the fan operating pressure ratio and the flight Mach number. At hot day TKO, the flight Mach number is substantially reduced relative to cruise or TOC, and the nozzle becomes unchoked ($M_e < 1$). This forces a decrease in flow (and therefore RPM) for a fixed fan pressure ratio. For a fixed corrected speed ($N/\sqrt{\theta}$), there is an increase in pressure ratio and decrease in flow. This necessarily moves the fan closer to the stall line.

The other major factor is the design pressure ratio of the fan, which substantially increases the BPR of the engine – something typically desirable for efficiency. From

Eq. 96, the Mach number at the nozzle exit will decline significantly for lower π_f (higher BPR). The impact of both flight condition and choice of engine BPR for a typical turbofan engine is shown in figure 40, where the operating line at hot day TKO and higher bypass ratio is much more stall critical.

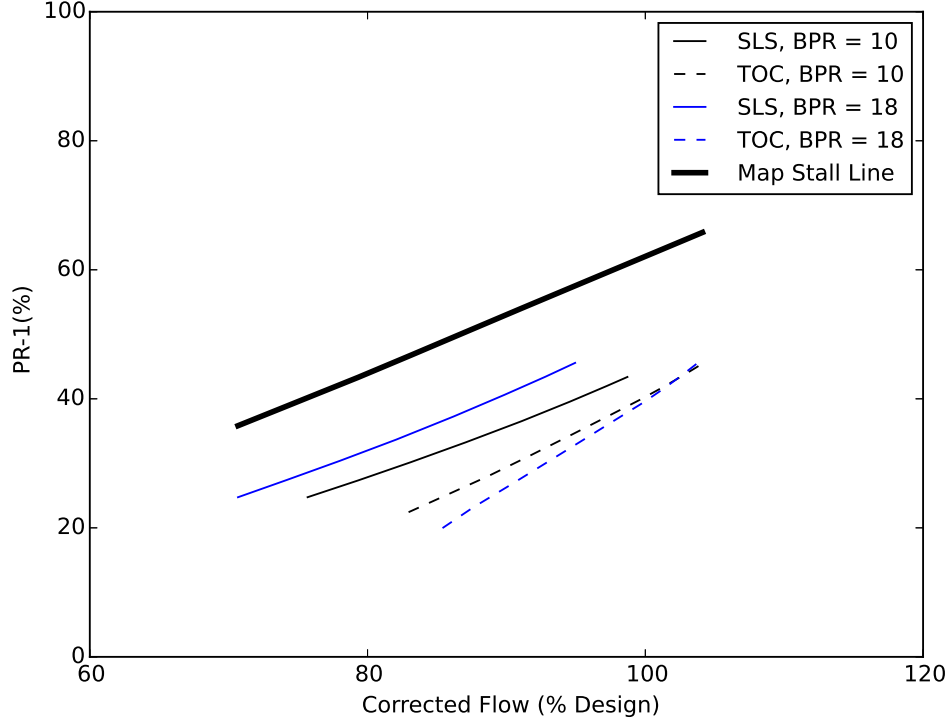


Figure 40: Commercial turbofan variation in fan operating line with flight condition. Trends show that SLS hot day is critical and is worse at higher BPR.

BLI Case

For BLI, the limiting stall condition will be that flight point where the fan operating line moves closest to the stability line after modification from the BLI related distortion. If any point is predicted to have a lacking stability margin after distortion is accounted for, then additional margin must be added to compensate. This must be done by either mitigating the effects of the distortion on the system or by modifying the fan exhaust area to move the operating line farther from the stability limit.

So, while the basic trend for a turbofan engine is that stall is generally much more critical at sea-level TKO conditions, the increased distortion at higher Mach numbers could make flight speeds at high power more critical. Conditions which require very high angles of attack should also be considered such as take-off and landing where large amounts of lift is required and the engines are generally at worse stall margin anyway. Cycle choices, such as the fan pressure and bypass ratios, will have also a significant impact on both the stall margin variation over the flight envelope, the amount of distortion ingested, and the stall margin loss due to distortion. As such, one major claim of this thesis is that the most critical stall condition for a given vehicle and requirements set cannot necessarily be assumed known prior to conducting the analysis. The following section discusses the potential ways this problem might be dealt with and discusses the reasoning for choosing the method implemented in the BLIPSS methodology.

Options for Determining Flight Conditions

The analysis from the previous sections showed that both the thrust target point and stall margin (distortion) constraint point for a BLI system might vary significantly depending on the choice of cycle design, the level of boundary layer ingested, and the flight requirements imposed on the system. One option for finding these conditions

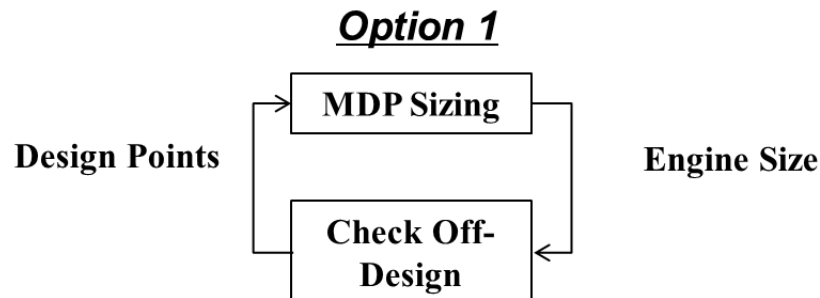


Figure 41: Option 1 of 3 for determining the flight conditions where all off-design conditions are checked and iterated with the MDP sizing procedure.

would be to check every single off-design flight condition within the mission flight

envelope – illustrated in figure 41. The problem with this is that it violates the purpose of the MDP methodology to begin with: to reduce the amount of design iterations needed to converge on the required engine size. Depending on the complexity of the cycle model, it may take many iterations and off-design cycle analysis runs to finish this process.

The second option for determining the flight conditions would be to include every condition in the multi-design point process as in figure 42. Given that there may be many conditions to check if the entire mission envelope is included, this would place an unmanageable level of program complexity on the cycle designer and may have convergence issues if a single initial iterate is used. The final option, as illustrated in

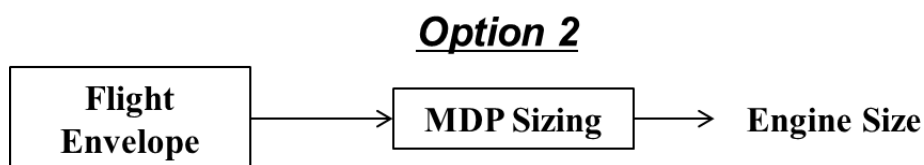


Figure 42: Option 2 of 3 for determining the flight conditions where all off-design conditions are included as constraint points within the MDP.

figure 43, is to assume that some subset of the total flight condition set will cover the majority of the critical conditions over the span of the design space. The process will then setup a screening design of experiments which represents a range of the design space to determine the likely critical flight conditions.

For screening cases, the first option is implemented and all off-design conditions are checked. For non-screening cases, off-design is not checked, and only the MDP sizing procedure is run. The final selected design can then also be run through the off-design check to ensure that it's critical sizing conditions were appropriate and that no off-design conditions have thrust or stall margin deficits.

Obviously option 3 is the one that seems most viable given the above analysis and is therefore implemented in the BLIPSS methodology algorithm description in figure 14. To verify that this process is acceptable, the following hypothesis is made and

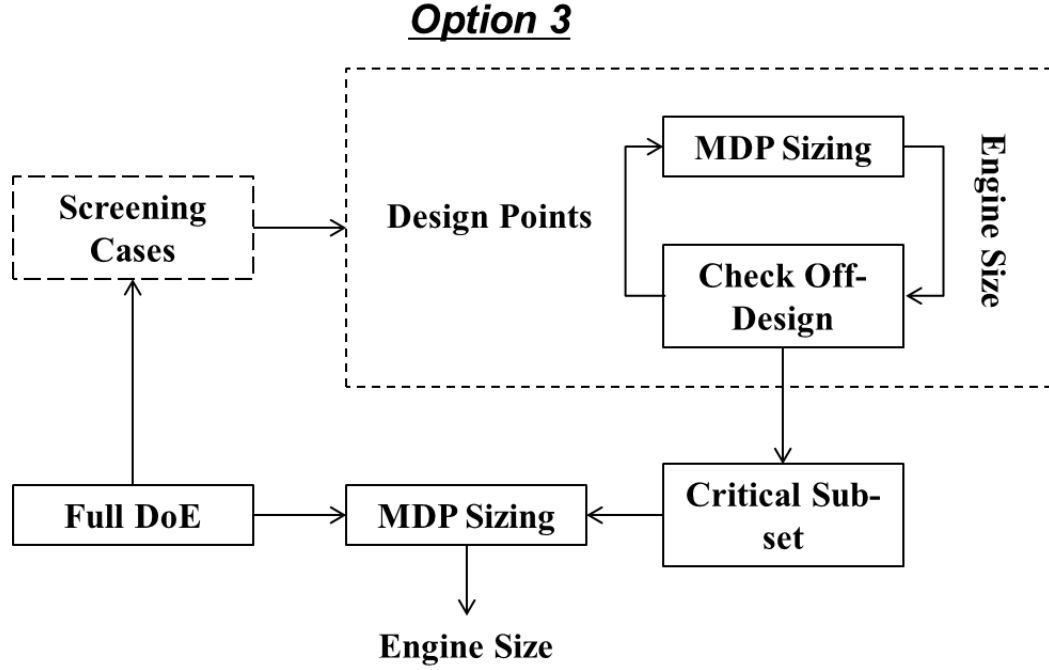


Figure 43: Option 3 of 3 for determining the flight conditions where a subset of critical conditions are identified using a screening design of experiments; all subsequent cases do not run off-design iteration checks.

will be tested thoroughly in chapter 6 with a numerical simulation and experiment on the canonical BLI problem.

Hypothesis 5:: Off-design flight conditions for BLI should be included as constraint points in the MDP requirements setup phase if thrust or stall margin loss due to BLI installation effects, which were not present in the podded case, become sufficiently high such that a larger engine size or additional design stall margin is required to accommodate the thrust and stability requirements at that flight condition. A small subset of all possible flight conditions can be found, for a given propulsion system architecture and requirements set, which captures the most critical conditions for a large majority of designs in the design space.

CHAPTER IV

BLI MODELING PHASE

In the previous chapter, the overall BLIPSS methodology was developed and hypotheses 1 and 2 were made based on observations from past literature and additional theoretical analysis. This chapter will demonstrate the BLI modeling phase, as outlined in Chapter 3, for a canonical design problem involving a hybrid wing body vehicle with boundary layer ingesting turbofan engines. The chapter will proceed according to the outline of the BLI modeling phase and the BLI component modeling process defined in Chapter 3. Furthermore, experiments intended to validate hypotheses 1 and 2 will be defined and conducted in order to justify the need for each of the components of the method and to determine which physical effects are relatively important for this canonical problem.

The chapter will first outline the baseline vehicle design and geometry and thrust requirements for the propulsion system. The baseline propulsion system will also be specified and defined in detail for purposes of comparison with the BLI designs. The BLI modeling components for the propulsion system will be defined in detail and verification/validation data will be provided to substantiate the models. Experiments 1 and 2 will be defined and the results will then be shown to draw conclusions in relation to hypotheses 1 and 2.

4.1 Baseline Design

4.1.1 Baseline Vehicle

The baseline vehicle used here is very similar to the Boeing N2A-EXTE design INSERT REFERENCE NASA LANGLEY. The vehicle is intended to carry 300 passengers and would therefore be a future potential replacement for a Boeing 777 (double aisle) type airplane. Some overall assumed parameters for the vehicle which are relevant to the BLI problem are shown below.

Parameter	Value
Gross Weight	536,282 lbs
Wing Span	240 ft
Max Fuel	197,000 lbs
Cruise Mach	0.84
Initial Cruise Alt	35,917 ft
Final Cruise Alt	43,000 ft
Initial Cruise L/D	21.6
Final Cruise L/D	20.0
SLS Thrust/Engine	72,400
Design Range	7530 nm
Payload	64,000 lbs

Table 7: Table showing key design parameters for the baseline HWB vehicle.

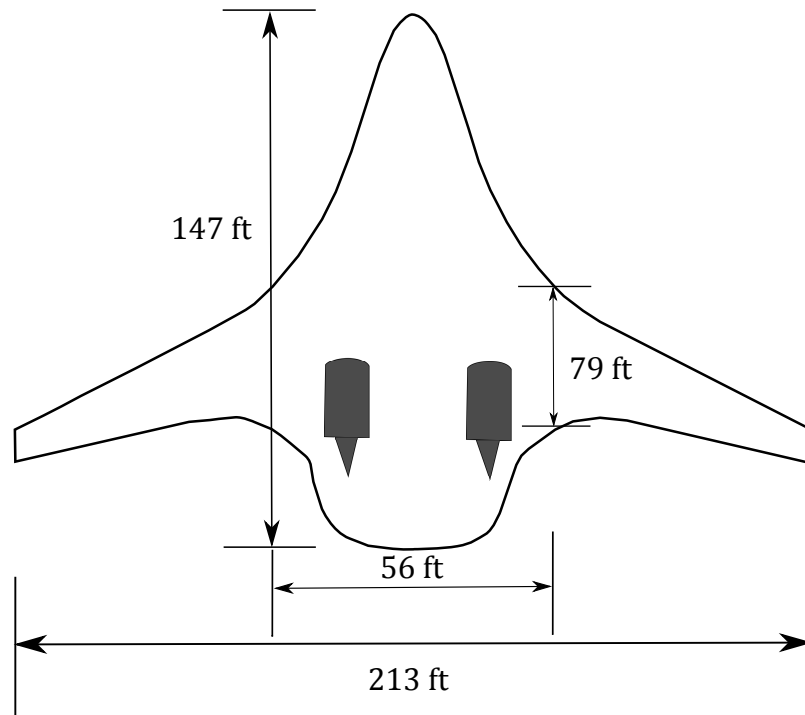


Figure 44: HWB baseline key design dimensions.

Available Vehicle Boundary Layer

4.2 Baseline Engine

4.3 BLI Modeling

4.3.1 Airframe Model

4.3.2 Power Balance and Drag Book-keeping

4.3.3 Inlet Model

4.3.4 Fan Model

General Model Architecture and Algorithm

4.4 Experiment 1 Results

4.4.1 Flight Condition Variation

Design Mach Number

Design AoA Impact

4.4.2 BLI Design Space Variation

CHAPTER V

ARCHITECTURE INTEGRATION PHASE

- 5.1 Implementation of Methodology on HWB Vehicle
- 5.2 Wake Correction Method
- 5.3 Experiment 3 Results
- 5.4 Experiment 4 Results

CHAPTER VI

VEHICLE MATCHING PHASE

6.1 Methodology Implementation

6.1.1 Algorithm Description

6.1.2 Solver Setup

6.1.3 Variable Area Nozzle Setup

6.2 Experimental Setup

6.2.1 Initial MDP Setup

6.2.2 Baseline Flight Envelope Requirements

6.2.3 Screening DoE Definition

6.2.4 Distortion Constraint Definition

6.3 Experiment 5 Results

6.3.1 Algorithm Validation

6.3.2 Screening Test Results

Variable Area Nozzle Results

6.4 Impact of BLI Design Variables on Critical Flight Conditions

6.5 Impact of Cycle Design Variables on Critical Flight Conditions

6.6 Impact of Requirements

6.7 Summary and Conclusions

CHAPTER VII

BLIPSS IMPLEMENTATION

- 7.1 Introduction
- 7.2 BLIPSS Process Description
- 7.3 BLI Modeling Phase
- 7.4 Architecture Integration Phase
- 7.5 Vehicle Matching Phase
- 7.6 Design Space Exploration
- 7.7 Results

CHAPTER VIII

SUMMARY AND CONCLUSIONS

REFERENCES

- [1] ALLAN, B. G. and OWENS, L. R., “Numerical modeling of flow control in a boundary layer ingesting offset inlet diffuser at transonic mach numbers,” in *44th AIAA Aerospace Sciences Meeting and Exhibit*, 2006.
- [2] ALLAN, B. G., OWENS, L. R., and BERRIER, B. L., “Numerical modeling of active flow control in a boundary layer ingesting offset inlet,” in *2nd AIAA Flow Control Conference*, 2004.
- [3] ALLAN, B. G., OWENS, L. R., and LIN, J. C., “Optimal design of passive flow control for a boundary- layer-ingesting offset inlet using design-of-experiments,” in *44th AIAA Aerospace Sciences Meeting and Exhibit*, 2006.
- [4] ANDERSON, J. D., *Fundamentals of Aerodynamics*. McGraw-Hill, 2001.
- [5] BERRIER, B. L. and ALLAN, B. G., “Experimental and computational evaluation of flush-mounted, s-duct inlets,” in *42nd AIAA Aerospace Sciences Meeting and Exhibit*, 2004.
- [6] BERRIER, B. L. and MOREHOUSE, M. B., “Evaluation of flush-mounted, s-duct inlets with large amounts of boundary layer ingestion.”.
- [7] BRADLEY, M. K. and DRONEY, C. K., “Subsonic ultra green aircraft research phase ii: N+4 advanced concept development,” tech. rep., NASA, 2012.
- [8] CAMPBELL, R. L., CARTER, M. B., PENDERGRAFT, O. C., FRIEDMAN, D. M., and SERRANO, L., “Design and testing of a blended wing body with boundary layer ingestion nacelles at high reynolds numbers,” in *43rd AIAA Aerospace Sciences Meeting and Exhibit*, 2005.
- [9] CARTER, M. B., CAMPBELL, R. L., PENDERGRAFT, O. C., FRIEDMAN, D. M., and SERRANO, L., “Designing and testing a blended wing body with boundary-layer ingestion nacelles,” *Journal of Aircraft*, vol. 43, pp. 1479–1489, 2006.
- [10] COMMITTEE, S. S.-., “Gas turbine inlet flow distortion guidelines,” Tech. Rep. ARP 1420, Revision B, Society of Automotive Engineers, 2002.
- [11] COUSINS, W. T. and DAVIS, M. W., “Evaluating complex inlet distortion with a parallel compressor model: Part 1 – concepts, theory, extensions, and limitations,” in *Proceedings of ASME Turbo Expo 2011*, 2011.
- [12] CUMPSTY, N. and HORLOCK, J., “Averaging aerodynamics flows for a purpose,” *Journal of Turbomachinery*, vol. 128, January 2006.

- [13] DOUGLASS, W., “Propulsive efficiency with boundary layer ingestion,” tech. rep., McDonnell Douglas, 1970.
- [14] DRELA, M., *Two-dimensional transonic aerodynamic design and analysis using the euler equations*. PhD thesis, Massachusetts Institute of Technology, 1985.
- [15] DRELA, M., “Power balance in aerodynamic flows,” *AIAA Journal*, vol. 47, July 2009.
- [16] FERRAR, A. M., O’BRIEN, W. F., and NG, W. F., “Active control of flow in serpentine inlets for blended wing-body aircraft,” in *45th AIAA/ASME/SAE/ASEE Joint Propulsion Conference & Exhibit*, August 2009.
- [17] FERRAR, ANTHONY M., O. W. F., “Flow in boundary layer ingesting serpentine inlets,” in *47th AIAA/ASME/SAE/ASEE Joint Propulsion Conference & Exhibit*, 2011.
- [18] FERRAR, ANTHONY M., O. W. F., “Progress in boundary layer ingesting embedded engine research,” in *48th AIAA/ASME/SAE/ASEE Joint Propulsion Conference & Exhibit*, 2012.
- [19] FLEMING, J., ANDERSON, J., NG, W., and HARRISON, N., “Sensing and active flow control for advanced bwb propulsion-airframe integration concepts,” tech. rep., NASA, 2005.
- [20] FLOREA, R. V., MATALANIS, C., HARDIN, L. W., STUCKY, M., and SHAB-BIR, A., “Parametric analysis and design for embedded engine inlets,” in *48th AIAA/ASME/SAE/ASEE Joint Propulsion Conference & Exhibit*, 2012.
- [21] FLOREA, R. V., VOYTOVYCH, D., TILLMAN, G., STUCKY, M., SHABBIR, A., SHARMA, O. P., and AREND, D. J., “Aerodynamic analysis of a boundary layer ingesting distortion-tolerant fan,” in *Proceedings of ASME Turbo Expo 2013: Turbine Technical Conference and Exposition*, 2013.
- [22] FREULER, P. N., “Boundary layer ingesting inlet design for a silent aircraft,” Master’s thesis, Massachusetts Institute of Technology, 2005.
- [23] GARG, M., CHOUDHARY, S., and KALLA, S. L., “On the sum of two triangular random variables,” *International Journal of Optimization: Theory, Methods, and Applications*, vol. 1, pp. 279–290, 2009.
- [24] GREITZER, E., “Mit n+3 final report, volume 2: Appendices design methodologies for aerodynamics, structures, weight, and thermodynamic cycles,” tech. rep., Massachusetts Institute of Technology, 2010.
- [25] GUO, J., JULIEN, P. Y., and MERONEY, R. N., “Modified log-wake law for zero-pressure-gradient turbulent boundary layers,” *Journal of Hydraulic Research*, vol. 41, no. 5, p. pp. 493, 2003.

- [26] HARDIN, L. W., TILLMAN, G., SHARMA, O. P., BERTON, J., and AREND, D. J., "Aircraft system study of boundary layer ingesting propulsion," in *48th AIAA/ASME/SAE/ASEE Joint Propulsion Conference & Exhibit*, 2012.
- [27] KAWAI, R. T., FRIEDMAN, D. M., and SERRANO, L., *Blended Wing Body(BWB) Boundary Layer Ingestion (BLI) Inlet Configuration and System Studies*. NASA. CR-2006-214534.
- [28] KESTNER, B. K., SCHUTTE, J. S., GLADIN, J. C., and MAVRIS, D. N., "Ultra high bypass ratio engine sizing and cycle selection study for a subsonic commercial aircraft in the n+2 timeframe," in *ASME Gas Turbine Exposition*, (Vancouver, Canada), 2011.
- [29] KIM, H. and LIOU, "Optimal inlet shape design of n2b hybrid wing body configuration," in *48th AIAA/ASME/SAE/ASEE Joint Propulsion Conference & Exhibit*, 2012.
- [30] KIM, H. D. and FELDER, J. L., "Control volume analysis of boundary layer ingesting propulsion systems with or without shock wave ahead of the inlet," in *AIAA Aerospace Sciences Meeting Including the New Horizons Forum and Aerospace Exposition*, (Orlando, Florida), 2011.
- [31] KIM, H. D., FELDER, J. L., and BROWN, G. V., "An examination of the effect of boundary layer ingestion on turboelectric distributed propulsion systems," in *Proc. AIAA Aerospace Sciences Meeting Including the New Horizons Forum and Aerospace Exposition*, (Orland, Florida), 2011.
- [32] KIM, H. D., "Distributed propulsion vehicles," in *27TH INTERNATIONAL CONGRESS OF THE AERONAUTICAL SCIENCES*, 2010.
- [33] KO, Y.-Y. A., *The Multidisciplinary Design Optimization of a Distributed Propulsion Blended-Wing-Body Aircraft*. PhD thesis, Virginia Polytechnic Institute and State University, 2003.
- [34] KOK, H., VOSKUIJL, M., and VAN TOOREN J.L., M., "Distributed propulsion featuring boundary layer ingestion engines for the blended wing body subsonic transport," in *51st AIAA/ASME/ASCE/AHS/ASC Structures, Structural Dynamics, and Materials ConferencejBRj 18th*, 2010.
- [35] LIEBECK, R., "Design of the bleded-wing-body subsonic transport," in *40th AIAA Aerospace Sciences Meeting & Exhibit*, 2002.
- [36] LIEBECK, R., "Blended wing body design challenges," in *AIAA/ICAS International Air and Space Symposium and Exposition: The Next 100 Years*, 2003.
- [37] LIOU, M.-S. and JOON LEE, B., "Minimizing inlet distortion for hybrid wing body aircraft," *Journal of Turbomachinery*, vol. 134, May 2012.

- [38] LONGLEY, J. and GREITZER, E., “Inlet distortion effects in aircraft propulsion system integration,” 1993.
- [39] LYNCH, F., “A theoretical investigation of the effect of ingesting airframe boundary layer air on turbofan engine fuel consumption,” tech. rep., Douglas Aircraft Company, 1960.
- [40] MATTINGLY, J., HEISER, W., and DALEY, D., *Aircraft Engine Design*. AIAA Education Series, second ed., 2002.
- [41] NICKOL, C. L., “Silent aircraft initiative concept risk assessment,” tech. rep., NASA, 2008.
- [42] NICKOL, C. L. and MCCULLERS, L. A., “Hybrid wing body configuration system studies,” in *47th AIAA Aerospace Sciences Meeting Including The New Horizons Forum and Aerospace Exposition*, 2009.
- [43] OATES, G., *Aircraft Propulsion Systems Technology and Design*. American Institute of Aeronautics and Astronautics, 1989.
- [44] OWENS, L. R., ALLAN, B. G., and GORTON, S. A., “Boundary-layer-ingesting inlet flow control,” *Journal of Aircraft*, vol. 45, p. 100, July-August 2008.
- [45] PLAS, A., “Peraircraft of a boundary layer ingesting propulsion system,” Master’s thesis, Massachusetts Institute of Technology, 2006.
- [46] PLAS, A., SARGEANT, M., MADANI, V., CRICHTON, D., GREITZER, E., HYNES, T., and HALL, C., “Performance of a boundary layer ingesting (bli) propulsion system,” in *AIAA Aerospace Sciences Meeting and Exhibit*, (Reno, Nevada), 2007.
- [47] QIAN, M., “Application of modified log-wake law in nonzero-pressure-gradient turbulent boundary layers,” Master’s thesis, National University of Singapore, 2004.
- [48] RODRIGUEZ, D. L., *A Multidisciplinary Optimization Method for Designing Boundary Layer Ingesting Inlets*. PhD thesis, Stanford University, 2001.
- [49] RODRIGUEZ, D. L., “Multi-disciplinary optimization method for designing boundary-layer-ingesting inlets,” *Journal of Aircraft*, vol. 46, no. 3, 2009.
- [50] SANDS, J., GLADIN, J., KESTNER, B., and MAVRIS, D. N., “Effects of boundary layer ingesting (bli) propulsion systems on engine cycle selection and hwb vehicle sizing,” in *AIAA Aerospace Sciences Meeting Including the New Horizons Forum and Aerospace Exposition*, (Nashville, TN), 2011.
- [51] SANDS, J. S., “Modeling the effects of boundary layer ingesting (bli) propulsion systems on vehicle sizing.” AE 8900 Special Problems, School of Aerospace Engineering, 2010.

- [52] SATO, S., PRITESH, M. C., HALL, D. K., DE LA ROSA BLANCO, E., and HILEMAN, J. I., “Assessment of propulsion system configuration and fuel composition on hybrid wing body fuel efficiency,” in *49th AIAA Aerospace Sciences Meeting including the New Horizons Forum and Aerospace Exposition*, 2011.
- [53] SCHUTTE, J., S.HERNANDO, J., and MAVRIS, D. N., “Technology assessment of nasa environmentally responsible aviation advanced vehicle concepts,” in *AIAA Aerospace Sciences Meeting Including the New Horizons Forum and Aerospace Exposition*, (Orlando, Florida), 2011.
- [54] SCHUTTE, J. S., *Simultaneous Multi-Design Point Approach to Gas Turbine On-Design Cycle Analysis for Aircraft Engines*. PhD thesis, Georgia Institute of Technology, 2009.
- [55] SHEDON, J., *Intake aerodynamics. 2nd ed.* Oxford: Blackwell Science., 1999.
- [56] SMITH, A. and ROBERTS, H., “The jet airplane utilizing boundary layer air for propulsion,” *Journal of the Aeronautical Sciences*, vol. 14, pp. 97–109, 1947.
- [57] SMITH, L. H., “Wake ingestion propulsion benefit,” *Journal of Propulsion and Power*, vol. 9, pp. 74–82, 1993.